MECHANISMS OF REGULATION OF *SLOPPY-PAIRED* GENES IN THE TEMPORAL PATTERNING PROGRAM OF THE OPTIC LOBE MEDULLA NEUROBLASTS IN *DROSOPHILA*

BY

ALOKANANDA RAY

DISSERTATION

Submitted in partial fulfillment of the requirements
for the degree of Doctor of Philosophy in Cell and Developmental Biology
in the Graduate College of the
University of Illinois Urbana-Champaign, 2022

Urbana, Illinois

Doctoral Committee:

Assistant Professor Xin Li, Chair and Director of Research
Professor Jie Chen
Associate Professor Rachel Smith-Bolton
Associate Professor Lori Raetzman

ABSTRACT

The generation of various neurons, each with specialized functional roles, from a small initial pool of neural stem cells presents a challenge for developing brains in higher animals. Temporal patterning, whereby neural stem cells specify distinct fates in their progeny in a birth-order dependent manner, is a crucial mechanism for achieving neural diversity and is conserved across species from fruit flies to mammals. However, detailed molecular mechanisms underlying temporal patterning are not entirely understood. In the work described in the following chapters, I have characterized the regulatory mechanisms controlling the expression of temporal patterning transcription factors Sloppy-paired 1 (Slp1) and Sloppy-paired 2 (Slp2) in optic lobe medulla neuroblasts in the model organism *Drosophila melanogaster*. I have demonstrated that at transcription, Slp1 and Slp2 are regulated by at least two *cis*-regulatory elements that function additively and drive expressions of these two genes in the pattern observed in medulla neuroblasts. I also showed that the Notch signaling pathway and the cell cycle contribute to the regulation of Slp1 and Slp2 protein expressions in this context. Together these results provide greater insight into how disparate cellular processes such as the cell cycle and signaling pathways such as Notch and temporal patterning interact to achieve precise developmental outcomes.

ACKNOWLEDGMENTS

I want to express my sincere gratitude to my research advisor Dr. Xin Li for her support. Her generosity with time and resources and providing professional opportunities have been critical to my development as an independent thinker and fledgling scientist. I hope I will find mentors like her to support my career in the future. My sincere thanks to my thesis committee members, Dr. Jie Chen, Dr. Rachel Smith-Bolton, and Dr. Lori Raetzman. Their insights and feedback have been central to giving my project structure. I am grateful and fortunate to have found such good mentors in them. I also thank members of the Li lab, Dr. Yu Zhang and Hailun Zhu, for having been wonderful friends and colleagues and for sitting through several presentations and providing feedback on them. I have been fortunate to have made many great friends during my time in graduate school. Their support and friendship have been critical in helping me through the joys and sorrows of life in the lab. Last but not least, I would like to thank my family for their love, encouragement, and putting up with a very pre-occupied me during these years. Thank you all.

TABLE OF CONTENTS

Chapter 1: A general introduction

A key question in developmental biology is how a small pool of progenitor cells undifferentiated from one another in terms of gene expression generates the final form of multicellular organisms in all their complexity. This question has inspired research over many decades. It has led to the description of developmental patterning programs- where progenitor cells proliferate and become increasingly differentiated from one another over time due to their expression of different lineage-defining transcription factors. This change is accompanied by a restriction of the cell types into which the progenitor may differentiate. Patterning begins early on and results in the formation of the commonly observed germ layers of eumetazoans. The appearance of more specialized tissues and cell types in higher animals calls for additional patterning programs that are at work until most progenitors have terminally differentiated. Molecular details of how patterning programs are regulated remain incompletely understood.

Work detailed in my thesis has been carried out with the hope of contributing a tiny bit toward understanding mechanisms regulating one such patterning program responsible for generating a very diverse population of neurons in the fruit-fly brain. Since patterning mechanisms are often conserved from flies to mammals, this research may help understand similar processes in mammals.

Temporal patterning of neural progenitors

The specific patterning mechanism that lies at the heart of my work is what is known as temporal patterning and is briefly discussed in this section. Subsequently, I review the literature relating to temporal patterning to provide a contextual backdrop for my studies.

Temporal patterning refers to the generation of differentiated progeny with distinct identities that differ based on the time of their birth (Pearson and Doe 2004, Kohwi and Doe 2013) (Figure 1.1). These cues may either be progenitor cell-intrinsic or environmental signals that impact progenitor gene expression and, ultimately, the identity of its progeny. Most temporal patterning events studied to date are driven by progenitor cell-intrinsic mechanisms. One may conceptualize the idea of cell-intrinsically driven temporal patterning as follows: a parent precursor cell expresses distinct transcription factors over separate developmental windows throughout its life controlled by internal factors such as cellular age, the presence of epigenetic modifications, etc.; as the same progenitor cell divides at each of these different stages of its life, these (different) transcription factors are transmitted to its progeny; inheritance of the temporal identity-defining factor (in this case the transcription factor) confers a unique identity on the progeny based on its time of birth. However, we will also encounter examples where an external temporal cue, such as a developmental stage-specific surge in hormone signaling, can impact the identities of progeny fates by affecting the progenitor. Temporal patterning as a differentiation program is particularly relevant to generating cell-type diversity typical of nervous systems.

Studies of temporal patterning in *Drosophila*

Pioneering studies in the embryonic neuroblasts of the ventral nerve cord (VNC) helped identify the first set of temporal transcription factors in *Drosophila*. In the developing VNC of the fly embryo, there are 30 neuroblasts per hemi-segment which have long been known to generate unique neuron types and glial cells in the embryonic central nervous system (CNS) (Hartenstein V. 1994, Broadus 1995). Earlier in development, these neuroblasts line the ventral surface. As they undergo asymmetric cell divisions, early-born neurons are differentiated closer to the ventral surface. In contrast, late-born neurons are 'stacked' on top, reaching 'up' toward the dorsal surface (Hartenstein V. 1994), thus resulting in a laminar arrangement of neurons reflecting their birth order. The subsequent positions of dividing neuroblasts and their neuronal progenies are predictable and constant with minimal migration, enabling the identification of these cells by row and column coordinates (for instance, NB7-1 refers to a neuroblast at row 7 and column 1) (Hartenstein V. 1994). These factors uniquely enable tracing the lineage of VNC neurons to their parent neuroblasts to re-construct their developmental histories. The transcription factors Hunchback (Hb, a fly TF of the Ikaros family), Pdm2 and Nubbin (POU domain-containing TFs), and Castor (Cas- a zinc finger family TF homologous to the Casz1 family of mammalian TFs) were first identified because of their laminar expression in the mature fly CNS (Kambadur 1998). Following these earlier observational studies, their function in determining neuron fates was reported soon after, as Hb was seen to be necessary and sufficient for specifying early-born neuron identities in multiple embryonic VNC neuroblast lineages such as NB7-1, NB7-3, and NB3-1(Isshiki 2001, Novotny 2002, Kanai, Okabe et al. 2005, Cleary and Doe 2006, Tran and Doe 2008). Subsequently, it was shown that

most embryonic VNC neuroblasts expressed five transcription factors sequentially over their dividing lives and gave rise to different neuron types over each of these temporal windows marked by the expression of each TF. These TFs expressed in order from young to old are Hb, Kruppel (Kr- a zinc finger TF), Pdm2/ Nubbin, Cas and Grainyhead (Grh- a CP2 domain containing TF) (Doe 2017).

These studies also highlighted another critical phenomenon accompanying temporal patterning- irreversible changes in progenitor competence to respond to environmental or cell-intrinsic cues with age, formally termed competence restriction. In the NB7-1 lineage of the embryonic VNC, the first temporal factor Hb usually specifies the U1 and U2 neuron fates(Bossing 1996, Schmidt 1997, Schmid 1999). If Hb is ectopically expressed later, it can specify additional U1 and U2 neurons, provided it is expressed before the fifth neuroblast division (Pearson and Doe 2007). Before the fifth division, despite being transcriptionally inactive, the *hb* locus is poised to be ectopically activated (Kohwi, Lupton et al. 2013). After the fifth division, the *hb* locus is relocated to the periphery of the nuclear lamina by its association with proteins Distal antenna and Distal antenna related (Dan/Danr), both members of the CENP-B/transposase protein family, thereby silencing its transcription (Kohwi, Hiebert et al. 2011, Kohwi, Lupton et al. 2013). If this intranuclear movement is inhibited, the Hb competence window is extended (Kohwi, Lupton et al. 2013). Competence restriction is regulated separately from temporal fate specification, although these two phenomena co-occur (Kohwi and Doe 2013).

Since the publication of reports on temporal patterning of embryonic VNC neuroblasts, similar patterning processes have been documented in several other neuroblast types in the fly- such as other embryonic neuroblasts of the central brain (CB) and the mushroom body (MB) (Ito, Masuda et al. 2013, Yu, Awasaki et al. 2013, Awasaki, Kao et al. 2014, Liu 2015, Ren, Yang et al. 2017) and post-embryonic larval neuroblasts of the optic lobe medulla (Li, Erclik et al. 2013, Bertet, Li et al. 2014).

Since challenges of specifying distinct progeny fates increase proportionally to the number of cells born from neuroblasts, temporal patterning programs' complexity also increases in neuroblasts that form more transit-amplifying intermediate progenitor cells. Neuroblasts exhibit three main modes of asymmetric divisions classified as Type 0, Type I, and Type II based on differences in the identity of progeny formed at each neuroblast division (Figure 1.2 adapted from (Doe, 2017)). A Type 0 division of a neuroblast generates one differentiated progeny neuron. These neuroblasts are relatively rare, seen in late embryonic VNC neuroblasts (Baumgardt, Karlsson et al. 2014) and medulla tips of the optic lobe (Bertet, Li et al. 2014). Type I division is the most common mode of division seen in most embryonic VNC neuroblasts (including CNS neuroblasts where the pioneering observations detailed earlier were made), most CB neuroblasts, and all medulla neuroblasts (Li, Erclik et al. 2013, Doe 2017). Type I neuroblasts divide into a daughter neuroblast and a daughter ganglion mother cell (GMC). The GMC, in turn, divides once to produce two daughter neurons. Type II neuroblasts have by far the most complicated developmental programs, and this division mode is seen in six dorsal medial (DM1-6) and two dorsal lateral (DL1-2) neuroblasts of the CB (Bello, Izergina et al. 2008,

Boone 2008, Bowman, Rolland et al. 2008). In this mode, neuroblasts divide into a daughter neuroblast and an intermediate progenitor cell (INP). The intermediate progenitors undergo between 4 to 6 self-renewing divisions forming a GMC and a daughter INP at each division until their exit from the cell cycle, therefore acting much like Type I neuroblasts. Type II divisions are capable of additional diversity beyond what is achievable with Type I divisions alone. Progenies of Type II neuroblasts DM2-6 in the fly central brain are patterned by two independent programs of temporal patterning, one based on the age of its parent type II neuroblast and the other based on the age of the INPs (Bayraktar and Doe 2013). Intermediate progenitors in this system, in effect, act as Type I neuroblasts expressing transcription factors Dichaete (D), Grainyhead (Grh), and Eyeless (Ey) in that order as they age.

In the fly central brain Type I neuroblasts, two RNA-binding proteins rather than transcription factors function as temporal patterning factors. These are IGF-II mRNA binding protein (Imp) and Syncrip (Syp) (Liu 2015, Ren, Yang et al. 2017). These two proteins are expressed in a complementary, nearly mutually exclusive gradient in CB neuroblasts, with Imp expression being highest in the youngest neuroblasts and gradually diminishing as neuroblasts age and Syp being expressed in gradually increased concentrations peaking in the oldest neuroblasts. In MB neuroblasts, Imp is required to differentiate early-born CB γ neurons and Syp for the late-born αβ neurons with the loss of each protein, abolishing its progeny neuron fate (Ren, Yang et al. 2017). A class of neurons born at an intermediate stage and named the α'β' neurons require lower concentrations of both Imp and Syp to be specified. Imp and Syp expression affect the

expression of other temporal patterning factors downstream. In MB neuroblasts Imp activates the expression of the transcription factor Chronologically inappropriate morphogenesis (Chinmo); here, Chinmo acts as a temporal patterning factor (Maurange, Cheng et al. 2008, Ren, Yang et al. 2017) and is required for γ neuron specification (Zhu, Lin et al. 2006). Chinmo translation is inhibited in older neuroblasts by let-7 miRNAs preventing specification of early-born fate in late-born neurons (Chawla and Sokol 2012, Liu 2015). In optic lobe medulla Type I neuroblasts, a cascade of temporal transcription factors has been reported (Li, Erclik et al. 2013, Bertet, Li et al. 2014). Due to their importance to the present work, temporal patterning in medulla neuroblasts is considered in detail separately.

Mechanisms of temporal patterning factor regulation in *Drosophila*

What regulates the precise expression of successive temporal patterning factors and the fixed duration of their expression? Studies in embryonic VNC Type I neuroblasts that consecutively express Hb, Kr, Pdm, Cas, and Grh show that some late temporal transcription factors can inhibit those expressed earlier (feedback inhibition). For instance, Pdm inhibits Kr in some but not all lineages (Grosskortenhaus, Pearson et al. 2005), Cas inhibits Pdm (Kambadur 1998, Grosskortenhaus, Pearson et al. 2005, Tran and Doe 2008) and Grh inhibits Cas (Baumgardt, Karlsson et al. 2009). However, factors required for activation of Hb are unknown (Kohwi and Doe 2013, Doe 2017), leading to a model where general activation and repression by the subsequent temporal patterning factors sustains this temporal cascade (Doe 2017). Interestingly, the VNC temporal cascade can be sustained in primary neuroblast-derived cell cultures *in vitro*, indicating

that the activation and maintenance of temporal patterning in this system are mediated by cell-intrinsic cues (Grosskortenhaus, Pearson et al. 2005). A class of factors known as switching factors is required in some systems to ensure that temporal patterning factors are expressed over a fixed duration (Doe 2017). Switching factors differ from temporal patterning factors in that they time the expression of temporal patterning factors but do not specify progeny fates (Kohwi and Doe 2013). Representative of this group is Seven-up (Svp) which is required to inhibit Hb expression beyond its temporal window in embryonic VNC neuroblasts (Kanai, Okabe et al. 2005, Tran and Doe 2008, Benito-Sipos, Ulvklo et al. 2011). In the same neuroblasts, Svp acts a second time to switch off the expression of Cas later in the cascade (Stratmann, Gabilondo et al. 2016).

However, prominent examples exist where progenitor extrinsic factors provide temporal cues determining progeny fates. Type II neuroblasts of the CB have been shown to express Ecdysone receptor B1 (EcRB1) 56 hours ALH (After Larva Hatching). Ecdysone signal transduced via the EcRB1 is required to express successive temporal patterning factors in these neuroblasts (Syed, Mark et al. 2017).

Early studies examining underlying mechanisms of temporal patterning in Type I embryonic VNC neuroblasts showed that the Hb temporal sequence was regulated at transcription (Grosskortenhaus, Pearson et al. 2005). However, regulation of temporal patterning by post-transcriptionally active factors has also been reported, making generalization difficult. For instance, in Type I MB neuroblasts, regulation of Chinmo

expression in late-stage neuroblasts is achieved by let-7 miRNA-dependent inhibition of Chinmo translation (Chawla and Sokol 2012, Liu 2015, Ren, Yang et al. 2017).

Temporal patterning in mammalian systems

Given the ubiquity of temporal patterning in specifying neuron fates in the fly CNS, is this mechanism conserved across species, and does it operate in mammals? Indeed, this seems to be the case, though specific details in temporal patterning mechanisms between these systems very likely differ. Three examples of neurogenic and gliogenic processes in mammals that show evidence of temporal patterning are discussed here, though it is likely that other examples exist.

Patterning of mammalian retinal progenitors

In vivo lineage tracing indicates that mammalian retinal progenitors give rise to distinct cell types in a characteristic order. Transcriptomic analyses of single retinal progenitor cells isolated at different times in development indicate that mammalian retinal progenitors express distinct transcription factors at different stages of development going through the expression of mouse orthologs of Hb, Kr, Pdm1/2, and Cas, thus bearing a striking resemblance to the pattern of TTF expression observed in fly ventral CNS (Elliott, Jolicoeur et al. 2008, Greig, Woodworth et al. 2013, Doe 2017). However, lineage analyses of single cells show that mammalian retinal progenitors exhibit significant variation in differentiation trajectories between cells (Trimarchi, Stadler et al. 2008). Even cells initially derived from clonal cultures diverge in development, with some choosing to

self-renewal and others to differentiation (Gomes, Zhang et al. 2011). The decision to either self-renew or differentiate is made stochastically. The basis of this variability in gene expression, including the expression of temporal patterning-related genes, is not well understood and presents a promising area for future research.

Patterning of the mammalian cortex

Like the embryonic fly CNS the mammalian cortex exhibits a laminar organization. Precursors of the cortical neurons arise from the ventricular and subventricular zones of the developing mouse brain. The first cortical neurons are born at the E11.5 stage of mouse development. These localize to the deeper layers of the cortex. Subsequently, waves of neurogenesis differentiate cortical neurons of the upper cortical layers (Molyneaux, Arlotta et al. 2007). Precursor cells called radial glia and the earliest born deep layer neuron express Pax6 and Foxg1 related to the fly genes Ey and Slp1/2, respectively (Hanashima 2004, Muzio and Mallamaci 2005, Elliott, Jolicoeur et al. 2008). The expression of Pax6 and Foxg1 in early-born cortical neurons in mice is reminiscent of the temporal cascade observed in optic lobe neuroblasts of fly larvae where Ey and Slp1/2 are expressed sequentially. However, lineage-tracing studies in the mammalian cortex have hinted at precursors being committed to late-born neuron fates (superficial upper layer neurons) at very early stages in development (Zimmer, Tiveron et al. 2004, Molyneaux, Arlotta et al. 2007). Further fate-mapping studies will be needed to resolve whether these precursors undergo sequential expression of patterning transcription factors before committing to a particular neuron fate.

The switch from neurogenesis to gliogenesis

As in flies, mammalian neural progenitors switch to gliogenesis at the end of neurogenic programs. Two transcription factors that mark this shift in neural progenitors from generating neurons to glia are COUP-TF1 and COUP-TF2 (Faedo, Tomassy et al. 2008, Naka, Nakamura et al. 2008), both orthologs of the fly Svp (Doe 2017). COUP-TF1 is required to enable the switch from generating neurons with an early-born identity to those with late-born identities. Additionally, COUP-TF1 also controls the transition from neurogenesis to gliogenesis. These roles of COUP-TF1 and 2 are comparable to the reported roles of Svp in promoting the generation of 'late-born' Kruppel expressing neurons in the fly embryonic ventral nerve cord and enabling the switch from expression of Cas to Grh, thereby marking the end of a neurogenic differentiation program.

The role of temporal patterning in restricting tumorigenic potential

Two studies in temporally patterned *Drosophila* neuroblasts have suggested that besides its central role in generating diversity of neuron types, a less appreciated but important consequence of temporal patterning is restricting the tumorigenic potential of neural progenitors (Narbonne-Reveau, Lanet, et al. 2016, Farnsworth, Bayratkar, et al. 2015). Typically fly neuroblasts segregate mRNAs of the transcription factor Prospero (Pros) in their ganglion mother cell progenies at the end of each asymmetric division (Knoblich 2008). Prospero regulates cell division and instructs ganglion mother cells to undergo one terminal division to two neurons. In a subset of early embryonic ventral nerve cord neuroblasts, loss of Prospero in younger neuroblasts results in aggressive malignant

tumors due to excessive division (Narbonne-Reveau, Lanet et al. 2016). Loss of Prospero in older neuroblasts of the same lineage had relatively modest effects, with smaller, fewer tumors formed. Prolonged induction of an early-born neuroblast identity by losing the switching factor Svp transformed older neuroblasts into aggressive tumor formers (Narbonne-Reveau, Lanet et al. 2016). In a separate study of intermediate progenitors born from Type II neuroblasts, more aged intermediate progenitors expressing the temporal transcription factor Ey were less susceptible to Notch induced tumorigenic proliferation. Young intermediate progenitors before the Ey expression stage formed tumors on ectopic expression of Notch, whereas Notch overexpression in Ey stage intermediate progenitors had no effect (Farnsworth, Bayraktar et al. 2015). The finding that prolonged expression of early temporal transcription factors increases the neuroblasts' susceptibility to proliferative signals indicates that dissecting mechanistic underpinnings of temporal patterning cascades may also be relevant to cancer research.

Connections between the cell cycle to temporal patterning in flies and mammals

Temporally patterned neuroblasts undergo a pre-programmed number of cell divisions simultaneously as they express patterning transcription factors. Given that these processes co-occur in the same cell and both show exquisite temporal regulation, investigators have long questioned whether the duration of the cell cycle serves as an intrinsic timer determining how long a temporal patterning factor is expressed and when its expression is to be terminated (Grosskortenhaus, Pearson et al. 2005, Okamoto, Miyata et al. 2016). Early studies in Drosophila embryonic VNC neuroblasts uncovered a requirement for cytokinesis in enabling the Hb to Kr transition (Grosskortenhaus, Pearson

et al. 2005); in these neuroblasts, the mRNA of switching factor Svp was exported outside of the nucleus for translation in a cytokinesis dependent manner (Mettler, Vogler et al. 2006). Studies in mammalian cortical progenitors have explored the possible connection between cell division and laminar fate specification (Okamoto, Miyata et al. 2016, Kawaguchi 2019). Transient cell cycle arrest in undifferentiated cortical progenitors induced by inhibiting Cdk9 while supplying Notch ectopically neither impaired laminar fate specification nor expression of temporal patterning genes in mice (Okamoto, Miyata et al. 2016). Most of this evidence points toward a poorly understood cell-intrinsic mechanism timing temporal transcription factor expression in flies and mammals.

An alternative model postulates that the length of the cell cycle, especially the G1 phase in cycling progenitors, may drive differentiation and temporal patterning since lengthening the cell cycle leads to premature neuronal differentiation in the mammalian cortex and the *Xenopus laevis* retina (Calegari and Huttner 2003, Decembrini 2009, Kawaguchi 2019). According to this model, critical fate specifying determinants such as microRNAs involved in temporal fate specification may accumulate at only certain cell cycle phases, such as the G1-S. Hence the length of these phases will determine whether these signals accumulate to functionally relevant concentrations (Calegari and Huttner 2003, Decembrini 2009). However, this model has not been rigorously verified, and the observed correlations between cell cycle length and differentiation may be functionally unrelated and inconsequential. Co-regulation of temporal patterning factors and genes regulating the cell cycle by mechanisms such as post-transcriptional adenine methylation

of their mRNAs may explain why cell cycle regulation and temporal patterning are so frequently seen as being associated (Yoon, Ringeling et al. 2017).

Temporal patterning in the fly larval optic lobe

To fully appreciate the extent to which temporal patterning of the optic lobe medulla generates neuron diversity, it is helpful to consider the anatomy of the adult medulla and its cell type diversity and examine how it originates. In the following section, I provide a primer on optic lobe development from the larval stages into adulthood. I also touch on some considerations that make the larval optic lobe medulla a remarkable parallel to mammalian cortical development, further strengthening this system's importance in understanding neuron diversity in mammalian brains.

The adult visual system of *Drosophila* and the optic lobe medulla

The visual system of the adult *Drosophila melanogaster* has around 120000 neurons of about 110 subtypes (Hofbauer 1990). The *Drosophila* compound eye is formed by 800 independent visual units called ommatidia. Each ommatidium transduces visual stimuli from a specific point in space, constituting a grid of 800 'pixels' in the fly's visual field (Kumar 2012). Within ommatidia, specialized neurons called photoreceptors containing light-sensitive rhodopsin proteins detect visual stimuli and transmit them onto structures called the optic lobes for further sensory processing (Behnia and Desplan 2015, Borst and Helmstaedter 2015, Neriec and Desplan 2016).

The optic lobe contains about 60% of the adult fly brain's neurons organized in sub-structures called neuropils (Fischbach 1989). The four neuropils that constitute each optic lobe listed from distal to proximal are the lamina (the most superficial part of the optic lobe lying just beneath the retina), the medulla, the lobula, and the lobula plate (located closest to the central brain). Each neuropil has a columnar organization. The columns in each neuropil number about 800 correspond to roughly one for each ommatidium in the compound eye, thus achieving a near-perfect representation of the visual field (Fischbach 1989, Meinertzhagen 2001, Morante and Desplan 2008). Neurons in each neuropil have specialized functions in visual signal processing, as inferred from adaptive learning experiments in flies. Laminar neurons carry out computations related to motion detection (Douglass 1995, Morante and Desplan 2008). Medullar neurons process motion detection and color vision (Morante and Desplan 2008). Lobular neurons perceive colors and detect features and ultimately relay all processed visual information from the optic lobes to higher visual processing centers in the central brain (Morante 2008, Behnia and Desplan 2015). Neurons in each neuropil are further sub-divided into categories based on their morphologies and which layer they project within a neuropil

The medulla has the largest and most complex organization of all optic lobe neuropils. The medulla alone has 40000 neurons comprising >80 subtypes which project to 10 different layers described (from distal to proximal) as layers M1 to M10. Medullar neurons are organized in repetitive columnar units across these layers. Uni-columnar medulla neurons arborize in a single medullar column and process visual information from a single

point in space. Multi-columnar medulla neurons send projections to multiple medullar columns and integrate information gathered from a wider expanse of the receptive field (Fischbach 1989, Morante 2008, Takemura, Lu et al. 2008). The nomenclature of medullar neurons considers their sites of origin and termination and their shapes. Neurons termed medullar intrinsic neurons (Mi) are interneurons whose cell bodies and processes are fully contained within the medulla. Neurons whose cell bodies or processes span the medulla and onto structures outside it are called transmedullary (Tm) neurons. Transmedullary neurons with a bifurcated Y-shaped morphology are categorized as transmedullary Y (TmY).

Development of the fly optic lobes at embryonic and larval stages

Pioneering anatomical studies undertaken over three decades have characterized the early stages of optic lobe development at great length (Hofbauer 1990, Green 1993, Urbach and Technau 2003).

The optic lobe develops from a plate of tightly packed epithelial cells called the optic placode at the Campos-Ortega/Hartenstein stage 11 in the Drosophila embryo (Hartenstein 1984). By stages 12 and 13, the optic placode constricts and invaginates to form the optic lobe primordium (OLP) and remains mitotically quiescent until the end of embryonic development. After larval hatching, cells of the OLP resume proliferation and subdivide into two different primordial clusters- the outer proliferation center OPC (also referred to as the outer optic anlage OAA) and the inner proliferation cluster IPC (also

inner optic anlage IOA) (White 1978, Hofbauer 1990). At the first larval instar, these proliferative clusters adopt a crescent shape and are positioned perpendicularly (Nassif, Noveen et al. 2003). The OPC and IPC are still connected at the second instar stage but are soon pushed apart by a group of cells delaminating from the IPC into a space between the IPC and the OPC. These migratory cells form a separate proliferative center called the distant IPC (dIPC) (Nassif, Noveen et al. 2003, Neriec and Desplan 2016).

Earlier divisions (during the 1st and 2nd instar stages) of neuroepithelial cells in the OPC and IPC are mitotic and symmetrical. However, by the third instar larval stage, both OPC and IPC start dividing asymmetrically to form optic lobe neurons; divisions of the OPC neuroblasts at the medial edge generate the medullar neurons. Divisions of the IPC neuroblasts form neurons of the lobula and lobular plate (Meinertzhagen 1993). The OPC also generates the laminar neurons from its distal edge (separated at this stage from the medial edge by a laminar furrow), whereby symmetrically dividing neuroepithelial cells of the OPC differentiate into neurons following a terminal cell division without undergoing an intermediary conversion to neuroblasts (Selleck 1991, Huang 1996, Nassif, Noveen et al. 2003). Secretions of Hedgehog (Hh) and the epidermal growth factor receptor ligand Spitz (Spi) by photoreceptor axons facilitate the terminal differentiation of OPC neuroepithelia to laminar neurons (Huang 1998).

Medulla neuroblasts are born from the medial edge of the OPC neuroepithelium. Several morphogenetic changes precede the formation of medulla neuroblasts from the OPC

neuroepithelium. OPC neuroepithelial cells at the medial edge first lose their adherens junctions and assume an ellipsoid shape but do not delaminate from the epithelium (Meinertzhagen 1993). They also undergo a cell cycle arrest mediated by changes in expression of cell cycle regulators E2F1 and CycD and by Fat-Hippo signaling (Reddy, Rauskolb et al. 2010). An activation event mediated by Notch-Delta signaling (Egger, Boone et al. 2007) then transforms the mode of division of these OPC medial-edge cells from symmetric to asymmetric, thus forming the first self-renewing medulla neuroblasts. The plane of the cell-division spindle in these new-formed neuroblasts then rotates relative to the original division plane within the OPC. As a result, neurons of the medulla are differentiated from these neuroblasts in a dorsal to ventral direction perpendicular to the plane of the OPC neuroepithelium (which is in the plane of the posterior to the anterior axis). Simultaneously an ordered activation of the proneural gene lethal of scute (l'sc) by EGFR (Yasugi, Umetsu et al. 2008, Yasugi, Sugie et al. 2010) takes place at the outermost cells of the OPC's medial edge and advances along the medial to the lateral axis, converting neuroepithelial cells to neuroblasts in its wake (Yasugi, Umetsu et al. 2008). Premature conversion of neuroepithelia to neuroblasts by l'sc is averted by active JAK/STAT signaling (Ngo, Wang et al. 2010, Yasugi, Sugie et al. 2010). Thus, the concerted action of Notch-Delta and the EGFR pathways rapidly shrinks the expanse of the OPC neuroepithelium. By the P+24% stage, the OPC neuroepithelium has been obliterated (Meinentzhagen 1993). The establishment of neuroblast identity is associated with the expression of typical medulla neuroblast markers – *Enhancer of split E(spl)* family proteins Deadpan (Dpn) and Asense (Ase).

The development of the optic lobe in fly larvae bears close similarities with the development of the mammalian cortex. Like the neuroepithelium of the optic lobe OPC, the mammalian cortex originates from a sheet of neuroepithelial cells that initially divide symmetrically, thereby greatly expanding the available pool of progenitors (Morrison and Kimble 2006, Farkas and Huttner 2008). Also, like optic lobe neuroepithelial cells that eventually form asymmetrically dividing neuroblasts, mammalian cortical progenitors change their mode of division from symmetric to asymmetric. However, the regulatory steps causing this change are not well understood (Molyneaux, Arlotta et al. 2007). These parallels between the developmental origins of the fly medulla neuroblasts and the mammalian cortical progenitors suggest that the larval optic lobe may be a critical model that can inform studies of mammalian cortical neurogenesis.

The question of neural diversity generation in the medulla

Though considerable advances had been made in studying the anatomical developments in the fly optic lobe, these early studies were unsuccessful at identifying the qualitative differences in neurons of the medulla except by their morphological distinctions, mainly due to a lack of known genetic markers and genetic tools for lineage tracing available at the time. Increasing knowledge of molecular markers of neurons and the advent of high throughput genomic technologies have deepened our understanding of molecular bases of neuron diversity generation.

Three primary mechanisms have been identified to contribute to the neuron diversity in the medulla. These are

1. Spatial patterning (fate specification based on spatial location within a tissue) - The neuroepithelial crescent of the OPC is divided by three prominent spatial domains expressing the transcription factors dVsx1 at the crescent center (Erclik, Hartenstein et al. 2008), Optix (Gold 2014) and Rx at the two tips of the crescent (Chen, Del Valle Rodriguez et al. 2016). The domain expressing Rx is further subdivided into regions expressing decapentaplegic (dpp) and wingless (wg) (Kaphingst 1994). Additionally, the OPC is divided along the dorsal-ventral axis by Hedgehog (Hh) (Evans, Olson et al. 2009, Chen, Del Valle Rodriguez et al. 2016). Together this divides the OPC in 8 spatial domains demarcated by expression of distinctive patterning transcription factors and signaling molecules (Erclik, Li et al. 2017).
2. Temporal patterning (fate specification based on time of birth) – Neuroblasts born from the OPC regions marked by dpp/rx, dVsx1, and Optix spatial TFs express a series of transcription factors over their lifetime, transitioning through each subsequent TF as they mature (Li, Erclik et al. 2013, Suzuki, Kaido et al. 2013). These transcription factors expressed by medulla neuroblasts from the time they are converted until they exit the cell cycle and terminally differentiate are (in the same order) Homothorax, Eyeless (Ey), Slp1 and 2 (Sloppy-paired 1 and 2), Dichaete (D) and Tailless (Tll). These transcription factors are inherited and determine the fates of their neuronal progeny. The expression of specific temporal genes correlates with downstream neuronal genes such as Bsh, Toy, Runt, Dfr,

and Dll (Li, Erclik et al. 2013). Together or in combination (as there are slight overlaps between consecutive TTFs in neuroblasts), these temporal patterning factors account for at least twelve different neuron types. Reciprocal interactions exist between successive temporal patterning factors from Ey onward in the medulla. Here Ey is required for activation of Slp, and Slp represses Ey. Similar interactions hold good between Slp and the next temporal factor, D, establishing Ey, Slp, and D as bonafide temporal patterning factors (Li, Erclik et al. 2013). However, like in the embryonic VNC neuroblasts, factors initiating expression of Hth (the first patterning factor of the medulla temporal sequence) are yet unknown, as are the factors that down-regulate it (Li, Erclik et al. 2013, Doe 2017). Since it is also unknown if this cascade can be sustained in cultured cells, it is not clear if maintenance of the medulla temporal cascade needs any external signals. Recent studies have expanded this network of temporal patterning factors in the optic lobe to include additional factors (Konstantinides, 2021, Zhu, 2022) (Figure 1.3).

3. Notch-dependent binary fate choice- The terminal cell division of GMCs born of medulla neuroblasts also partitions some cell fate determinants asymmetrically between daughter neurons. As a consequence, one of the daughter neurons born from the GMC division expresses Notch (depicted as Notch ON), and the other lacks Notch expression (Notch-OFF) (Li, Erclik et al. 2013, Suzuki, Kaido et al. 2013). The binary state of Notch activation in the progeny neurons combined with their expression of genes induced by temporal TFs doubles the plausible variety of neurons in the medulla.

Together, these three mechanisms have accounted for 70 different neuron types in the medulla. Since other members of the temporal cascade remain to be discovered, these mechanisms may generate more neuron types than are currently known.

Outstanding questions about temporal patterning in fly medulla neuroblasts

Despite sharing a thematic commonality, details of temporal patterning vary between different systems, even within the same model organism. An excellent recent review has summarized unresolved questions concerning temporal patterning (Doe 2017). Here I limit my discussions to my system of interest, the *Drosophila* optic lobe medulla neuroblasts.

As mentioned earlier, three bonafide temporal transcription factors have been identified in medulla neuroblasts- these are Eyeless (Ey), Sloppy-paired1/2 (Slp1/2), and Dichaete (D). Ey is necessary for activation of Slp1/2 but is not sufficient in this role as ectopic expression of Ey in younger neuroblasts using an *inscuteable*- Gal4 driver that is expressed in all neuroblasts does not lead to Slp1/2 expression (Li, Erclik et al. 2013). The insufficiency of Ey at activating Slp1/2 expression indicates that other unidentified factors act in concert with Ey in initiating Slp1/2 expression. Also, the regulatory requirement of Ey for Slp activation was inferred from genetic experiments. Since a genetic interaction does not demonstrate if Ey acts to activate Slp1/2 expression at transcription, the precise mechanism of Slp1/2 regulation at the time of initial reporting was unknown.

Several other questions also remain about temporal patterning in this system. It is unknown what activates the expression of Hth, the earliest temporal patterning factor identified. Factors up-regulating Ey expression are also unknown, indicating that additional temporal patterning factors between Hth and Ey remain undiscovered. Another intriguing question is, how does the patterning of the outer proliferation center (the original neuroepithelium from which medulla neuroblasts are born) by the same set of spatial patterning transcription factors Vsx1, Optix, and Rx result in two different temporal cascades at the medulla 'proper' and the tips of the medulla crescent (Doe 2017). Although significant progress has been made to understand the consequences of integrating spatial and temporal patterning signals in this system (Erclik, Li et al. 2017), the molecular details that cause two different temporal sequences to originate from the same spatially patterned tissue are unclear.

The control of developmental gene expression by enhancers

Since a significant fraction of my doctoral work has focused on the regulation of the patterning genes Slp1/2 by transcriptional enhancers, I believe it will be helpful to introduce the reader to enhancers and prevailing ideas about their activation and function to understand the motivations of my experiments better.

Temporal patterning at its core is a differentiation program that sets in action an elaborate gene regulatory network. Several studies across various systems have demonstrated that

enhancers in progenitor cells undergoing differentiation are dynamic. Consistent with these observations, studies of temporal patterning in embryonic VNCs have shown that earliest born Hb expressing neural progeny born of neuroblasts NB7-1, NB7-3, and NB5-1 each maintain Hb expression via a discrete enhancer (Hirono, Margolis et al. 2012, Kohwi and Doe 2013). Enhancers are vital in establishing observed gene expression patterns during development; hence a lot of focus in developmental biology has rightly been directed at understanding enhancer function.

Core promoters of genes, while competent at assembling functional transcriptional complexes, lead to very weak transcription of their associated genes when acting alone. Their association with more distal regulatory elements called enhancers increases the output of gene transcription by several thousand-fold. Enhancers are segments of noncoding DNA that contain sequences recognized by transcription factors for site-specific binding. These transcription factors often recruit additional cofactors that activate or repress transcription from the associated gene. On binding their cognate transcription factors in response to extrinsic or intrinsic cues, enhancers modulate transcription of their target genes, integrating all incoming stimuli. Some enhancers often exhibit preferences for activating promoters with specific sequence features such as TATA boxes (Butler and Kadonaga 2001). Enhancers can influence transcription irrespective of their orientation relative to their target gene (Shlyueva, Stampfel et al. 2014). Distance between active enhancers and their targets exhibits wide variability. In *Drosophila*, most enhancers regulate genes in close physical proximity, with the median distance between enhancers and their targets being 10 kb (Kvon, Kazmar et al. 2014, Shlyueva, Stampfel et al. 2014).

Some enhancers, however, can activate more distant target genes while skipping one or even two intervening ones; the distant target may be as far away as 70 -100 kb (Levine 2010, Spitz and Furlong 2012, Shlyueva, Stampfel et al. 2014). Though enhancers are often referred to as *cis*-acting elements because they usually activate target genes located on the same DNA strand, enhancers may be able to act in *trans* and activate transcription from a target on a different DNA strand. This phenomenon, known as transvection (Lewis 1954, Fukaya and Levine 2017), is of particular importance to *Drosophila*, where autosomes remain paired together in interphase (Morris 1998), raising the likelihood of regulation by transvection.

In the last few decades, many studies have attempted to use new high-throughput technologies to glean insights into enhancer activation. The fact that enhancers are regulatory elements has complicated their identification. Several approaches have been used to identify enhancers in genomes based on their association with specific types of proteins or their co-occurrence with identifiable genomic features (Shlyueva, Stampfel et al. 2014). Prominent among these include attempts at identifying enhancers by their association with crucial patterning transcription factors, association with transcriptional co-activators, association with specific histone marks, and association with accessible regions of chromatin -each has yielded results with varying degrees of success. More recent approaches have tried to identify potential enhancers by mapping contact points between non-regulatory DNA regions and gene-promoters using variations of conformation capture assays (van Steensel and Dekker 2010, Li, Ruan et al. 2012). However, the most direct approach to testing enhancer function that exploits the modular

nature of enhancers involves reporter assays where putative enhancer elements are placed in proximity of a minimal promoter driving expression of a reporter gene (Shlyueva, Stampfel et al. 2014, Small and Arnosti 2020). Recent technical advancements have enabled the screening of potential enhancers in the *Drosophila* embryo in a high-throughput manner, demonstrating how reporter assays in combination with next-generation sequencing can identify thousands of latent enhancer elements (Arnold 2013, Kvon, Kazmar et al. 2014). Reporter assays remain the 'gold standard' of enhancer identification but are not without problems (Shlyueva, Stampfel et al. 2014, Small and Arnosti 2020). Traditionally *in vivo* reporter assays have required the insertion of transgenes at random sites within the genome. Variations in genomic context may significantly impact the strength of enhancer function and their spatiotemporal expression patterns (Kvon, Kazmar et al. 2014). Observing enhancers in their native genomic context using genome editing tools such as CRISPR/Cas9 will circumvent many of these issues (Shlyueva, Stampfel et al. 2014, Small and Arnosti 2020). With this hope, CRISPR/Cas9 based genome editing is used to interrogate enhancer function in studies summarized in this thesis.

Another commonly seen feature of transcription regulation by enhancers is that multiple enhancers may regulate the same gene. Enhancers located closest to the transcription start sites of their target genes are referred to as the primary enhancer. Those located farther away are called distal or 'shadow' enhancers (Spitz and Furlong 2012, Shlyueva, Stampfel et al. 2014) (the term shadow enhancers were initially used to describe an enhancer that regulated a distant target while being physically proximal to a different

gene; thus being present 'in the shadow' of the non-target gene (Barolo 2012)). Regulation by multiple enhancers is more common than initially thought. A study on mesoderm patterning genes in flies indicates that multiple enhancers regulate 64% of observed genes; some genes are regulated by as many as five enhancers (Cannavo, Khoueiry et al. 2016). Though one of these redundant enhancers can often be deleted with no phenotype, the same study concluded that shadow enhancers face as much selective constraint as non-redundant enhancers and are therefore not dispensable. The evolutionary significance of shadow enhancers is not entirely understood. Beyond ensuring the robustness of deterministic processes in development and buffering against environmental fluctuations (Frankel, Davis et al. 2010), multiple enhancers have also been suggested to contribute to gene expression in an additive manner, with transcription aided by multiple enhancers being necessary for achieving the critical threshold of active gene products (Ghiasvand, Rudolph et al. 2011, Lagha, Bothma et al. 2012).

The *sloppy-paired* locus in flies: previous studies on the regulation of *sloppy-paired* gene

Lastly, I would like to briefly introduce the genes whose activations I have investigated- Sloppy paired 1 and 2. First identified in a screen for lethal mutations in embryonic pattern formation (Nusslein-Volhard 1984), the Slp1 and Slp2 proteins were soon revealed to be crucial pair-rule genes acting in the segmentation of the *Drosophila* embryo (Grossniklaus 1992, Cadigan 1994, Prazak, Fujioka et al. 2010). The two genes encode related transcription factors that likely arose from a gene duplication event and are orthologous to the mammalian forkhead box transcription factors (Cadigan 1994). During *Drosophila*

embryo segmentation, Slp1/2 are expressed in multiple stripes regulated by different enhancers. These enhancers are activated by combinatorial site-specific transcription factor binding (Prazak, Fujioka et al. 2010). Early studies of Slp1 and Slp2 function in segmentation showed that they are biochemically equivalent and that the observed greater importance of Slp1 in segmentation was likely because of its earlier expression (Cadigan 1994). In the context of the optic lobe medulla neuroblasts, Slp1 and Slp2 act as temporal patterning genes (Li, Erclik et al. 2013), similar to the observation of a mammalian forkhead box-containing transcription factor Foxg1 specifying neural fates in cortical neurons (Hanashima 2004).

Conclusions

The discovery that optic lobe medulla neuroblasts in *Drosophila* are temporally patterned has opened exciting new opportunities to further our understanding of the mechanisms of neuron differentiation. A rich body of work about temporal patterning in flies and the novelty of this discovery creates a unique opportunity to utilize insights from previous studies to make discoveries in the current context. The conclusions we arrive at will complement what we have learned from other instances of temporal patterning. Additionally, the similarities between the developmental histories of the optic lobe medulla neuroblasts and mammalian cortical progenitors underscore the potential importance of our work in understanding far more complicated mammalian brain development. Together with the wealth of available resources for genetic manipulation in flies, these factors make this a promising study target and one with an enormous scope.

For my studies, I have identified enhancer elements driving the expression of the genes Slp1/2, two components of the medulla temporal cascade, to help identify regulators of Slp1/2 activation. By probing transcription factor binding to enhancers at critical points in development, I have tried to establish whether these regulators directly bind to slp1/2 enhancers. I have also tried to demonstrate how local system-specific regulators can interact with more pervasive developmental pathways such as Notch signaling to facilitate temporal patterning gene expression outcomes. Lastly, my work has uncovered that inducing cell cycle arrest in medulla neuroblasts leads to a halted temporal cascade. However, further work will be required to identify the basis of this phenotype. This work will add crucial insights to our knowledge of fly medulla neuroblasts' differentiation.

List of abbreviations used in text

CB- Central Brain

CNS- Central Nervous System

Chinmo- chronologically inappropriate morphogenesis

COUP-TF- Chicken Ovalbumin Upstream Promoter-Transcription Factor

Cas - Castor

CycD- Cyclin D

D- Dichaete

Dll- Distalless

Dpp- Decapentaplegic

dVsx1- drosophila Visual system homeobox 1

Ey- eyeless

EcRB1- Ecdysone Receptor B1

Foxg1- Forkhead box g1

G1/S- post-synthetic Gap1 / Synthetic phase

Grh- Grainyhead

GMC- Ganglion Mother Cell

Hth- Homothorax

Hh- Hedgehog

Hb- Hunchback

IPC- Inner Proliferation Centre

IP- Intermediate Progenitor

Imp- IGF-II mRNA binding protein

Kr- Kruppel

L'sc- lethal of scute

miRNA- micro RNA

mRNA- messenger RNA

MB- Mushroom body

N- Notch

NB- Neuroblast

OPC- Outer Proliferation center

Pros- Prospero

Pdm- POU domain protein (POU: Pituitary-specific 1 (Pit1), Octamer Transcription Factors (Oct) and Unccordinated-86 (Unc-86))

Rx- retinal homeobox

Slp1- Sloppy-paired 1

Slp2- Sloppy-paired 2

Spi- Spitz

Svp- Seven up

Syp- Syncrip

TF- Transcription Factor

TTF- Temporal patterning transcription factor

VNC- Ventral nerve cord

Wg- wingless

Figures

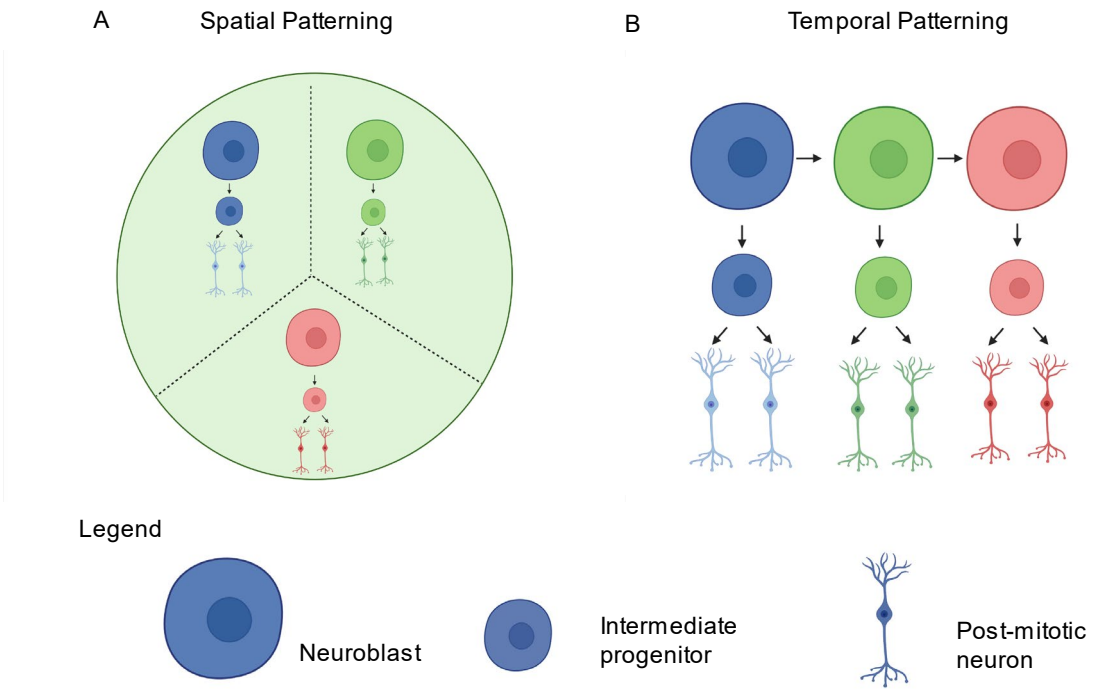

Figure 1.1 Spatial and temporal patterning are two central mechanisms for neural diversity generation in animals. A. A schematic illustrating the idea of spatial patterning. Neural stem cells are located at different spatial positions within the brain. A summation of morphogen gradients and other developmental signals diffusing inside the brain creates unique combinations of developmental signals at specific locations. Depending on their position, stem cells are subjected to a unique blend of developmental stimuli, and so they follow subtly different developmental trajectories. The difference in developmental signals received by a stem cell leading to heritable changes is indicated by different colors in the cartoon. B. A schematic illustrating temporal patterning. As neural stem cells divide

Figure 1.1 (cont.) asymmetrically, they produce intermediate progenitors that produce post-mitotic neurons and daughter stem cells which continue the cycle until their terminal differentiation. As the neural stem cell ages, the complement of transcription factors that it produces changes, leading to heritable differences in the subtype of progenies specified. The age-associated changes in the identity of a neural stem cell have been indicated by changes in its color in the schematic. Image created using BioRender.

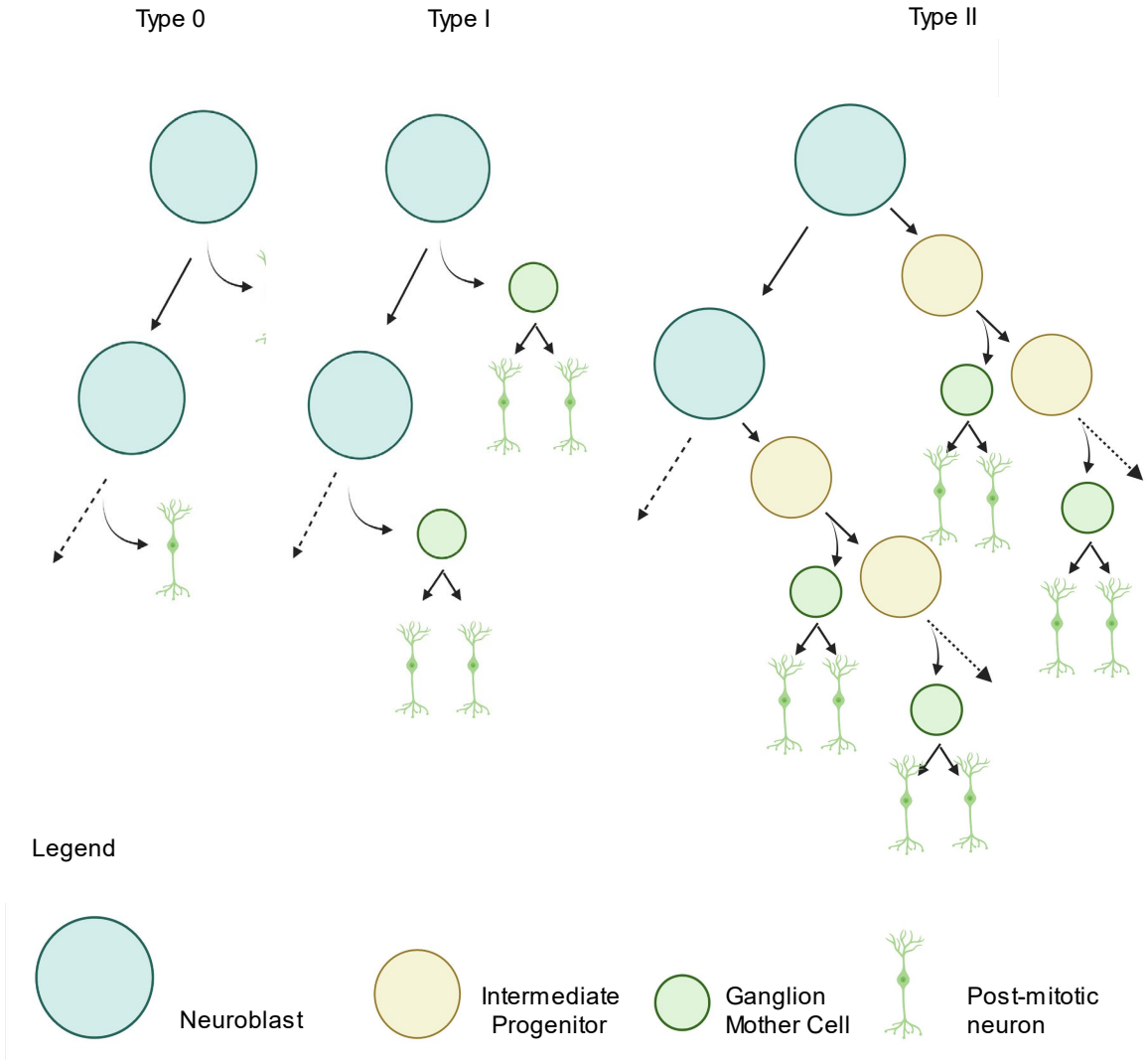

Figure 1.2 Neural stem cells exhibit three modes of cell division: Type 0, Type I, and Type II. In Type 0 division, asymmetric neural stem cell divisions produce a daughter stem cell and a post-mitotic daughter neuron (schematic to the left). Type I division of a neuroblast asymmetric divisions form a daughter neuroblast and an intermediate progenitor that divides once to produce two post-mitotic progeny neurons (schematic at the center). Intermediate progenitors born from neuroblasts undergoing Type I division are called Ganglion Mother Cells or GMCs.

Figure 1.2 (cont.) Type II neuroblast divisions (schematic to the right) result in a daughter neuroblast and a transit-amplifying intermediate progenitor that acts like a neuroblast with restricted potential. These intermediate progenitors of Type II neuroblasts divide a fixed number of times. They self-renew at each division, forming a daughter intermediate progenitor and a ganglion mother cell that divides once to produce two post-mitotic neurons. In all schematics, dotted lines indicate that the process repeats until the neuroblast, or the intermediate progenitor exits the cell cycle and terminally differentiates. Image created using BioRender.

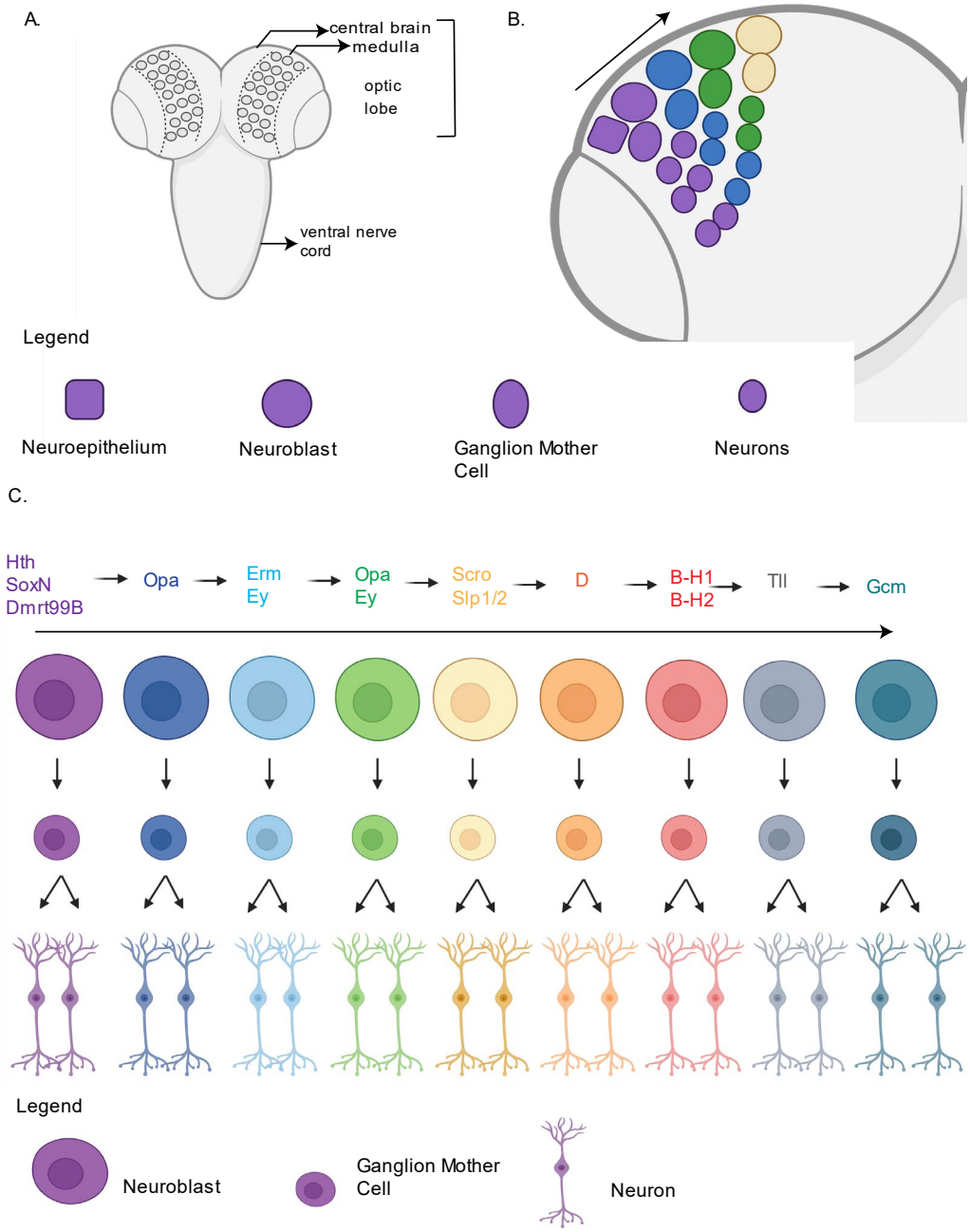

Figure 1.3 Temporal patterning contributes to neural diversity in the optic lobe medulla of *Drosophila melanogaster*. A. A cartoon showing the structure of the fly's central nervous system, which consists of the ventral nerve cord and two optic lobes. The optic lobe medulla (demarcated within dotted lines) has numerous superficial neuroblasts

Figure 1.3 (cont.) (indicated by small circles within the medulla). B. Cartoon of a section through the optic lobe medulla. In the medulla neuroepithelial cells (rectangle) are transformed into medulla neuroblasts (circles) following neurogenic signaling at the late second instar larval stage. Neuroepithelial cells closest to the central brain are converted first, and this wave of neurogenesis migrates outward from the central brain toward the periphery. As a result the earliest born neuroblasts are located close to the central brain with younger neuroblasts occupying more peripheral locations. An arrow indicates the progressively increasing age of the medulla neuroblasts. A thin layer of neuroepithelium persists closest to the youngest neuroblasts. Medulla neuroblasts undergo Type I divisions, forming a daughter neuroblast and a Ganglion Mother Cell (GMC; oval). GMCs divide in a plane perpendicular to the neuroblasts' plane of division and form two daughter neurons (small circle). The neurons are located deep within the brain. Medulla neuroblasts are temporally patterned, so the identity of neural progenies depends on the fate-specifying transcription factor it inherits from its parent neuroblast. In the diagram different colors represent a temporal patterning transcription factor. C. The sequence of temporal patterning transcription factors expressed in medulla neuroblasts. Complex interactions between the temporal patterning transcription factors maintain their activity at defined developmental stages and have been inferred through genetic experiments, but the simplified diagram above does not show these interactions. The arrowhead indicates the direction of increasing neuroblast age. Medulla neuroblasts begin by expressing the temporal factors at the left and go through stages of expression of each until they express the last transcription factor Gcm and get transformed into glial cells. Abbreviations used: Hth (Homothorax), SoxN (Sox Neuro), Dmrt99B (Doublesex- Mab

Figure 1.3 (cont.) related 99B), Opa (Odd-paired), Erm (Earmuff), Ey (Eyeless), Scro (Scarecrow), Slp1/2 (Sloppy-paired 1 and 2), D (Dichaete), B-H1/2 (Bar H1 and 2), Tll (Tailless), Gcm (Glial cells missing). Figure made using BioRender.

Chapter 2. Identification of enhancer elements and regulatory factors driving the transcription of *sloppy-paired* genes in medulla neuroblasts

Introduction

Temporal patterning in medulla neuroblasts constitutes the expression of successive patterning transcription factors in a pre-programmed birth-order dependent manner(Doe 2017). As they age, medulla neuroblasts express a series of transcription factors Homothorax (Hth), Eyeless (Ey), Sloppy-paired 1, and Sloppy-paired 2 (Slp1, Slp2), Dichaete (D), and Tailless (Tll) and then stop dividing and terminally differentiate into glial cells (Li, Erclik et al. 2013). Recent studies have further expanded this network of temporal-patterning transcription factors (TTFs) using insights from single-cell RNA sequencing (Konstantinides, Rossi et al. 2021, Zhu, Zhao et al. 2022). Since a sequential expression of transcription factors temporally patterns *Drosophila* neuroblasts, it is often assumed that transcription control is the predominant stage at which expression of TTFs is regulated. A study of temporal patterning Type I neuroblasts of the ventral nerve cord of *Drosophila* remains the only study to demonstrate that activation of temporal patterning factors is regulated at transcription and to have identified enhancers regulating TTF expression at various stages in development (Hirono, Margolis et al. 2012). However, no analogous study exists for medulla neuroblasts, and previous studies that reported the temporal patterning program in this system did not show direct transcriptional regulation.

TTFs may be regulated at either the transcriptional or post-transcriptional level, and the observed protein expression pattern is not necessarily the same as that of the mRNA transcripts. A case in point is the expression pattern of the Sox Neuro (SoxN) protein recently reported to function alongside Doublesex-Mab related 99B (Dmrt99B) and Hth to specify identities of early-born neurons in the medulla (Zhu, Zhao et al. 2022). While mRNA transcripts of the *soxN* gene are distributed in neuroblasts of all ages, the SoxN protein is expressed only in the youngest neuroblasts, suggesting that post-transcriptional mechanisms are at work to confine the actual domain of SoxN protein expression. However, the presence of transcriptional enhancers regulating the expression of a TTF is strong evidence for its regulation by transcription. Identification of enhancers and transcription factor (TF) binding sites present within their sequence will demonstrate whether the observed sequential expression of TTFs is controlled primarily at transcription.

In the fly optic lobe medulla temporal sequence, Ey is the earliest known bonafide TTF required for activating the next TTFs Slp1/2 and is repressed by them. The existence of this clear regulatory relationship between Ey and the subsequent TTFs Slp1/2 led us to choose the transition from Ey expression to Slp1 and Slp2 expression in medulla neuroblasts to test whether the TTF transitions in the medulla may be regulated at transcription.

Results

Expressions of mRNA transcripts of *slp1* and *slp2* closely coincide with the expressions of the corresponding proteins

We performed fluorescence *in situ* hybridization (FISH) to detect *slp1* and *slp2* transcripts using a library of fluorescently labeled 20-bp DNA probes (custom ordered Stellaris probes) and antibody-staining to detect Slp1 and Slp2 proteins in the medulla of fly third instar larval brains. The observed pattern of *slp1* and *slp2* mRNA detected by FISH closely reflected the respective proteins (Figure 2.1B, C). This close correspondence indicated that expressions of Slp1 and Slp2 are very likely regulated at transcription.

At least two enhancers function redundantly to regulate transcription from the *slp* locus in medulla neuroblasts

We next tried to identify transcriptional enhancers that might regulate Slp1/2 expression in medulla neuroblasts. Initially, we looked at images of *UAS-GFP* expression patterns in the fly larval central nervous system (CNS) driven by various Gal4 lines fused to potential regulatory elements (Pfeiffer 2008, Pfeiffer, Ngo et al. 2010) (available from the Janelia FlyLight image database https://flweb.janelia.org/cgi-bin/flew.cgi). One of the enhancer lines, *GMR35H02-Gal4*, stood out for its expression pattern resembling endogenous Slp1 and Slp2 proteins. We experimentally verified this by crossing the *GMR35H02-Gal4* line to a *UAS-GFP* line and observed by immunostaining the expressions of GFP and endogenous Slp1 and Slp2 (Figure 2.2 A-A'''). We then narrowed down the minimal

enhancer element within the *GMR35H02* sequence by performing two consecutive rounds of enhancer bashing experiments to a 220bp sequence.

For the first iteration of enhancer bashing experiments, we cloned smaller sub-segments of the 3.75 kbp DNA element contained within the *GMR35H02* line into a GFP reporter vector pJR12 and made transgenic flies. Three partially overlapping fragments of 2.1 kbp, 973 bp, and 1.5 kbp, respectively (sequences are listed in Figure 2.3), were cloned into the pJR12 vector upstream of a GFP reporter gene driven by a minimal promoter derived from the *hsp* gene (Rister 2015). DNA constructs containing the enhancer fragments were injected into fly embryos, where they were incorporated at the same genomic site by φC31 transgenesis. Incorporation at the same site minimized variation due to genomic position differences and ensured direct comparability between transgenic lines. The transgenic line containing a 1.5 kbp enhancer fragment named SlpL1.5 prominently expressed GFP in the same pattern observed for *GMR35H02-Gal4* (Figure 2.2 B-B"), indicating that the active enhancer of *slp1* and *slp2* genes in *GMR35H02* is located within this smaller 1584 bp sequence.

Subsequently, we looked for conserved sequences within the SlpL1.5 fragment. Previous cross-taxa comparative studies have indicated that in many cases, circuits regulating critical patterning processes are conserved across vast evolutionary distances (Awgulewitsch 1992, Malicki 1992, Wray, Hahn et al. 2003, Brody, Rasband et al. 2007). Therefore, we reasoned that enhancers of genes essential for temporal patterning might

be conserved at least across various related *Drosophila* species. To this end, we compared the sequence of SlpL1.5 using Evoprinter (Odenwald 2005) between 12 *Drosophila* species (Listed in Figure 2.4B). We identified three segments within the SlpL1.5 element that showed high conservation (conserved across all 12 *Drosophila* species used for comparison) (Figure 2.4 A, highlighted by rectangular frames). These three conserved DNA segments of sizes 220 bp, 592 bp, and 123 bp, respectively (sequences in Figure 2.5), were cloned into the pJR12 vector, and transgenic flies were generated as previously described. Transgenic flies containing the 220bp fragment (Slpf1) expressed GFP very similar to the *GMR35H02-Gal4* line we had earlier observed (Figure 2.6 B-B" and A-A"), indicating that we had narrowed down the active enhancer within the *GMR35H02* sequence to a 220bp element.

Deleting the endogenous 220 bp enhancer by CRISPR-Cas9 led to a modest yet noticeable reduction in Slp1 expression but not to a complete loss of either Slp1 or Slp2 (Figure 2.7 A-A", B-B" and Figure 2.8). This phenotype indicated that other enhancers besides the 220bp enhancer also regulated the transcription of the *slp* genes.

To discover other enhancers of *slp* expression, we scanned through the REDfly database (Gallo, Li et al. 2006) of curated enhancers reported for *Drosophila melanogaster* genes. Here we found several other enhancer elements that regulated *slp1* and *slp2* in different developmental contexts, most prominently during parasegment boundary formation at embryonic segmentation, where *slp1* and *slp2* serve as pair-rule genes (Prazak, Fujioka

et al. 2010, Fujioka and Jaynes 2012). An earlier study had conducted an exhaustive analysis of a 30 kbp genomic region surrounding the *slp* transcription units to better understand the regulation of *slp* expression during embryonic segmentation (Fujioka and Jaynes 2012). In this study, segments of regulatory DNA within 30 kbp of *slp1* and *slp2* transcription start sites, averaging 2kbp in size, were incorporated in a *lacZ* reporter, and patterns of lacZ expression were then observed in transgenic flies (listed in Figure 2.9). We obtained transgenic lines used in this study from the authors and then tested by antibody staining whether the expression of *lacZ* by these enhancers colocalized with endogenous Slp1 and Slp2 proteins. These screens led us to identify a second enhancer reported in REDfly as d5778 (Figure 2.10 Q-Q"). This enhancer is activated slightly later than the 220 bp enhancer. It may also control *slp* expression in surface glial cells and glia bordering the medulla and central brain. Interestingly, our 220bp enhancer identified earlier was also reported to function as a stripe enhancer for *slp* at segmentation and was located within the REDfly enhancer u8772. In addition to enhancers reported in the REDfly database, we observed expression of GFP driven by tiling *Gal4* lines available from Vienna Drosophila Stock Centre and additional potential enhancer-*Gal4* lines from Janelia. Of the *Gal4* lines characterized, the VT001979 line showed an interesting expression pattern, driving *UAS-GFP* in some late-stage Slp2 expressing neuroblasts (2.11 C-C"). However, since this line also showed strong expression in the central brain, we concluded that the encoded enhancer is not expressed specifically in medulla neuroblasts and did not analyze it further.

Bioinformatic analyses of the d5778 enhancer (procedure detailed in a later section and Methods) revealed several binding sites predicted to bind Eyeless (Ey), a TTF and a known regulator of Slp1 and Slp2 in medulla neuroblasts, in an 850bp stretch of the d5778 enhancer. We, therefore, cloned the 850bp segment within the d5778 enhancer into the pJR12 GFP reporter vector to observe if it could recapitulate the expression driven by the d5778 enhancer. We found that this 850 bp segment could indeed reproduce the pattern of GFP reporter expression as the original 2.131 kbp d5778 enhancer (Figure 2.12 B-B'"). To avoid size-related ambiguities, we refer to the two enhancers of Slp1/2 activation in medulla neuroblasts as u8772 220bp and d5778 850bp (Figure 2.12 A-A"', B-B"'). As with the u8772 220bp enhancer, individual deletion by CRISPR-Cas9 of the d5778 850bp enhancer did not eliminate Slp1 and Slp2 expression (Figure 2.7 C-C" and Figure 2.8). Reduction in Slp1 expression was even milder on d5778 deletion than on the deletion of u8772 220bp enhancer and was statistically insignificant. The sequences of the two enhancers, u8772 220bp and d5778 850bp, are listed in Figure 2.13.

Bioinformatic identification of transcription factor binding sites within enhancers of *slp1/2* transcription

To find potential binding sites for transcription factors in our enhancers, we carried out an initial bioinformatic assessment of the enhancer sequences using the MEME suite (Bailey, Johnson et al. 2015), TOMTOM (Gupta, Stamatoyannopoulos et al. 2007)) and a FIMO (Grant, Bailey et al. 2011) based online resource (available at https://biss.epfl.ch.) developed by the Deplancke group (Dr. Bart Deplancke, EPFL, personal communication).

This initial analysis revealed several binding sites for Ey, Slp1, ventral nervous system defective (vnd), and the Notch co-factor Suppressor of Hairless (Su(H)) in both enhancers. Earlier studies on medulla neuroblasts have shown that Ey is required but insufficient for Slp expression in genetic experiments (Li, Erclik et al. 2013). Though we did not observe transcripts for *vnd* by single-cell RNA-sequencing (Zhu, Zhao et al. 2022), mRNA of Scarecrow (Scro), a related transcription factor of the NK-2 family, expressed in medulla neuroblasts at about the same time as *slp1* mRNA. These results corroborated our hypothesis that Ey and Scro may activate *slp1* and *slp2* mRNA transcription by directly binding to identified *slp* enhancers. Finding Su(H) binding sites suggested that the Notch pathway may also play a role in regulating *slp1* and *slp2* transcription.

To exhaustively identify all possible binding sites of Ey, Su(H), and Scro on the *slp* enhancers, first, we obtained position weight matrices (PWMs) for Ey, Su(H), and Slp1 binding from Fly Factor Survey (Zhu, Christensen et al. 2011) and JASPAR (Sandelin, Alkema et al. 2004, Fornes, Castro-Mondragon et al. 2020). For Ey, we also found a consensus binding sequence of the Ey paired-box motif reported in the literature (Tanaka-Matakatsu, Miller et al. 2015). Using information from these position weight matrices and available literature, we inferred a most-probable DNA-binding consensus sequence for each transcription factor. We then used this consensus sequence to look for transcription binding sites within our enhancers using the DNA Pattern Recognition Tool of the Sequence Manipulation Suite (abbreviated as SMS in figures) (Stothard 2000). Our

findings from these analyses are summarized in the following figures: Figure 2.14 for Ey binding sites, Figure 2.15 for Su(H) binding sites, and Figure 2.16 for Slp1 binding sites.

For Scro, we did not find position weight matrices of transcription factor binding. Therefore we used available position weight matrices of 20 other related NK-2 domain factors to 'guess' likely sites of Scro binding on the d5778 enhancer. First, we searched for possible transcription factor binding sites for the 20 NK-2 domain family transcription factors (listed in Figure 2.18 with their respective position weight matrices and inferred DNA binding consensus motifs) within the d5778 enhancer. Next, we identified the five most commonly occurring sequence motifs among the 20 NK-2 TFs as plausible sites for Scro binding (Figure 2.19). Given the small size of the u8772 220bp enhancer, we identified just the binding sites predicted for vnd (whose position weight matrix was available) within this enhancer as probable Scro binding sites (Figure 2.17) to avoid mutating a significant fraction of its sequence length. The transcription factor vnd is the closest NK-2 family relative of Scro in *Drosophila* (Zaffran 2000), so vnd binding sites, we reasoned, could be a close substitute for Scro binding sites.

Genetic experiments support that Ey and Su(H) regulate *slp1/2* transcription via enhancers identified

We observed the expressions of the GFP reporters of the u8772 220bp and the d5778 850bp enhancers in neuroblasts within and outside of RNAi knockdown clones of *ey* and *su(h)* – potential regulators of *slp1/2* transcription. We reasoned that if these factors

initiated *slp1/2* transcription by binding directly to the two enhancers identified, we would observe a change in GFP expression in cells where they were absent. GFP reporter expression was obliterated in *ey RNAi* expressing neuroblasts and *su(h) RNAi* expressing neuroblasts for both enhancers (Figure 2.20 A-A', B-B' and Figure 2.20 C-C', D-D' respectively). Since our enhancers also showed binding sites for Slp1, we also observed the expression of GFP reporters in mitotic clones that lacked expressions of both Slp1 and Slp2. GFP reporter expressions from both enhancers remained unaffected in *slp* mutant clones suggesting Slp1 was not involved in initiating *slp1/2* transcription (Figure 2.20 E-E', F-F'). This observation, however, does not preclude a role for Slp1 in later stages of Slp1/2 expression for maintaining high steady-state concentrations of Slp1/2 proteins at later stages in neuroblast development. Thus, we established that the factors Ey and Su(H) indeed initiate *slp1/2* transcription by acting upon the u8772 220 bp and the d5778 850 bp enhancers.

Mutagenesis of transcription factor binding sites on GFP reporters confirms direct binding of Ey, Scro, and Su(H) to *slp* enhancers

We mutated the transcription factor binding sites (TFBSs) for Ey, Su(H), Slp1, and Scro identified by bioinformatic analyses as described earlier to generate enhancers that should lack, in theory, the ability to bind the individual transcription factors. We cloned custom-made gene blocks that lacked or had mutated all sites for binding either Ey, Su(H), Slp1, or Scro in the pJR12 GFP reporter vector (Rister 2015) and observed GFP expression in transgenic flies. Details of transcription factor binding sites deleted and sequences of gene blocks synthesized to eliminate sites for each transcription factor's

binding are listed in Figures 2.21 and 2.22 for Ey, 2.23 and 2.24 for Su(H), 2.25 and 2.26 for Slp1, 2.27 and 2.28 for Scro. 21 bp fragments (corresponding to two turns of the DNA double helix) encompassing the transcription factor binding sites were mutated to preserve the major/minor groove orientations of other transcription factor binding sites.

Loss of Ey binding sites reduced GFP expression significantly compared to the wild-type enhancers for both the u8772 220bp (Figure 2.29 B-B'") and the d5778 850bp enhancers (Figure 2.30 C-C"'). Loss of potential Scro binding sites nearly eliminated GFP expression from the u8772 220bp reporter (figure 2.29 D-D"') and reduced it to a large extent for the d5778 850bp reporter (Figure 2.30 B-B"'). Loss of Su(H) binding sites significantly reduced expression from both enhancers (Figure 2.29 C-C"' and Figure 2.29 D-D"'). However, in the case of the d5778 enhancer, loss of Su(H) binding sites up-regulated GFP expression in surface glial cells (Figure 2.30 D-D"', F). Intensity measurements from the d5778 Su(H) mutant GFP reporter were thus confounded by the GFP signal from surrounding glial cells. They did not accurately reflect the reduction of GFP expression from neuroblasts (Figure 2.30 F). In contrast, loss of Slp1 binding sites did not significantly affect the pattern of GFP reporter expression from either enhancer, although the GFP signal intensity was reduced (Figure 2.29 E-E"', F and Figure 2.30 E-E"'). Overall, our results from reporter assays using transcription factor binding site mutated enhancers agreed well with our observations from genetics studies. Thus, we have identified possible sequences that Ey, Scro, and Su(H) bind to on the u8772 220bp and d5778 850bp enhancers for activating expressions of *slp1* and *slp2*.

DamID-sequencing shows the binding of Ey and Su(H) to *slp* enhancers *in vivo*

Finally, to establish that Ey and Su(H) bind to the u8772 220bp and the d5778 850bp enhancers *in vivo,* we performed targeted DamID-sequencing (van Steensel 2000, Marshall, Southall et al. 2016). We observed reproducible Ey and Su(H) binding peaks at the u8772 220bp and the d5778 850 bp enhancers (Figure 2.31 A). We identified reproducible peaks by IDR analysis (https://github.com/nboley/idr) of two replicate samples for each transcription factor (Figure 2.31A; IDR reproducible peaks at each enhancer are enclosed within blue rectangles for emphasis). These findings further support that Ey and Su(H) activate transcription from *slp* enhancers by direct binding.

Discussion

Here we have established that at least two enhancers regulate the expression of *slp1* and *slp2* in medulla neuroblasts. The Slp proteins are likely regulated at transcription, given mRNA transcripts of *slp1* and *slp2* closely mirror the patterns of corresponding proteins. Initially, we found a 220 bp element that functions as an enhancer of *slp* gene transcription through enhancer bashing experiments. However, CRISPR deletion of this element resulted in only a partial loss of Slp1, suggesting that other enhancers also activate *slp1/2* transcription.

An analysis of enhancer phenotypes utilizing resources generated for a prior study (Fujioka and Jaynes 2012) revealed that several non-coding DNA elements near the *slp1* and *slp2* coding loci might potentially function as enhancers of slp1/2 transcription in a

variety of cell types in the medulla. Some, such as the REDfly enhancers u8772, and u8781, showed prominent expression in neuroblasts. On examining their sequences, we found they contained the 220bp enhancer fragment we had discovered by enhancer bashing experiments starting with the *GMR35H02-Gal4* encoded sequence. Others such as u8166 showed striking expression in the deeper neural layers of the medulla but not in neuroblasts. Another fragment, the u5534 enhancer, also drove reporter expression in the medulla but did not coincide with the endogenous expression of Slp1/2. Some sequences closer to the *slp2* gene, such as i2330 and d6383, drove the expression of reporters in glial cells. However, we found a second enhancer element of *slp1/2* transcription in medulla neuroblasts- the d5778 enhancer. Thus we have identified at least two enhancers that control the transcription of *slp1* and *slp2* genes in medulla neuroblasts. The genomic distance between the identified enhancers is about 29.375 kbp. We also note that the authors of the study that first reported these enhancers (Fujioka and Jaynes 2012) also observed the expression of some of these enhancers in 'a ring-like pattern in the brain' referring to the medulla and were intrigued to find *slp* mRNA transcripts in the same brain region. Our observations made using their reporters are consistent with and provide a new context for this earlier report.

The functions of the two enhancers in this role are partially redundant since deletion of either individually did not abolish Slp1 or Slp2 expression but subtly changed the width of the domains over which each protein expressed. The two enhancers likely contribute to Slp1/2 expression patterns additively since endogenous deletion of the u8772 220bp enhancer leads to a partial reduction in Slp1 expression. Our observations of multiple

enhancers regulating transcription from the *slp* locus parallel *slp* transcription in other contexts. Others have noted that various enhancers regulate Slp1/2 expression at segmentation, and like in our system, the loss of an individual enhancer has modest effects. However, a full complement of stripe enhancers is required to properly maintain parasegment boundaries and Wingless (Wg) expression (Fujioka and Jaynes 2012). It is currently unknown whether the deletion of these enhancers together will lead to a loss of Slp1/2 expression. Future experiments deleting both enhancers will address this question.

A detailed analysis of the sequences of our enhancers using bioinformatic tools shows several sites for binding Ey, Scro, and the Notch pathway TF Su(H). We have also established the requirement of these factors to activate the two enhancers from mutagenesis and genetic experiments. Ey is required for the function of both the u8772 220bp and the d5778 850bp enhancers. Su(H) is necessary to ensure the correct timing of Slp1 and Slp2 expressions. We have also seen that the loss of potential binding sites for Scro results in loss of reporter expression for the u8772 220bp enhancer and a significant reduction in reporter intensity for the d5778 850bp enhancer. These observations are consistent with reports that Scro is required to ensure optimal expression of Slp1 and Slp2; loss of Scro results in significantly low levels of Slp1 and Slp2 transcription and a failure to correctly specify neurons (Zhu, Zhao et al. 2022). We further verified Ey and Su's (H) binding *in vivo* to these enhancers by DamID-seq. In the future, DamID-seq of Scro will help demonstrate the *in vivo* binding of this transcription factor to the *slp* enhancers.

Commonly used abbreviations in the text

TTF- Temporal patterning transcription factor

TF- Transcription Factor

PWM- Position Weight Matrix

Slp1, Slp2- Sloppy-paired 1 and Sloppy-paired 2

Ey- Eyeless

Scro- Scarecrow

Su(H)- Suppressor of Hairless

Vnd- ventral nervous system defective

Materials and Methods

Fly stocks used

UAS-ey-RNAi (BDSC 32486)

UAS-Su(H)-RNAi (VDRC 103597)

UbiFRT40ARFP/CyO flies (BDSC 34500)

GMR35H02-Gal4 (BDSC 49923)

GMR79H09-Gal4 (BDSC 40058)

VT001971-*Gal4* (VDRC ID 200611)

VT001979-*Gal4* (VDRC ID 205045)

VT001980-*Gal4* (VDRC ID 205920)

UAS GFPnls (BDSC 4776)

ayGal4 UAS lacZ (BDSC 4410)

ywhsFlp; ayGal4>UAS GFP; UAS Dcr2/Tm6B

ywhsFlp; ayGal4>UAS lacZ; eyRNAi (this study)

ywhsFlp; Sp/CyO; u8772 220bp>GFP (this study)

ywhsFlp; Sp/CyO; d5778 870bp>GFP (this study)

Dcr2; Su(H) RNAi; u8772 220>GFP (this study)

Dcr2; Su(H) RNAi; d5778 870> GFP (this study)

ywhsFlp; Ubi>RFPFRT40A; u8772 220bp>GFP (this study)

ywhsFlp; Ubi>RFPFRT40A; d5778 870bp>GFP (this study)

ywhsFlp; SlpS37A/Sm6-Tm6B

ywhsFlp; Sp/CyO; UAS-Dam/ Tm6B

ywhsFlp; Sp/CyO; UAS-Dam-Ey/ Tm6B (this study)

ywhsFlp; Sp/CyO; UAS-Dam-Su(H) /Tm6B (this study)

Dcr2; tubG80ts; SoxNGal4 (this study)

y[1] M{w[+mC]=nos-Cas9.P}

ZH-2A w[*] (BL54591)

y[1] w[1118]; PBac{y[+]-attP-9A}VK00027 (BL9744)

Plasmids and DNA constructs

pJR12 vector (a kind gift from Dr. Jens Rister)

pCFD5 (Addgene plasmid #73914, a kind gift from Dr. Simon Bullock)

BAC clone CH321-94O18

cDNA clone GH10914 (DGRC)

Antibodies

rabbit anti-Slp1, guinea-pig anti-Slp2 (1:500) (kind gifts from Dr. Claude Desplan)

guinea-pig anti-Dpn (1:500) (a kind gift from Dr. Chris Doe)

sheep anti-GFP (1:500) (AbD Serotec, 4745-1051)

Chicken anti-beta-gal (1:500, Abcam ab9361)

Secondary antibodies are from Jackson or Invitrogen.

Experimental Procedures

Flies were reared on yeast food at 25°C unless otherwise stated.

Enhancer identification- Flies carrying the *GMR35H02-Gal4* insertion (BDSC 49923) were crossed with transgenic flies expressing *UAS GFPnls* (BDSC 4776). GFP driven by the *GMR35H02-Gal4* was then compared to endogenous Slp1 and Slp2 expression. The procedure for making transgenic constructs and strains is described separately.

RNAi experiments

ayGal4 (*actin*>FRT-y^{+}-STOP-FRT-Gal4, in which *actin* promoter drives Gal4 expression after the action of heat shock-activated flippase excises a STOP cassette (Ito 1997)) was used to drive RNAi of *ey*, and *su(h)*. Flies of genotype *ywhsFlp; ayGal4>UAS GFP; UAS. Dcr2/Tm6B* were crossed to the RNAi lines. Larvae were heat-shocked at 37°C for 10 minutes 48 hours after egg laying and then raised at 29°C until the brains of third instar larvae were dissected and stained.

Flies of genotype *ywhsFlp; ayGal4> UAS lacZ; eyRNAi* were made by combining *ayGal4> UAS lacZ* on chromosome II (BDSC 4410) with *UAS-ey RNAi* on chromosome III. These flies were then crossed to flies with genotype *ywhsFlp; Sp/CyO; u8772 220bp>GFP* or *ywhsFlp; Sp/CyO; d5778 870bp>GFP, respectively,* to observe the effect of *ey RNAi* on the GFP reporter expression driven by the u8772 220bp and d5778 850bp enhancers (Figure 2.20 A-A’ and B-B’).

For studying the effects of *su(h) RNAi* on GFP reporter expression from the u8772 220bp and d5778 850bp enhancers, flies of genotype *ywhsFlp; ayGal4>lacZ; Tm2/Tm6B* were crossed to flies of genotype *Dcr2; su(h) RNAi; u8772 220>GFP* or *Dcr2; su(h) RNAi; d5778 870> GFP* (Figure 2.20 C-C', D-D').

Negative labeling of *slp* loss of function clones

UbiFRT40ARFP/CyO flies (BDSC 34500) were crossed with flies of genotype *ywhsFlp;Sp/CyO; u8772 220bp>GFP* and *ywhsFlp ;Sp/CyO; d5778 870bp>GFP* to create strains with genotypes *ywhsFlp; Ubi>RFPFRT40A; u8772 220bp>GFP* and *ywhsFlp; Ubi>RFPFRT40A; d5778 870bp>GFP* ,respectively. Flies of genotype *ywhsFlp; SlpS37A/Sm6-Tm6B* flies (a kind gift from Dr. Andrew Tomlinson) were then crossed to *ywhsFlp; Ubi>RFPFRT40A; u8772 220bp>GFP* and *ywhsFlp; Ubi>RFPFRT40A; d5778 870bp>GFP* and larvae were heat-shocked for 45 minutes 48 hours after egg-laying. Third instar larvae were then dissected. The *ywhsFlp; SlpS37A/Sm6-Tm6B* strain carries a deletion on chromosome II that spans both Slp1 and Slp2 genes. Clones carrying two copies of this deficiency are seen as dark regions amidst Ubi>RFP marked wild type neuroblasts.

Bioinformatic identification of transcription factor binding sites

The procedure followed to identify all potential binding sites for Ey, Su(H), Slp1, and Scro is explained in detail in the main text. For determining the most probable motif for binding each transcription factor, we allowed for a maximum number of two mismatches to the stringent consensus sequence we inferred by combining information from literature and the position weight matrices of each transcription factor. We then used this 'relaxed' motif as input for the DNA Pattern Find program in the Sequence Manipulation Suite (Stothard 2000). All motifs used to find possible binding sites for a transcription factor are listed in Figures 2.14, 2.15, 2.16, 2.17, and 2.19.

Plasmids constructs and transgenic fly stocks

Primer sequences for all cloning are provided in Figure 2.33.

For making all recombinant DNA constructs, DNA was amplified from a template using Expand High-Fidelity Polymerase (Roche) unless stated otherwise, and all constructs were verified by sequencing. All fly embryo injections for making transgenic flies were carried out by Bestgene Inc, Chino Hills, CA.

Generating constructs for reporter assays and enhancer bashing and making transgenic reporter expressing stocks

Sequences encoded in *GMR35H02* and the d5778 REDfly enhancer were cloned from the BAC clone CH321-94O18 (Venken, Carlson et al. 2009) (BACPAC resources).

Sequences were PCR amplified from this BAC and cloned into the pJR12 vector (a kind gift from Dr. Jens Rister) between *AscI* and *NotI* sites.

Mutated enhancers were custom synthesized as gene blocks (gBlocks, IDT DNA) and cloned as above into the pJR12 vector. Sequences of gBlocks used for cloning mutated enhancers are detailed in the following figures: Figures 2.21 and 2.22 for Ey binding site mutant enhancers, 2.23 and 2.24 for Su(H) binding site mutant enhancers, 2.25 and 2.26 for Slp1 binding site mutant enhancers, and 2.27 and 2.28, for Scro binding site mutant enhancers.

pJR12 plasmids containing enhancer fragments were injected into fly embryos. All enhancer constructs were inserted at the landing site VK00027 on the third chromosome (BL9744) by φC31 integrase mediated transgenesis (Groth 2004). Transgenes were incorporated at the genomic site to minimize position-specific effects and ensure comparability across experiments. Positive transformants were screened using the w+ marker present in the pJR12 plasmid.

Generation of CRISPR enhancer deletion constructs and transgenic stocks

CRISPR gRNAs were designed by entering sequences of genomic DNA of the target +/- 20 kbp into the CRISPR Optimal Target Finder web utility (Gratz, Ukken et al. 2014) (https://www.targtfinder.flycrispr.neuro.brown.edu). Four gRNAs-two upstream and two

downstream of the target region to be deleted, were then selected (sequences of gRNAs used are listed in Figure 2.35). All four gRNAs were then cloned into the vector pCFD5 (Port and Bullock 2016) (Addgene plasmid #73914, a kind gift from Dr. Simon Bullock) using NEB-Builder HiFi DNA Assembly master mix.

pCDF5 vectors with gRNAs were then injected into embryos of the fly strain containing y[1] M{w[+mC]=nos-Cas9.P}ZH-2A w[*] (BL54591) along with a custom repair oligonucleotide 120bp long, that contained 60bp of wild type genome sequence flanking both ends of the expected double-stranded break (sequences of oligonucleotides used listed in Figure 2.36). After injection, the *nos-cas9* source was eliminated in the subsequent generations by crossing individual G0 progeny flies to a double balancer of genotype *ywhsFlp; Sp/CyO; Tm2/Tm6B* and selecting male G1 progeny. Individual G1 males were then crossed to the same double balancer line to create stocks. We genotyped individual G1 males by PCR (using the RedExtract-n-Amp tissue PCR kit from Sigma-Aldrich) to identify whether their genome had been edited. G2 progeny of genome-edited males were then raised until homozygous stocks were established. Sequences deleted by CRISPR was determined by sequencing genomic DNA of homozygous final stocks (sequences deleted listed in Figure 2.37)

Generation of DamID-fusion constructs (*U.A.S. Dam-Ey* and *UAS-Dam-Su(H)*) and transgene expressing stocks

Su(H) coding sequence was amplified from a cDNA clone GH10914 (DGRC) by PCR. The amplified Su(H) coding sequence was cloned into the pUAST-Dam-attB vector (Southall, Gold et al. 2013) (a kind gift from Dr. Andrea Brand) between the *NotI* and *XhoI* sites. The Ey coding sequence's custom gene block (IDT gBlock) was cloned into the pUAST-Dam-attB vector. Constructs were then incorporated into fly embryos at the VK00027 landing site (BL 9744) by φC31 mediated integration. Transformants were identified by expression of the w+ marker gene. Final stocks were established by crossing to a double balancer line of genotype *ywhsFlp; Sp/CyO; Tm2/Tm6B*.

Immunofluorescence staining

Antibody staining was carried out using minor modifications to a previously described protocol (Li, Erclik et al. 2013). The protocol is as follows: brains from climbing third instar larvae were dissected in 1XPBS and fixed in 4% Formaldehyde solution in 1X PBS for 30 minutes on ice. Brains were then incubated in primary antibody solution overnight at 4^{o}C, washed three times for 30 minutes each at 4^{o}C using 1X PBS and 10% Tween-20 (PBST). Subsequently, the brains were incubated in fluor conjugated- secondary antibody solution overnight at 4^{o}C and then washed in PBST three times at room temperature each time for 30 minutes. Samples were mounted in Slowfade Gold antifade reagent (Invitrogen). Images are acquired using a Zeiss LSM500 Confocal Microscope.

Fluorescence In situ hybridization (FISH)

FISH was carried out with minor modifications to a previously described protocol (Long, Colonell et al. 2017) and the incubation of fixed brain tissue with sodium borohydride for autofluorescence quenching was skipped. 20bp tiling Stellaris RNA FISH probes were designed using the *slp1* mRNA and *slp2* mRNA sequences as templates and custom-ordered. Concurrent FISH and immunofluorescence staining were carried out as described in the same publication.

DamID-Seq

Flies of genotype *ywhsFlp; Sp/CyO; UAS-Dam/ Tm6B, ywhsFlp; Sp/CyO; UAS-Dam-Ey/ Tm6B* or *ywhsFlp; Sp/CyO; UAS-Dam-Su(H) /Tm6B* were crossed with *Dcr2; tubG80ts; SoxNGal4*. Mating crosses were incubated at 25 °C. Eggs laid within an 8-hour window were then shifted to 18°C for three days until hatching. The expressions of the Dam-fusion proteins were then induced in larval brains by shifting the larvae to 29°C for 72 hours. Climbing third instar larvae were then dissected. Only the optic lobes were used for further sample preparation. For each sample, around 100 brains were dissected.

Dam-ID libraries were made as previously described (Marshall, Southall et al. 2016). Briefly, fly brains were dissected in 1X PBS, and genomic DNA was isolated using QIAamp D.N.A. Micro kit (Qiagen). Genomic DNA was then digested with DpnI and purified using spin column purification (Qiagen PCR-purification kit). To the DpnI digested D.N.A. DamID-PCR adaptors were ligated. Subsequently, the adaptor-ligated DNA

fragments were digested with DpnII. The DpnII digested genomic DNA fragments were then amplified by PCR to enrich for bound GATC fragments. For making sequencing libraries, the PCR enriched genomic DNA sample was sonicated using a Bioruptor bath sonicator (Diagenode), purified using AMPure XP beads, end-repaired, and 3'-adenylated. Illumina sequencing indexes were then ligated to these fragments. Index-labeled DNA. fragments were then further enriched by PCR amplification, checked for quality and fragment size distribution on an Agilent Bioanalyzer, and qPCR (Quality control of all libraries was carried out at the Functional Genomics Unit of Roy J. Carver Biotechnology Center, UIUC). Libraries deemed acceptable were then sequenced on a single SP100 lane of an Illumina NovaSeq sequencer. Read lengths were 100bp. Two replicates of *Ey-Dam*, *Su(H)-Dam,* and *Dam* only samples were sequenced. The number of reads obtained was as follows: Dam replicate1: 53745480 reads, Dam replicate 2: 85637355 reads, Ey-Dam replicate 1: 81121107 reads, Ey-Dam replicate 2: 82085708 reads, Su(H)-Dam replicate 1: 77448608 reads, replicate 2: 80015207 reads. All samples exhibited good QC scores.

DamID-Seq data analysis

DamID-seq data was analyzed using the damidseq-pipeline (Marshall and Brand 2015). Duplicate samples of Ey-Dam and Su(H)-Dam samples and Dam-only controls were aligned to the *Drosophila* reference genome UCSC dm6. The alignment rate for individual samples was as follows:(Ey-Dam replicate 1- 97.04%, Ey-Dam replicate 2 -97.82%, Su(H)-Dam replicate 1- 97.91%, and Su(H)-Dam replicate 2 – 97.82%. The main utility-the damid-seqpipeline was used to align reads to the genome using bowtie2, bin, and

count reads, normalize counts and generate log-2 ratio bedgraph files for each DamID-sample and its corresponding Dam-only control. The provided gatc.track file was used for running the script. Next, the findpeaks utility was used with an FDR <0.01 to identify peaks. We then used the provided peaks2genes utility to assign peaks to genes. To assess the reproducibility of our data, we also ran the findpeaks script using FDR <0.1 to discover peaks with weaker statistical confidence and used this as input for the IDR Python package (https://github.com/nboley/idr). 984 of 1810 (54.4.%) Ey-Dam and 972 of 1996 (48.7%) of Su(H)-Dam peaks passed an IDR threshold of 0.05. Lists of genes bound reproducibly by Ey-Dam and Su(H)-Dam were used in BioVenn (Hulsen, de Vlieg et al. 2008) to visualize the overlap between these two lists and estimate the percentage of genes regulated by both transcription factors. Enriched gene ontology terms in this list were identified using DAVID (Huang da, Sherman et al. 2009),(Huang da, Sherman et al. 2009). All replicate tracks for Ey and Su(H) and reproducible peaks identified using IDR were visualized in IGV (Robinson, Thorvaldsdottir et al. 2011).

Imaging and image analysis for comparison of wild type and mutant GFP reporter intensities

All images were acquired using a Zeiss LSM 500 confocal microscope. Samples were imaged at sub-saturating illumination conditions, with stack intervals of 1 micron. The same laser settings and imaging conditions were used across all variants of the same enhancers. Image analysis was carried out using Fiji (Schindelin, Arganda-Carreras et al. 2012). Signal intensities in the GFP and the Dpn channels were measured over a small rectangular selection for all variants. For the same enhancer, a ‘scaling factor’ was

calculated for each mutant by dividing the Dpn channel intensity for the mutant reporter by the channel intensity of the corresponding wild-type reporter. The GFP channel intensities for each variant were then multiplied by this scaling factor. Finally, a ratio of the scaled GFP channel intensity to the Dpn channel intensity was calculated for each GFP reporter variant. Ratios of scaled GFP/Dpn intensities were then plotted using GraphPad Prism. For each enhancer, ordinary one-way ANOVA and Tukey's multiple comparisons were carried out between reporter variants. Five sets of data were acquired for each enhancer (one set- wild type and all mutant variations all imaged using the same conditions).

Image analysis for CRISPR enhancer deletion experiments

All images were acquired using a Zeiss LSM 500 confocal microscope under sub-saturating illumination conditions. For each sample, the width of Slp1, Slp2, and Dpn expression domains was measured in Fiji at five different locations and averaged. The brain size of the sample was estimated by measuring the length of the brain at its widest point perpendicular to the neuroblast division axis. The width of each protein expression domain was divided by the brain size to normalize expression domain size estimates to the brain size. These ratios were then plotted in GraphPad Prism, and pairwise comparisons between wild-type and CRISPR enhancer deleted brains were carried out. Ordinary one-way ANOVA and Tukey's multiple comparisons test were used to estimate variation between the wild type and CRISPR deletion lines. Seven brains of each genotype were quantified.

Figures

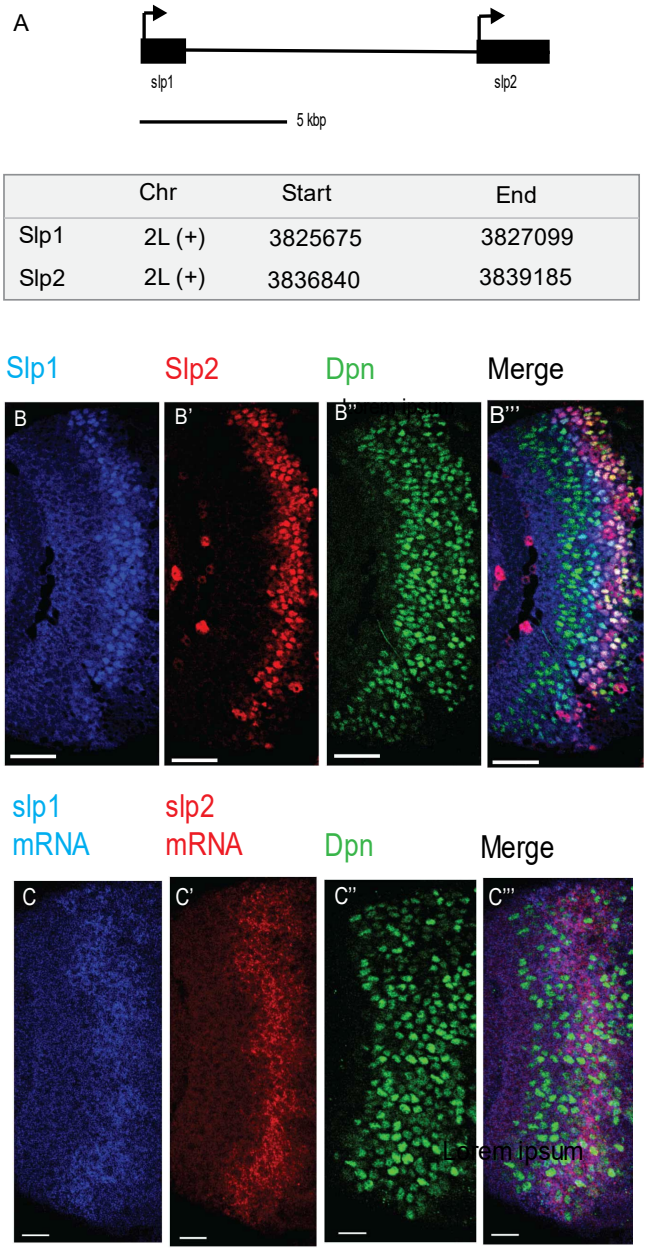

Figure 2.1. *slp1* and *slp2* expression in medulla neuroblasts are transcriptionally regulated. A. Schematic showing the two genes *sloppy-paired 1* (*slp1*) and *sloppy-paired 2* (*slp2*) as located in the *Drosophila melanogaster* genome (drawn to scale). The *sloppy-paired* locus has two related genes resulting from a gene duplication event. The genes

Figure 2.1 (cont.) *slp1* and *slp2* are located about 9.7 kbp apart and are regulated similarly in embryonic development and the optic lobe medulla. Both function as temporal transcription factors in patterning the fly optic lobe medulla. B. Protein expression pattern of Slp1, Slp2 in medulla neuroblasts identifiable by their expression of the neuroblast marker Deadpan (Dpn). C. Expressions of *slp1* and *slp2* mRNA in medulla neuroblasts. The mRNA expressions coincide with expressions of the respective proteins suggesting transcriptional regulation. Scale bar: 20 microns.

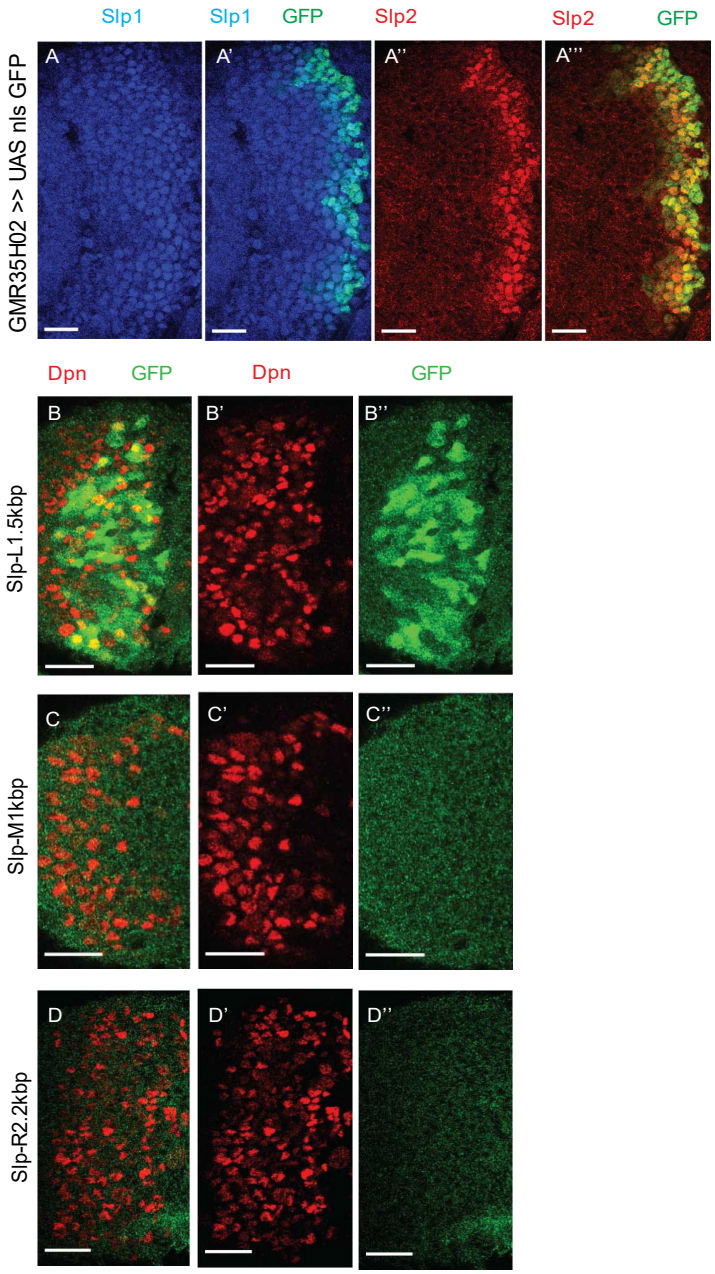

Figure 2.2. Identification of an enhancer of *slp1 and slp2* transcription by screening Janelia Farm Gal4 lines and subsequent enhancer bashing. (A-A''''). *UAS-GFP* expression driven by the Janelia line *GMR35H02-Gal4* containing a 3.75 kbp regulatory DNA fragment fused to a Gal4 sequence closely corresponds to the expression of endogenous Slp1 and Slp2 proteins, indicating that the sequence encoded by the

Figure 2.2 (cont.) GMR35H02-Gal4 contains an enhancer of slp genes. Subsequently, smaller overlapping fragments of sizes 1584 bp, 973 bp, and 2143 bp were cloned from the *GMR35H02* sequence into a GFP reporter vector, and transgenic flies were created. GFP reporter expression driven by the (B-B''). SlpL1.5 fragment (1584 bp), (C-C''). SlpM1.0 fragment (973 bp) and (D-D''). by the SlpR2.0 fragment (2143 bp) are shown. Prominent GFP reporter expression in neuroblasts was observed only for the SlpL1.5 fragment indicating the active enhancer within the *GMR35H02* sequence is located within this sequence. Scale bar 20 microns.

A. Sequence name: SlpL1.5

Chromosomal Location: 2L: 3817261-3818808

Size: 1584 bp

Sequence

GAATCGAAATGCTTCCCCGCCTCGCCCAAATGCATTTGAATCGAGTGGTGAGCGATAGTTTTCA
CATGTTTTGTTCGAGCATTAATTCCGTTTAAATGATTTCCGCAACAGATTTGAGCTTTGCACGTAA
TCAAGTGGAAATGAATTTGACCAACACAAGAGGTTTATACACACATCACATTTTCTGCCTTTATG
TTTTTGCGGTGTCCCATTAGTTTGATTGTTTCGAAGGCCACTGAGCCGTGAAAAATATCAGAGAA
ATAAAAATCGAAATACCGAAATGAGCTGGTTTTTTGTTAGCGAAAGTGCAGATTTTTCAGGACTC
GCAAAGGGATGTGATTGAAGATCTTCAGGATATTTCAGCACATGCATCGATATTTGTCCCAAACT
GGAAGTCATTGACCCAGTTACTTTTCAACTATATATTGAATTTATATATTTATGTATTTACCATACA
GGGCCATGCTCAAAATCAACGCCCAAACCAAAATACCACTTTAATCGAGGCCAACTTCCCTCAG
TTCGACCTTGTAGTGGCAAGCAAAAAAACCAAAAATTACAAACACCAAACTTGAGATTTGCTAAC
ATATCGTGACTGTGACTGTGACCAAATAACGCGACAGGATCCTCGAAGGACTCCAGTCGAAGG
TCAATGTATGGCCACAGTTTTGCGTTAGATCCCAAAGTTTCAAGCAATACTGCGTACGGTTAACC
AGGAGAGGCCAAAATATGCCATTTACTTTGGCCACATATCGTTCTACGGGCCAAGGACATACCT
CGGCCGGTCCAAGGACGTTTCTCGGGCAAACTGAAGGAAACACGAGATACGAGGACCAGCAG
CAGCAGCAGCAGCAGCAGCTGAGTTTGGCCTGCTTGCTGTCGTCGGGATGTCAATGTCAGCGG
GTGCCGTTCGAGTCCTTTATTCCGGCATCCTTACTCGAGGCTCATCATCACGCAGGCAGGCGC
ATCCTGCCGCGTGGATACCCCCCTGGCTCTGGATTCCCATTCGCATTCCCATTCCTATTCCCGA
TTTCCAATTCCGATTCCTGGTGCCACCTCCGGTGCACCGCTGGTGCAAATCGCCGGCATTTAAC
ACTAACCTTCCGATCTCCGCTGCCGTCCAAGGAATTTGCCAGCGGGCTAAGAGGACAAAAGCG
GAACGGCAAGACGCTTTCCAAAATCAAAACAGCACCTGAGTTTTGGGCTGGTCCTTTAGGCAAA
AAACACCTTTGACTTGTGTCAATTGTGAAAATCCTAGCACTGCGACGAATTCTAAAGGATGCACG
TGGAAATATACTTTAAAATTAAAGATGAAATTTTGACATAGGAGTTTTTCCAAGTGCAAGGACCAA
TTATACCCTGTATTTACTGTAGCATGTTCCCAACTTCCTCCTTCTGGACTCACTGCATTCTATTTC
TAACCATTCTCCTTGTTGCTCCTCACATATTTACCCAATGATAACCAAATATTTTCGATGCGAAGA
CATTTTCCAATTTGAAGCAATGAAAACATACAAGTCGCTGGCGGCCTTTGATGTTGCACGTTCA

Figure 2.3

B. Sequence name: SlpM1.0

Chromosomal Location: 2L: 3818785-3819757

Size: 973 bp

Sequence

GCGGCCTTTGATGTTGCACGTTCATCTGCGACTTGCCTCGCTCGACTCCTTGCCGCATGAAATT
TGAGTGAGTCAGTCAAGTGCTCAAGTGCGTGTCTGCCCTTTCATTTTGAATGTGTGTGTAGATG
TTTCGATTCTTTTTTGTAATTAACCGACTTTCGAACACATCGGCGGCACCTCCTACTTTTTGTTTC
CTTTTCCGTACGCGATGTTGCCACGTCCACGCCTAAACACTTCACTTGCCGCATGTGTTTCTTGT
CCCCAATCCTGGCTGCACTGAAAGAAAACTATATATATCTAATGGAATAAGGTAGATGATTTTAT
GGTATGCAGTATGCAATACCCATTATATTGATTGATTTCAACTAGTACTTGAGTCAGTTAGCCAT
ATACTTTTTTTTCCGGTGTACTCTGCATATTTTCCACTGCTGTATCGGATTTCCCCGATTCAAAAG
ACATTAGCTCGAAGTTAGGCAGGCGCCTAGAAATGTCAGCGAATTTTGACCGCCTGCGCCTGTT
TGTGTTAATGAGAAAGTGTCATCGATTTGACGTGGCGGCAAAAGACCAAACGCATTTTCCCATC
TTGTCATTATGTCAAAGAGGTGTGATCTGACTCGTTTTTTGTGGCCATAACTTGGGGAAGTTGTT
CCGCAGTGTGGAGATGTGAGCCATGAATGGAGCTGACACACTTTCACGTGGCCACGGAAGGAA
GTCGTTTAATTGGAAGTGGGAAATTCGATCGGGTAAATAGCCAAGTGTTAAATAAATTACATCTT
GTGTTTGTCGAGGAATACAAAAGCTAGCAGTGAGATGATAAAGTAAAACGAAATTTTATTAATAA
TCCAGAAAGAATACATTAATCATATCTTTAATGTGGTATTCTCATTTCTCAAGGTGTTATTTTCTTT
TTTTAAAATTTTCAACTGCCATTTTGATCTTCACACCTGAATTCGAGGCACATTCCGAACTGTCC

Figure 2.3 (cont.)

C. Sequence name: SlpR2.2

Chromosomal Location: 2L: 3818872-3821014

Size: 2143 bp

Sequence

AGTGCGTGTCTGCCCTTTCATTTTGAATGTGTGTGTAGATGTTTCGATTCTTTTTTGTAATTAACC
GACTTTCGAACACATCGGCGGCACCTCCTACTTTTTGTTTCCTTTTCCGTACGCGATGTTGCCA
CGTCCACGCCTAAACACTTCACTTGCCGCATGTGTTTCTTGTCCCCAATCCTGGCTGCACTGAA
AGAAAACTATATATATCTAATGGAATAAGGTAGATGATTTTATGGTATGCAGTATGCAATACCCA
TTATATTGATTGATTTCAACTAGTACTTGAGTCAGTTAGCCATATACTTTTTTTTCCGGTGTACTC
TGCATATTTTCCACTGCTGTATCGGATTTCCCCGATTCAAAAGACATTAGCTCGAAGTTAGGCA
GGCGCCTAGAAATGTCAGCGAATTTTGACCGCCTGCGCCTGTTTGTGTTAATGAGAAAGTGTCA
TCGATTTGACGTGGCGGCAAAAGACCAAACGCATTTTCCCATCTTGTCATTATGTCAAAGAGGT
GTGATCTGACTCGTTTTTTGTGGCCATAACTTGGGGAAGTTGTTCCGCAGTGTGGAGATGTGAG
CCATGAATGGAGCTGACACACTTTCACGTGGCCACGGAAGGAAGTCGTTTAATTGGAAGTGGG
AAATTCGATCGGGTAAATAGCCAAGTGTTAAATAAATTACATCTTGTGTTTGTCGAGGAATACAA
AAGCTAGCAGTGAGATGATAAAGTAAAACGAAATTTTATTAATAATCCAGAAAGAATACATTAAT
CATATCTTTAATGTGGTATTCTCATTTCTCAAGGTGTTATTTTCTTTTTTTAAAATTTTCAACTGCC
ATTTTGATCTTCACACCTGAATTCGAGGCACATTCCGAACTGTCCATAAACCGATCATCTCGAGA
TCCTTCTCAACCATTGGTCATCAAAAATTTGCCAGCTGTTCGATCTTGTTTTTGGTCCTTTCATAT
CCTGTTGCTGCATAAATCGAACATAAATTCCTGCTCCTTAGCAGCCCTTGTAAAAGTTAATTGCT
ATGTTAACACGTCCAGGCCAAAACACAATGAGCCGTCTGCTGCTCATTTCAATAAGGCTCAAAA
AGGAATCGATTTTTAAGACTATTAAAGGCCGAATCCGCTTAGCGGAGCGTCTGCTTTTCTGACT
TCTTAATTGTGTTTCTGGTTTACTGGATTTGGATCGTAGGGGTTGGGGCGGTACTAACGATTCC
TCAAACATTCTGCACGCGCTGCGATCATTTGTGGTGATTATATATTGTTTGAATTTCTCCTTTGAT
TGCGTCCACAGTCCACAGTCCGCAGGATCGAGGATCAAGGATCGCCGAGGCATAAATCAAGGA
CTCCCGCTGCGGTGCATTCCCAATCGAGGGTATATTTTCCAAAAGGCGTGGCCCAAAGTCGGT
CGAACAGAATTAAAGTCAAAGCCAAAGGCCGAAAATAAGAAATAATTGAGACATTTGTTGGCAG

Figure 2.3 (cont.)

CAGCGGCGGCGGCTGTTTCTTTTTGGTATATTTTTGGTCTACCCGCAATGACAATGTGATAAAAT
GTACCTAAAACAATGACATCAAAGTCGGTTTCCGAATTTCTTTTATTTCGTCCATGGGCGGCAGCT
CCTTGCATTTTTCAGGTGACATCTTATTTCCACCTTTCGGCACGTTTCGAACAATGAGTGTCCTTT
TTTGTCGTGGTACGCTACTCCCGCTCATCAAAGGATATATGCGGCCACTCTGATCTCTGCCGATC
TCGCCTTGATTATGTTGTCACACAAGAATCACAAGATTAGACGAAAATCACGGCGACGATGATAA
GGCGATATAGATCAAAGGATCATCGAGATCGGCTCCTTTTGGCTACTTTATGTGGATTATGTTGT
CACATTTGGCACAATCGGTTCAATGCGTTTTCGTGGAACTTGCTATGCGCAAAAGGATATTGTAA
TCGATATGGGAAGATCAGTGCCGAGATCAGCGGGATAATATTTTATTATCGTGAAGGTGAGAAAT
TCCTCAAAGGTGTCAACCAAACTGTGAATAAACAATGGAATTGGATCATACAAAACTGTATAAGCT
GGTAATGAGGTCCTAAAATAGGTCTACAGATTTATACTTGATCGAAGAAGAGTGAAGGGAGCTAG
CTGGG

Figure 2.3 (cont.) Sequences of enhancer fragments derived from the GMR35H02 encoded sequence used for cloning in pJR12 vector and transgenesis in the first round of enhancer bashing experiments. Sequences, sizes, and chromosomal locations of the three fragments SlpL1.5, SlpM1 and SlpR2.2 are indicated in A, B and C.

A

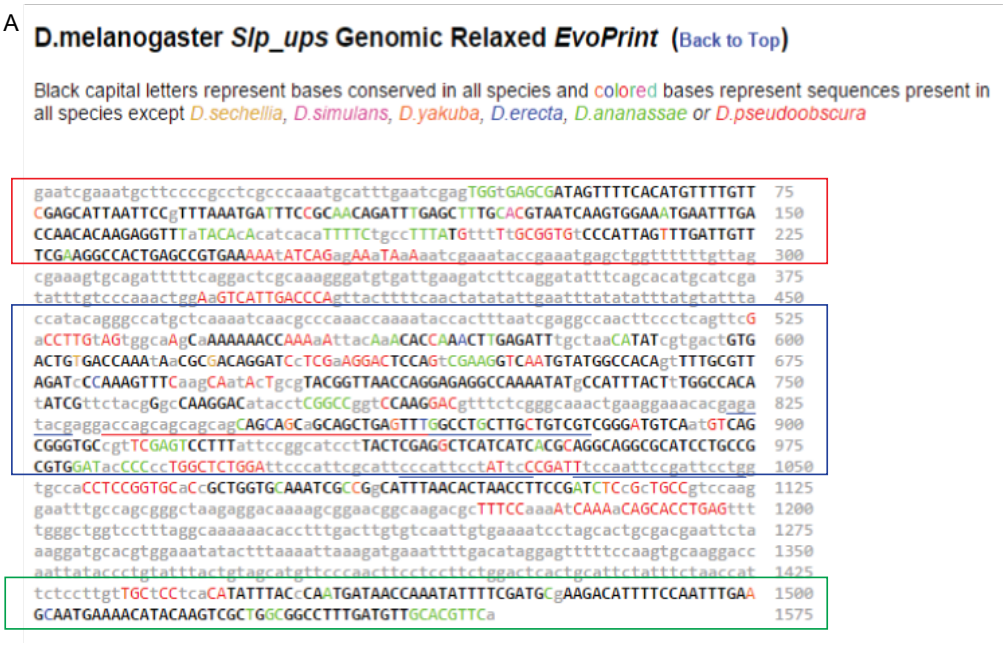

B. *Drosophila* species used for Evoprinter comparison

Drosophila melanogaster
Drosophila sechellia
Drosophila simulans
Drosophila yakuba
Drosophila erecta
Drosophila pseudoobscura
Drosophila virilis
Drosophila willistoni
Drosophila grimshawi
Drosophila mojavensis
Drosophila ananassae
Drosophila persimilis

Figure 2.4 Analysis of evolutionary conservation of the SlpL1.5 sequence reveals three highly conserved segments. A. Screenshot of output from Evoprinter showing the relative conservation of the SlpL1.5 sequence across 12 *Drosophila* species. Most

Figure 2.4 (cont.) conserved sequences are indicated by bold black letters. Three segments of conserved sequences were identified within SlpL1.5 by Evoprinter and cloned into a GFP reporter vector for the second round of enhancer bashing experiments. These were named Slpf1 (sequenced enclosed within the red rectangle), Slpf2 (sequence within the blue rectangle), and Slpf3 (sequence enclosed within the green rectangle). B. Species of *Drosophila* used for sequence conservation analysis in Evoprinter.

A. Sequence name: Slpf1

Size: 220 bp

Sequence

GAATCGAGTGGTGAGCGATAGTTTTCACATGTTTTGTTCGAGCATTAATTCCGTTTAAATGATTT
CCGCAACAGATTTGAGCTTTGCACGTAATCAAGTGGAAATGAATTTGACCAACACAAGAGGTTT
ATACACACATCACATTTTCTGCCTTTATGTTTTTGCGGTGTCCCATTAGTTTGATTGTTTCGAAGG
CCACTGAGCCGTGAAAAATATCAGA

B. Sequence name: Slpf2

Size: 592 bp

Sequence

TTCGACCTTGTAGTGGCAAGCAAAAAAACCAAAAATTACAAACACCAAACTTGAGATTTGCTAAC
ATATCGTGACTGTGACTGTGACCAAATAACGCGACAGGATCCTCGAAGGACTCCAGTCGAAGG
TCAATGTATGGCCACAGTTTTGCGTTAGATCCCAAAGTTTCAAGCAATACTGCGTACGGTTAACC
AGGAGAGGCCAAAATATGCCATTTACTTTGGCCACATATCGTTCTACGGGCCAAGGACATACCT
CGGCCGGTCCAAGGACGTTTCTCGGGCAAACTGAAGGAAACACGAGATACGAGGACCAGCAG
CAGCAGCAGCAGCAGCAGCTGAGTTTGGCCTGCTTGCTGTCGTCGGGATGTCAATGTCAGCGG
GTGCCGTTCGAGTCCTTTATTCCGGCATCCTTACTCGAGGCTCATCATCACGCAGGCAGGCGC
ATCCTGCCGCGTGGATACCCCCCTGGCTCTGGATTCCCATTCGCATTCCCATTCCTATTCCCGA
TTTCCAATTCCGATTCCTGGTGCCACCTCCGGTGCACCGCTGGTGCAAATCGCCGGCATTTAAC
ACTAACCTTCCGATCTCCG

Figure 2.5

C. Sequence name: Slpf3
Size: 123 bp
Sequence TCTCCTTGTTGCTCCTCACATATTTACCCAATGATAACCAAATATTTTCGATGCGAAGACATTTTC CAATTTGAAGCAATGAAAACATACAAGTCGCTGGCGGCCTTTGATGTTGCACGTTCA

Figure 2.5 (cont.) Sequences of three highly conserved DNA segments within SlpL1.5 were tested further for enhancer activity. For the second round of enhancer bashing experiments, sequences of enhancer segments derived from the SlpL1.5 fragment were cloned into pJR12 vector for transgenesis. The sequences of the three fragments- Slpf1, Slpf2, and Slpf3 cloned are shown in A, B, and C respectively.

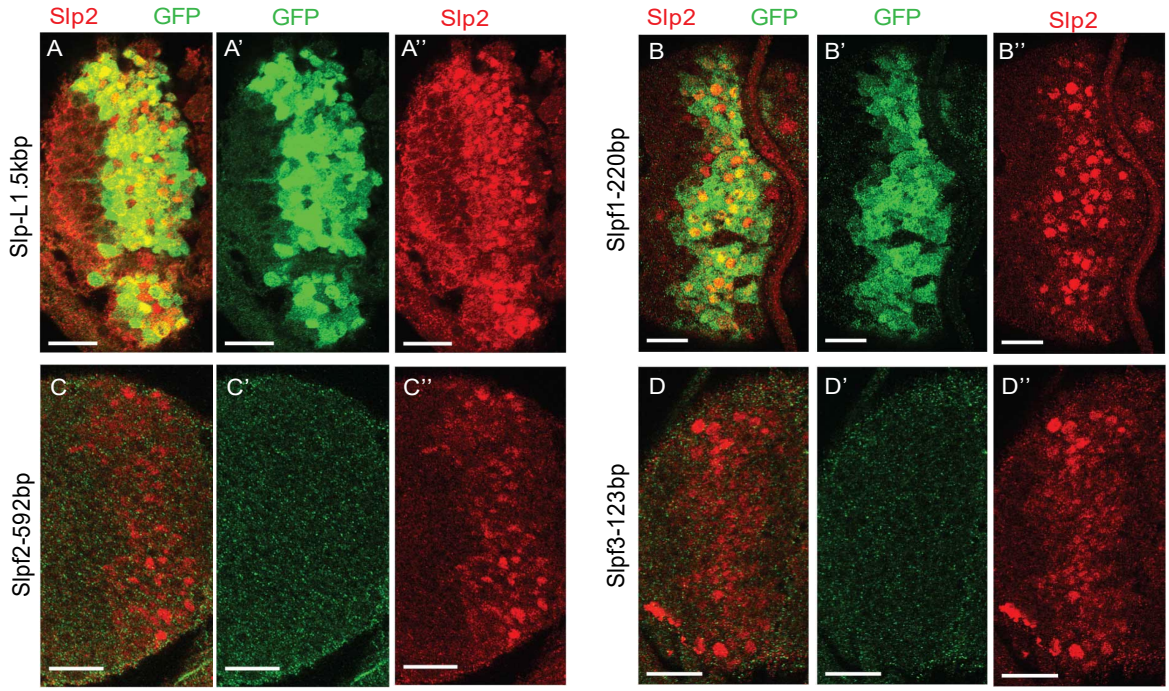

Figure 2.6. A 220bp segment within the SlpL1.5 fragment functions as an enhancer of *slp1/2* transcription in medulla neuroblasts. Expressions of GFP reporter driven by SlpL1.5 (A-A'') and its sub-segments Slpf1(B-B''), Slpf2 (C-C''), and Slpf3 (D-D''). Of the three sub-segments of SlpL1.5, only the Slpf1 fragment (220bp in size) shows enhancer activity. Scale bars 20 microns.

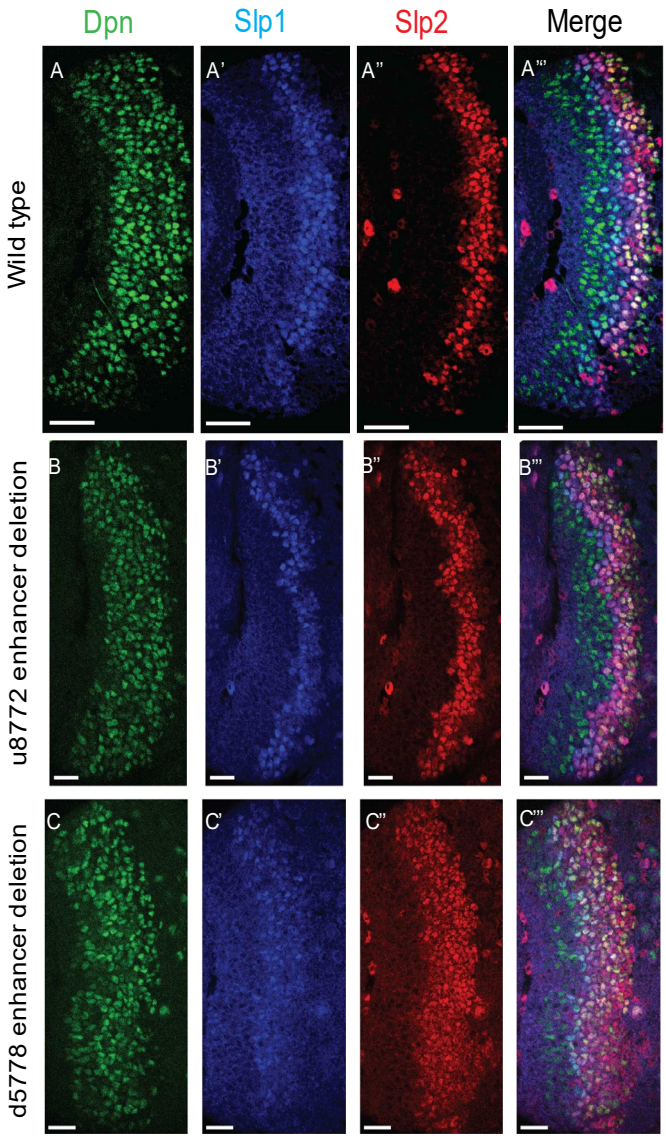

Figure 2.7 Deleting the u8772 220bp enhancer and the d5778 850bp enhancer individually by CRISPR-Cas9 results in modest changes in the extent of Slp1 and Slp2 expressions. Deleting the u8772 220bp enhancer (B-B"') results in a slight reduction in Slp1 expression compared to wild-type brains (A-A"'). Effects of deletion of the d5778 850bp enhancer did not result in a conspicuous loss of either Slp1 or Slp2.

Figure 2.7 (cont.) Neither enhancer when deleted led to a complete loss of Slp1 or Slp2 proteins indicating these enhancers act redundantly. Scale bars 20 microns.

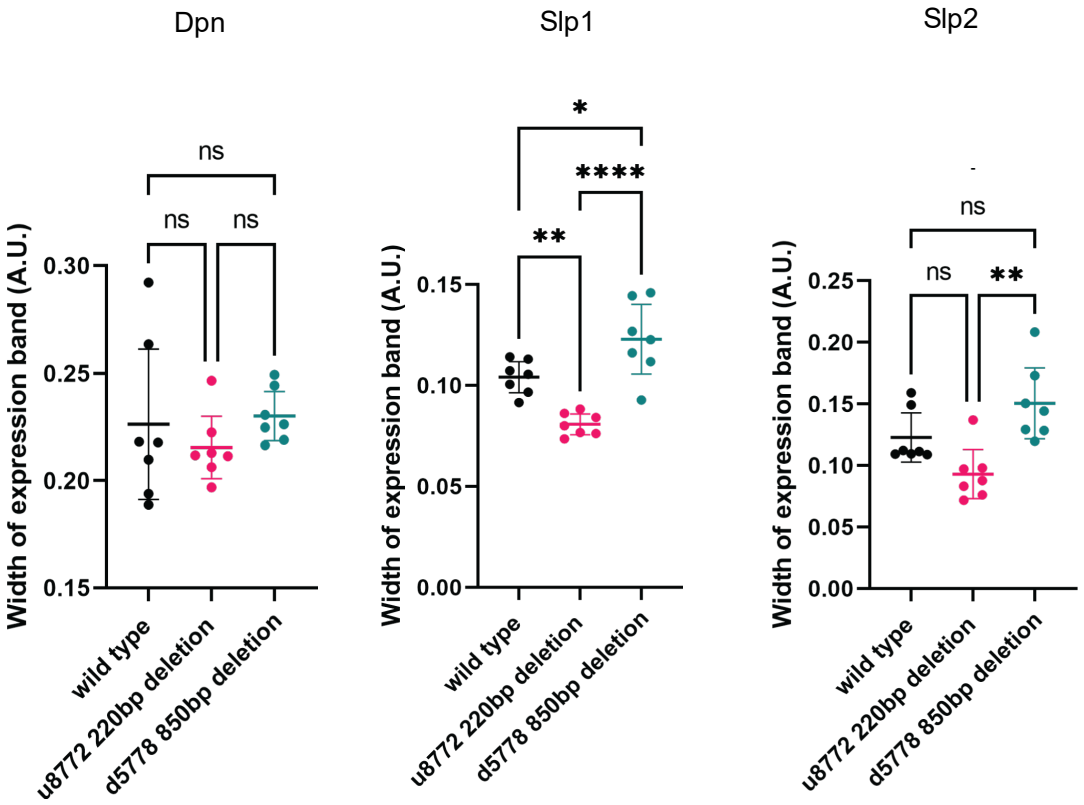

Figure 2.8 Quantification of the effects of enhancer deletion on the expression of Slp1 and Slp2 proteins. The width of each protein expression band normalized to brain size was computed for wild-type brains and brains where each of the two enhancers had been deleted (n=7 for each genotype). Sample means were compared using ordinary one-way ANOVA and Tukey's multiple comparisons test. The scatter of individual values is plotted for each sample, and the mean and 95% confidence intervals are indicated. Neither deletions had any effect on Dpn expression. Slp1 expression was significantly reduced relative to wild type when the u8772 220bp enhancer was deleted and expanded when the d5778 850bp enhancer was deleted. Slp2 expression is reduced on the deletion

Figure 2.8 (cont.) of the u8772 850bp relative to wild type, although this reduction is statistically insignificant and slightly expanded on the deletion of the d5778 850bp enhancer.

Enhancer fragment	Chromosome	Start	End
u8772	2L	3816967	3818532
u8781	2L	3816967	3817608
u8172	2L	3817605	3818532
u8166	2L	3817605	3819171
u5534	2L	3820168	3822240
u5547	2L	3820168	3821009
u3925	2L	3821751	3823158
u3725	2L	3822001	3823158
u2316	2L	3823356	3824032
u1609	2L	3824033	3824739
i1523	2L	3827196	3827972
i2330	2L	3827970	3828686
i4053	2L	3829629	3830998
i4060	2L	3829629	3831819
i5882	2L	3831440	3833928
d2445B	2L	3839285	3841364
d5778	2L	3842530	3844660
d6383	2L	3843114	3845187
GMR35H02	2L	3,817,265	3,821,014
VT001971	2L	3,828,414	3,830,695
GMR79H09	2L	3,830,094	3,833,128
VT001979	2L	3,844,454	3,846,610
VT001980	2L	3,846,245	3,848,335

Figure 2.9 REDfly enhancers and enhancer-Gal4 lines screened for identifying other enhancers of *slp1/2* transcription in medulla neuroblasts. Table summarizing names and chromosomal locations of enhancer fragments screened to identify the second enhancer of *slp1* and *slp2* transcription. Enhancer fragments with names beginning in u, i, or d are enhancers from the study (Fujioka and Jaynes 2012).

Figure 2.9 (cont.) Those with names beginning with GMR are Janelia Farm enhancer-Gal4 lines with names beginning VT are enhancer Gal4 lines from the Vienna Drosophila Stock Centre.

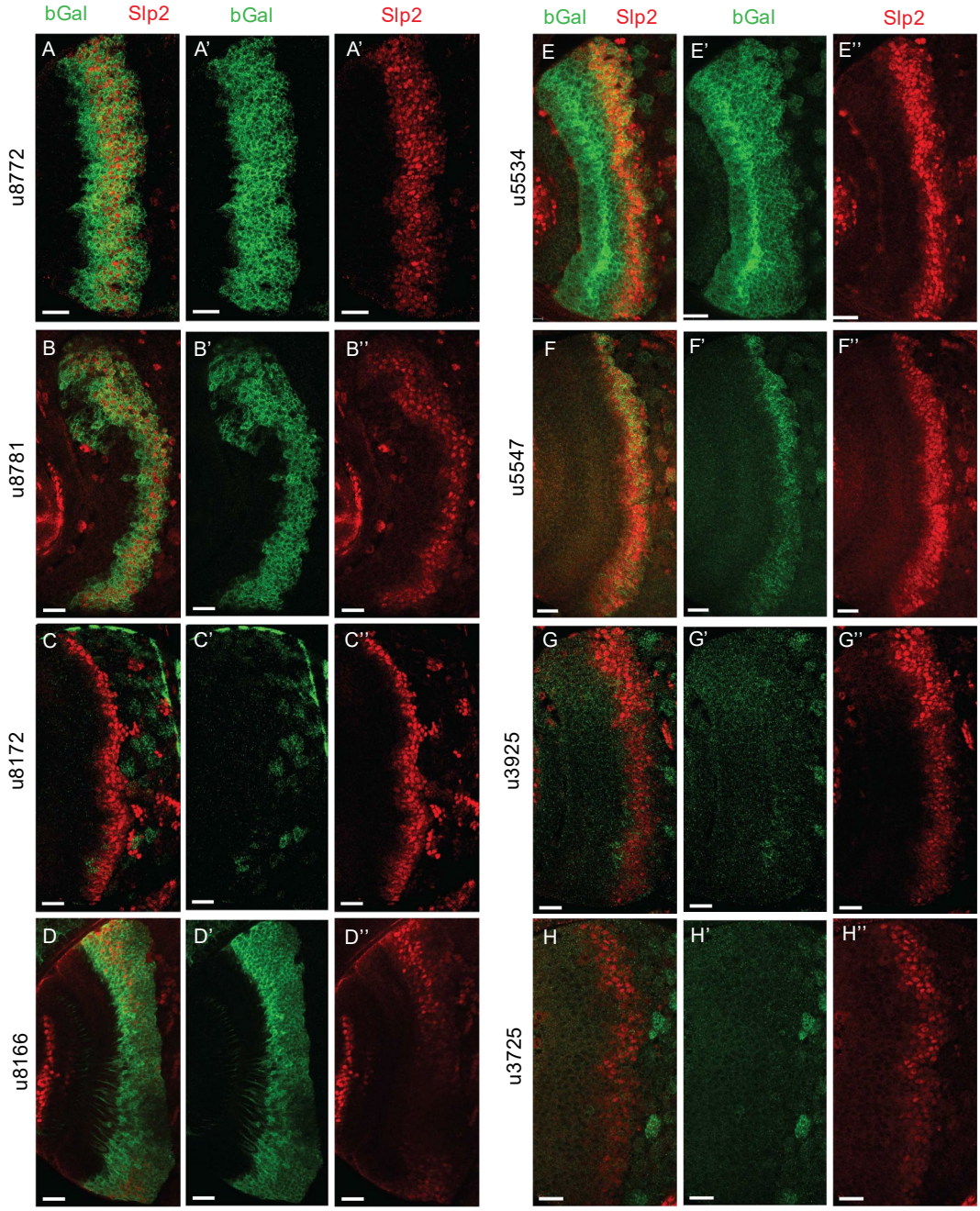
bGal
Slp2
bGal
Slp2
bGal
Slp2
bGal
Slp2
u8772
u8781
u8172
u8166
u5534
u5547
u3925
u3725
A
A'
A'
B
B'
B''
C
C'
C''
D
D'
D''
E
E'
E''
F
F'
F''
G
G'
G''
H
H'
H''

Figure 2.10

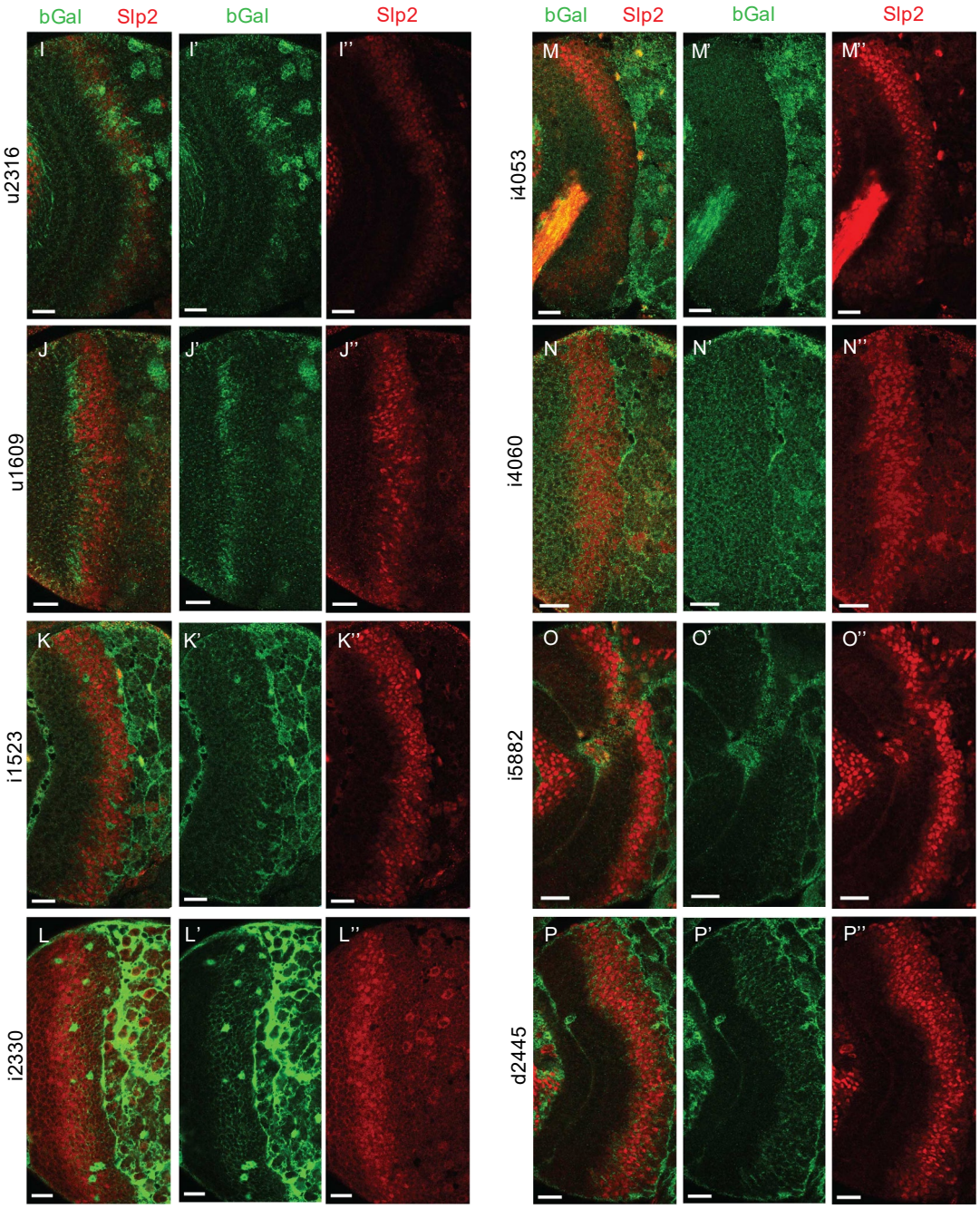

Figure 2.10 (cont.)

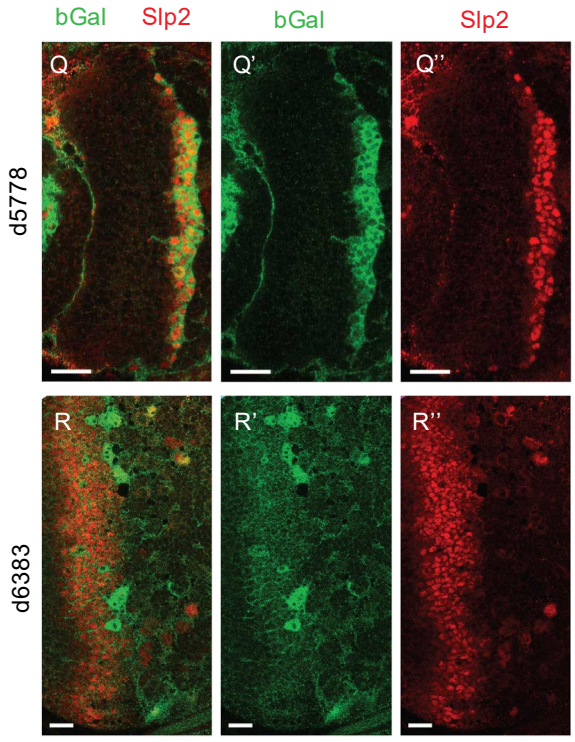

Figure 2.10 (cont.) Screen of REDfly enhancers identifies d5778 as an enhancer of slp1/2 transcription in medulla neuroblasts. Results of the screen showing lacZ reporter gene expressions driven by REDfly enhancers are listed in Figure 2.9. Of the reporters tested, u8772 (A-A'') and u8781 (B-B'') recapitulated the expression patterns driven by the previously identified 220bp slp enhancer, thereby supporting our findings. Both u8772 and u8781 contain within them the 220 bp enhancer element. Additionally, patterns of *lacZ* expression driven by u8166 (D-D'') and u5547 (F-F'') are also interesting in that they somewhat overlap with the expression of endogenous Slp2. However, the u5547 enhancer was contained within the *GMR35H02* sequence, and enhancer bashing experiments encoding this part of *GMR35H02* did not show reporter expression. The u8166 line drove reporter expression primarily in neurons than in neuroblasts. For these

Figure 2.10 (cont.) reasons, the u5547 and u8166 enhancers were not considered for further analysis. However, the screen of REDfly enhancers identified d5778 as a potential enhancer of slp1 and slp2 transcription since it drove reporter expression in neuroblasts in a pattern overlapping endogenous Slp2 (Q-Q''). Scale bars 20 microns.

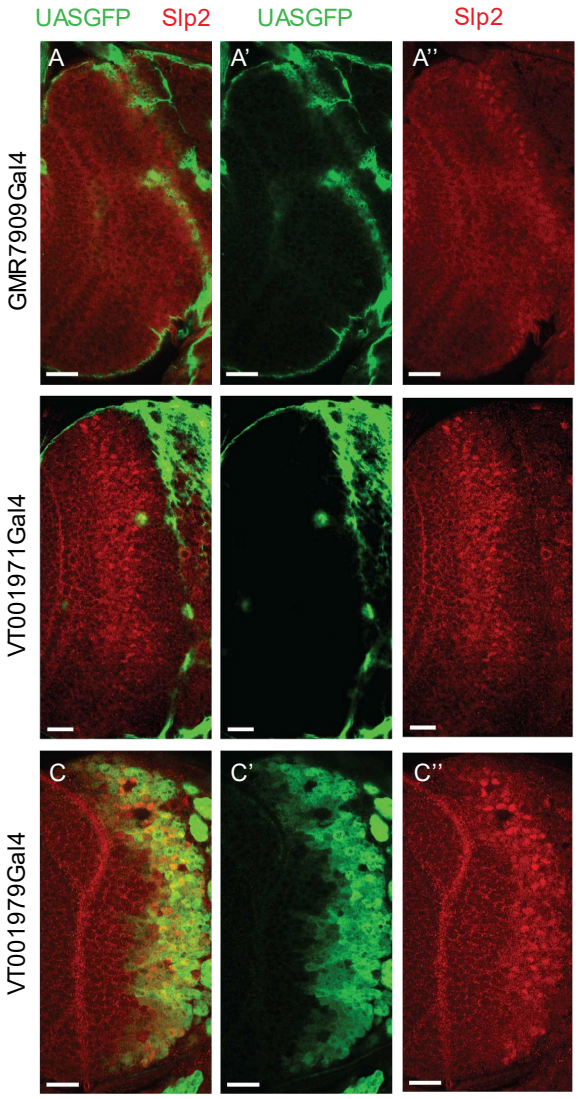

Figure 2.11 The VT001979 enhancer-Gal4 line may regulate Slp2 transcription in the medulla and central brain neuroblasts. Results of the screen of other Janelia Farm lines and tiling Gal4 lines from the Vienna Drosophila Stock Center encoding putative enhancer elements. The candidate enhancer-Gal4 lines were crossed to *UAS-GFP* reporter flies, and the GFP expression pattern was compared to endogenous Slp genes' expressions. Only the VT001979 line showed expression partly overlapping Slp2 in

Figure 2.11 (cont.) medulla neuroblasts (C-C''). However, we did not analyze the enhancer encoded by this line because of its prominent expression in the central brain neuroblasts and consequent lack of medulla neuroblast specificity. Scale bars 20 microns.

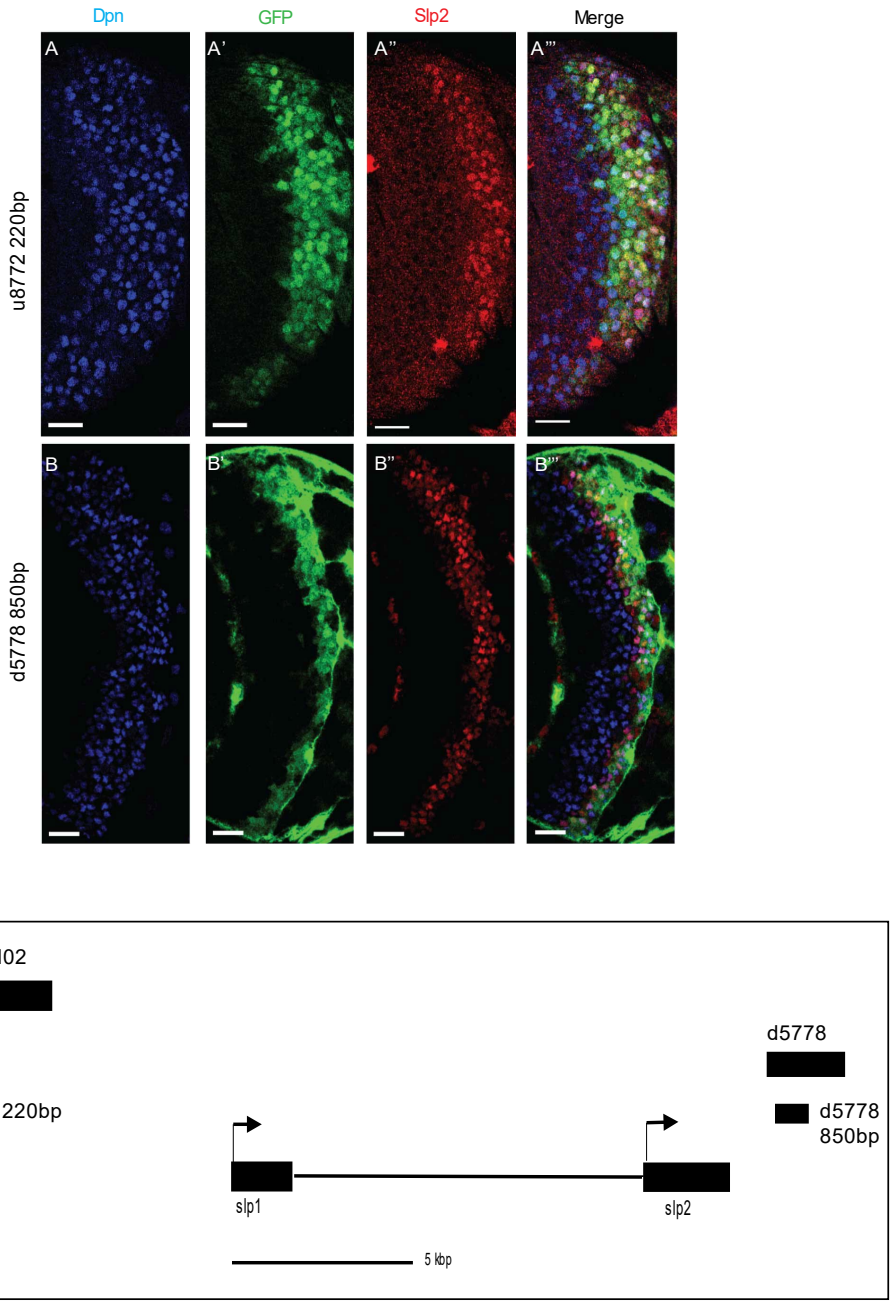

Figure 2.12. u8772 220bp and d5778 850bp are two enhancers regulating transcription of *slp*1/2 genes in medulla neuroblasts. (A-A'') Expressions of GFP reporter driven by the u8772 220bp enhancer and (B-B'') by the d5778 850bp enhancer. Colocalization of GFP with the neuroblast marker Deadpan (Dpn) confirms the activity of

Figure 2.12 (cont.) these two enhancers in medulla neuroblasts. As inferred from its expression in older neuroblasts, the d5778 850bp enhancer is activated later in development than the u8772 220bp. Scale bars 20 microns. C. A schematic (drawn to scale) of the *slp1* and *slp2* coding units relative to one another and the enhancers of *slp* genes in medulla neuroblasts. The genes *slp1* and *slp2* are located 9.7 kbp apart. The *GMR35H02* enhancer is located 8.4 kbp upstream of the *slp1* transcription start site, whereas the d5778 enhancer is located 3.3 kbp downstream of the *slp2* coding region. The genomic distance between the GMR35H02 and the d5778 enhancers is around 27 kbp.

A. u8772 220bp wild type enhancer sequence

Sequence

GAATCGAGTGGTGAGCGATAGTTTTCACATGTTTTGTTCGAGCATTAATTCCGTTTAAATGATTTC
CGCAACAGATTTGAGCTTTGCACGTAATCAAGTGGAAATGAATTTGACCAACACAAGAGGTTTAT
ACACACATCACATTTTCTGCCTTTATGTTTTTGCGGTGTCCCATTAGTTTGATTGTTTCGAAGGCC
ACTGAGCCGTGAAAAATATCAGA

B. d5778 850bp Wild type

Sequence

CATTAACTCGAGTCTGGTTTCCGATTCCGATTTCGCTTCCTCCTGCCAACTTATTTCTATATCTTC
TCCCTTTGTGCCCTGTGTGTGTGAAACAAAAACGTTTGTTTCAATACGTTGGCTTCGTGCATTTTA
CGGTGTTGGGAAACAGACGAAATGGACTCATTGATTCCAATTGACTGATTTCAATTGATGTTAAG
TGTCTGCCACAGTCGCAGCCGCAAATTCAGTGGCACAACTCCGTCGCAGCCAAATGCCATTTGC
TTTTCACATCCAGGTCGAACGGCGTTGCCTTGTTGACTTTGTTTTTGCTACTCATTGCCGCGATTT
GGGTTAGGCATGGGGTATGTGCGCACTGTGGGAACTTTGGATTACTCAGATGAAACAGCATTTA
GGACACTATGCAGCTGGAAAGATAAACTAGTTGATAGCTACTCATTTACTCATTTACTACTTACTA
CTAATTTAATGCATTTTTAACAACTTTAAGCTACACAAGCCAAAACTAATGGGTATTTTATAGTCCT
ATTTAACCCCTTTAACGAATGCATCCTTTTACCTTTTTTGGTCACGGCAGCTGAACTCTGCCCTTT
CGTTGGGGGTGACTCCTCCCTCCCGTACTCCCTCCCTCCCTCCCCTCCCTCTCCGCGCCACAGT
CGACCTTGTCAAGTACCTTGTTAGCTGTTGGGCAAATGTGCCACACAAGTGGCTCACATCAGCG
GGATCGAAAATAAAAAGCGAAACGCATCGAGAACTTCCCAAGAAAACGGCGAGTCAAAGTTGAG
AAAACGCTGCTTCCGTTTAATTGACAATTGAACCCGAACCCGGACCGAACTCCTGGAGAATATGT
ACG

Figure 2.13 Sequences of the two enhancers regulating slp1/2 expression in medulla neuroblasts. Sequences of the u8772 220bp enhancer (A) and the d5778 850bp enhancer (B).

A

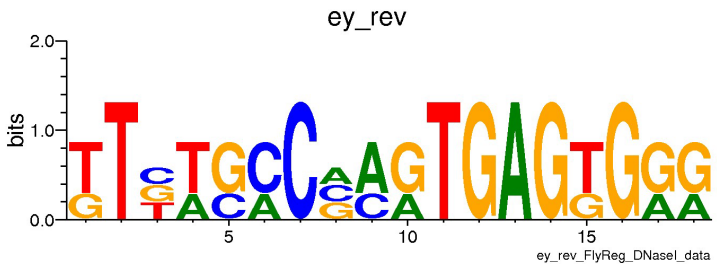

B. Consensus Ey binding site based on PWM above

[GT]T[CTG][AT][CG][AC]C[AGC][AC][AG]TGAG[TG]G[AG][AG]

C. Consensus Ey paired domain binding site based on literature

[AT][AT][ATCG][AC]C[AG][AC][ATCG]T[GC]A[ATCG]TG[AG][AG][CT]

D. Common Ey binding consensus based on PWM and literature

[ATGC][AT][ATGC][AC]C[ACG][AC][ATGC]T[GC]A[ATGC]TG[G]

E. Common Ey binding consensus used as input for SMS

[ATGC][AT][ATGC][AC]C[ACG][ACtg][ATGC]T[GCat][tA][ATGC]TG[G]

F. u8772 220bp wild type enhancer sequence with Ey sites highlighted

Sequence

GAATCGAGTGGTGAGCGATAGTTTTCACATGTTTTGTTCGAGCATTAATTCCGTTTAAATGATTTC
CGCAACAGATTTGAGCTTTGCACGTAATCAAGTGGAAATGAATTTGACCAACACAAGAGGTTTATA
CACACATCACATTTTCTGCCTTTATGTTTTTGCGGTGTCCCATTAGTTTGATTGTTTCGAAGGCCA
CTGAGCCGTGAAAAATATCAGA

Figure 2.14

G. d5778 wild type enhancer with Ey sites highlighted

Sequence

CATTAACTCGAGTCTGGTTTCCGATTCCGATTTCGCTTCCTCCTGCCAACTTATTTCTATATCTTC
TCCCTTTGTGCCCTGTGTGTGTGAAACAAAAACGTTTGTTTCAATACGTTGGCTTCGTGCATTTTA
CGGTGTTGGGAAACAGACGAAATGGACTCATTGATTCCAATTGACTGATTTCAATTGATGTTAAG
TGTCTGCCACAGTCGCAGCCGCAAATTCAGTGGCACAACTCCGTCGCAGCCAAATGCCATTTGC
TTTTCACATCCAGGTCGAACGGCGTTGCCTTGTTGACTTTGTTTTTGCTACTCATTGCCGCGATTT
GGGTTAGGCATGGGGTATGTGCGCACTGTGGGAACTTTGGATTACTCAGATGAAACAGCATTTA
GGACACTATGCAGCTGGAAAGATAAACTAGTTGATAGCTACTCATTTACTCATTTACTACTTACTA
CTAATTTAATGCATTTTTAACAACTTTAAGCTACACAAGCCAAAACTAATGGGTATTTTATAGTCCT
ATTTAACCCCTTTAACGAATGCATCCTTTTACCTTTTTTGGTCACGGCAGCTGAACTCTGCCCTTT
CGTTGGGGGTGACTCCTCCCTCCCGTACTCCCTCCCTCCCTCCCCTCCCTCTCCGCGCCACAGT
CGACCTTGTCAAGTACCTTGTTAGCTGTTGGGCAAATGTGCCACACAAGTGGCTCACATCAGCG
GGATCGAAAATAAAAAGCGAAACGCATCGAGAACTTCCCAAGAAAACGGCGAGTCAAAGTTGAG
AAAACGCTGCTTCCGTTTAATTGACAATTGAACCCGAACCCGGACCGAACTCCTGGAGAATATGT
ACG

Figure 2.14 (cont.) Bioinformatic analyses of the u8772 220bp and the d5778 850bp enhancers reveal potential binding sites for Ey in both enhancers. A. Position weight matrix of Ey binding from Fly Factor Survey. B. Consensus sequence for Ey binding based on A. The consensus motif is written following the same rules as required to find patterns in a DNA sequence using the DNA Pattern Find program of the Sequence Manipulation Suite. If two or three bases are found with an equal likelihood at a specific position in a consensus pattern, this is reflected by incorporating the bases inside square brackets. For example, a consensus sequence written as att[ca] will find both attc and atta motifs. C. Ey binding consensus from a paper (Tanaka-Matakatsu, Miller et al. 2015). D. Most likely Ey binding consensus incorporating patterns from both B and C.

Figure 2.14 (cont.) E. Consensus sequence used to find Ey binding sites used as input for Sequence Manipulation Suite's DNA Pattern Find program. This consensus was less stringent than in D, allowing for alternative bases (underlined and in lower case) at certain positions. Ey binding sites in F. the u8772 220bp enhancer and G. the d5778 850bp enhancer.

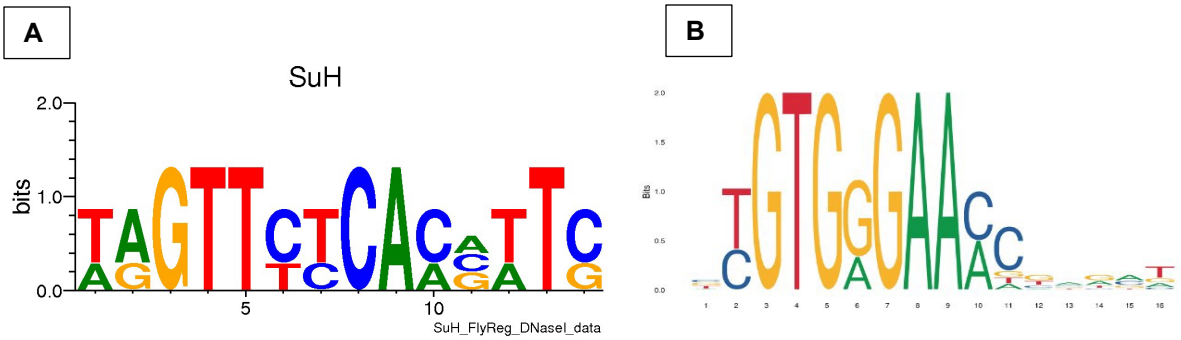

C. Consensus Su(H) binding site based on PWM from Fly Factor Survey

[TA][AG]GTT[CT][TC]CA[CA][AGC][TA]T[CG]

D. Consensus Su(H) binding site based on PWM from JASPAR

[GT]TTC[TC]CAC[AG]

E. Consensus Su(H) binding site based on both PWMs used as SMS input

TT[CT][CTg]CAC

F. u8772 220bp wild type enhancer sequence with Su(H) sites highlighted

Sequence

GAATCGAGTGGTGAGCGATAGTTTTCACATGTTTGTTCGAGCATTAATTCCGTTTAAATGATTTC
CGCAACAGATTTGAGCTTTGCACGTAATCAAGTGGAAATGAATTTGACCAACACAAGAGGTTTATA
CACACATCACATTTTCTGCCTTTATGTTTTTGCGGTGTCCCATTAGTTTGATTGTTTCGAAGGCCA
CTGAGCCGTGAAAAATATCAGA

Figure 2.15

G. d5778 850bp wild type enhancer with Su(H) sites highlighted

Sequence

CATTAACTCGAGTCTGGTTTCCGATTCCGATTTCGCTTCCTCCTGCCAACTTATTTCTATATCTTC
TCCCTTTGTGCCCTGTGTGTGTGAAACAAAAACGTTTGTTTCAATACGTTGGCTTCGTGCATTTTA
CGGTGTTGGGAAACAGACGAAATGGACTCATTGATTCCAATTGACTGATTTCAATTGATGTTAAG
TGTCTGCCACAGTCGCAGCCGCAAATTCAGTGGCACAACTCCGTCGCAGCCAAATGCCATTTGC
TTTTCACATCCAGGTCGAACGGCGTTGCCTTGTTGACTTTGTTTTTGCTACTCATTGCCGCGATTT
GGGTTAGGCATGGGGTATGTGCGCACTGTGGGAACTTTGGATTACTCAGATGAAACAGCATTTA
GGACACTATGCAGCTGGAAAGATAAACTAGTTGATAGCTACTCATTTACTCATTTACTACTTACTA
CTAATTTAATGCATTTTTAACAACTTTAAGCTACACAAGCCAAAACTAATGGGTATTTTATAGTCCT
ATTTAACCCCTTTAACGAATGCATCCTTTTACCTTTTTTGGTCACGGCAGCTGAACTCTGCCCTTT
CGTTGGGGGTGACTCCTCCCTCCCGTACTCCCTCCCTCCCTCCCCTCCCTCTCCGCGCCACAGT
CGACCTTGTCAAGTACCTTGTTAGCTGTTGGGCAAATGTGCCACACAAGTGGCTCACATCAGCG
GGATCGAAAATAAAAAGCGAAACGCATCGAGAACTTCCCAAGAAAACGGCGAGTCAAAGTTGAG
AAAACGCTGCTTCCGTTTAATTGACAATTGAACCCGAACCCGGACCGAACTCCTGGAGAATATGT
ACG

Figure 2.15 (cont.) Bioinformatic analyses of the u8772 220bp and the d5778 850bp enhancers reveal potential binding sites for Su(H) in both enhancers. Position weight matrices for Su(H) binding from A. Fly Factor Survey and B. from JASPAR. C. Su(H) binding consensus inferred from the matrix in A. D. Su(H) binding consensus inferred from the matrix in B. E. Su(H) binding consensus motif incorporating common elements from C and D used as input for the Sequence Manipulation Suite DNA Pattern Find program. F. Potential Su(H) binding sites found in the u8772 220bp enhancer. G. Potential Su(H) binding sites found in the d5778 850bp enhancer.

A.

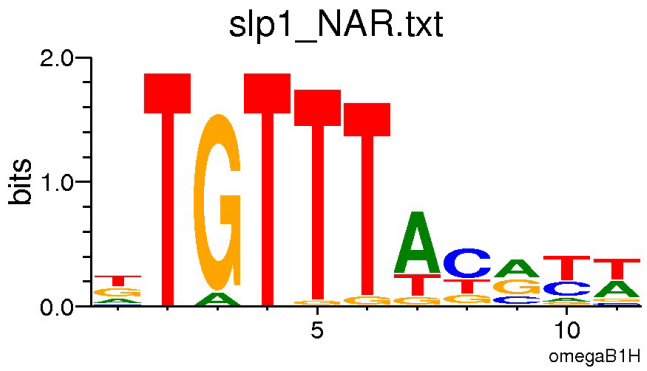

B. Consensus Slp1 binding site based on PWM from JASPAR used as SMS

TGTT[GT][ATG][CTG][AGCT][TCA]

C. u8772 220bp wild type enhancer sequence with Slp1 sites highlighted

Sequence

GAATCGAGTGGTGAGCGATAGTTTTCACATGTTTTGTTCGAGCATTAATTCCGTTTAAATGATTTC
CGCAACAGATTTGAGCTTTGCACGTAATCAAGTGGAAATGAATTTGACCAACACAAGAGGTTTATA
CACACATCACATTTTCTGCCTTTATGTTTTTGCGGTGTCCCATTAGTTTGATTGTTTCGAAGGCCA
CTGAGCCGTGAAAAATATCAGA

Figure 2.16

D. d5778 850 bp wild type enhancer with Slp1 site highlighted

Sequences

CATTAACTCGAGTCTGGTTTCCGATTCCGATTTCGCTTCCTCCTGCCAACTTATTTCTATATCTTC
TCCCTTTGTGCCCTGTGTGTGTGAAACAAAAACGTTTGTTTCAATACGTTGGCTTCGTGCATTTTA
CGGTGTTGGGAAACAGACGAAATGGACTCATTGATTCCAATTGACTGATTTCAATTGATGTTAAG
TGTCTGCCACAGTCGCAGCCGCAAATTCAGTGGCACAACTCCGTCGCAGCCAAATGCCATTTGC
TTTTCACATCCAGGTCGAACGGCGTTGCCTTGTTGACTTTGTTTTTGCTACTCATTGCCGCGATTT
GGGTTAGGCATGGGGTATGTGCGCACTGTGGGAACTTTGGATTACTCAGATGAAACAGCATTTA
GGACACTATGCAGCTGGAAAGATAAACTAGTTGATAGCTACTCATTTACTCATTTACTACTTACTA
CTAATTTAATGCATTTTTAACAACTTTAAGCTACACAAGCCAAAACTAATGGGTATTTTATAGTCCT
ATTTAACCCCTTTAACGAATGCATCCTTTTACCTTTTTTGGTCACGGCAGCTGAACTCTGCCCTTT
CGTTGGGGGTGACTCCTCCCTCCCGTACTCCCTCCCTCCCTCCCCTCCCTCTCCGCGCCACAGT
CGACCTTGTCAAGTACCTTGTTAGCTGTTGGGCAAATGTGCCACACAAGTGGCTCACATCAGCG
GGATCGAAAATAAAAAGCGAAACGCATCGAGAACTTCCCAAGAAAACGGCGAGTCAAAGTTGAG
AAAACGCTGCTTCCGTTTAATTGACAATTGAACCCGAACCCGGACCGAACTCCTGGAGAATATGT
ACG

Figure 2.16 (cont.) Bioinformatic analyses of the u8772 220bp and the d5778 850bp enhancers reveal potential binding sites for Slp1 in both enhancers. A. Position weight matrix of Slp1 binding from JASPAR and Fly Factor Survey. B. Slp1 D.N.A. binding consensus motif inferred from A. The same consensus was used as input for the Sequence Manipulation Suite DNA Pattern Find program. C. Potential Slp1 binding sites found in the u8772 220bp enhancer using the consensus in B. D. Potential Slp1 binding sites found in the d5778 850bp enhancer using the consensus in B.

A

B. Consensus vnd/Scro binding site based on PWM used as SMS input

[TAC][CTG][AG]AG[TA][GA]

C. u8772 220bp wild type enhancer sequence with vnd/Scro site highlighted

Sequence

GAATCGAGTGGTGAGCGATAGTTTTCACATGTTTTGTTCGAGCATTAATTCCGTTTAAATGATTTC
CGCAACAGATTTGAGCTTTGCACGTAATCAAGTGGAAATGAATTTGACCAACACAAGAGGTTTAT
ACACACATCACATTTTCTGCCTTTATGTTTTTGCGGTGTCCCATTAGTTTGATTGTTTCGAAGGCC
ACTGAGCCGTGAAAAATATCAGA

Figure 2.17 Bioinformatic analyses of the u8772 220bp enhancer reveal potential binding sites for Scro. A. Position weight matrix of vnd binding from JASPAR. B. Consensus motif for vnd binding inferred from A. The same sequence was used as input in the Sequence Manipulation Suite DNA Pattern Find program. C. Potential vnd binding site within the u8772 enhancer that could be a site for Scro binding.

Transcription Factor	Position Weight Matrix	Pattern searched (SMS)
Bap	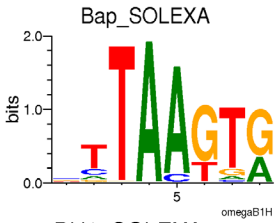	[TCA]TA[AC][GT][TGA][GA]
BH1	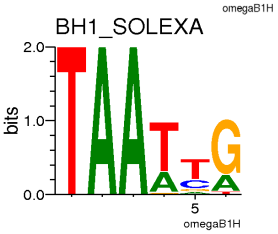	TAA[TA][TCG][GA]
BH2	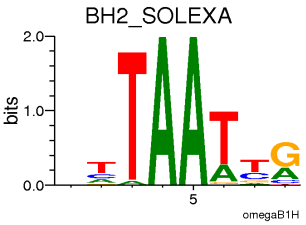	[TCA]TAA[TAG][TCG][GA]
Bsh	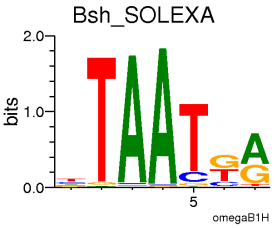	TAA[TCG][GTC][AG]
C15	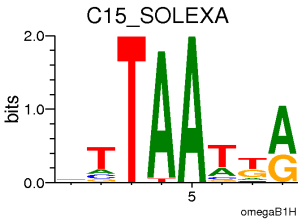	[TAGC]TAA[TAC][TGA][AG]
CG11085	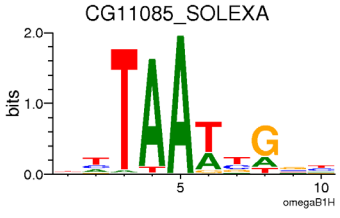	[TGA]T[AT]A[TAG][TC G][GAT] -

Figure 2.18.

Transcription Factor	Position Weight Matrix	Pattern searched (SMS)
CG15696	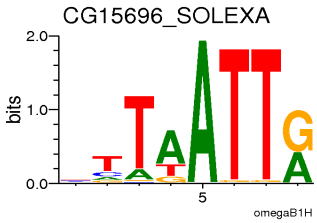	[TGAC][TAG][ATG]ATT[GA] -
CG18599	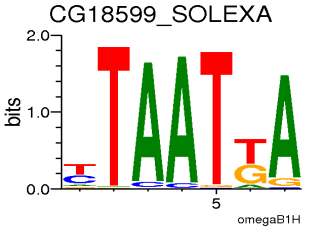	[TCAG]T[AC][AC][TG][TGA][AG] -
CG34031	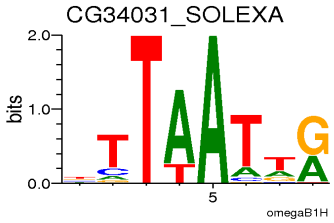	[T CAG]T[AT]A[TAC][TAG][- -
DII	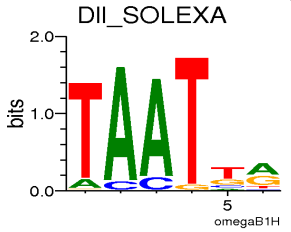	[TA][AC][AC][TG][TGC][AGT] -
Dr	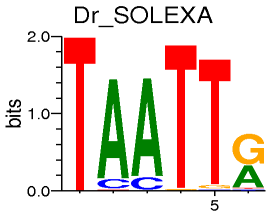	T[AC][AC]T[TG][GA]
E5	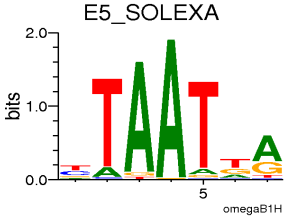	[TCG][TA][AGT]A[TAG][TGA][AGT] -

Figure 2.18 (cont.)

Transcription Factor	Position Weight Matrix	Pattern searched (SMS)
Ems	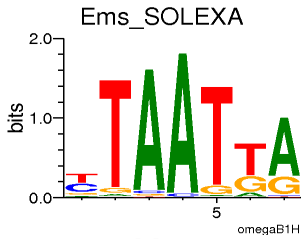	[TCG][TGA][AGC]A[TG][TGA][AG] -
Exex	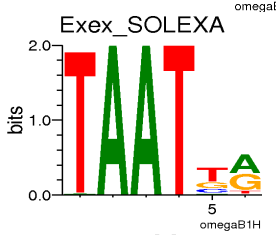	TAAT[TGC][AGT]
Hgtx	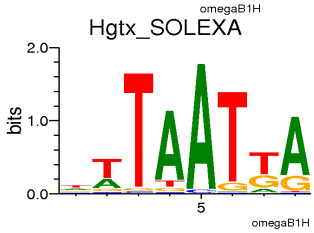	[TAG]T[ATG]A[TG][TGA][AG] -
Hmx	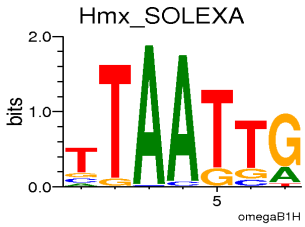	[TGCA][TG]A[AC][TG][TGC][GAT] -
inv	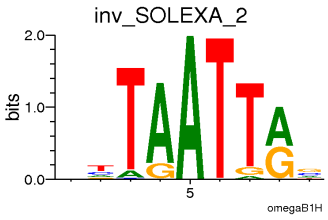	[TA][AG]AT[TGA][AG]
NK7.1	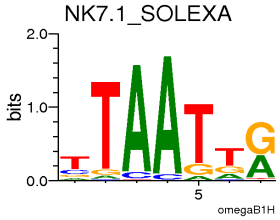	[TCGA][TGA][AC][AC][TGA][TGA][GA] -

Figure 2.18 (cont.)

Transcription Factor	Position Weight Matrix	Pattern searched (SMS)
Unpg	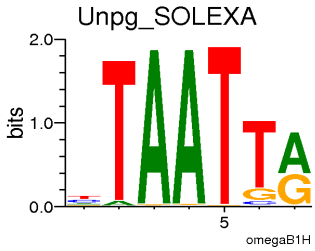	[TA]AAT[TGC][AG]
Vnd	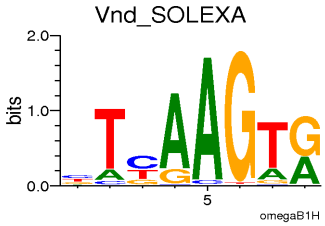	[TAC][CT - G][AG][AG]G[TAG][GA]

Figure 2.18 (cont.) NK-2 family transcription factors with known binding consensus motifs were used to identify potential Scro binding sites in the d5778 850bp enhancer. The transcription factor is listed in the column to the left. Its position weight matrix, from Fly Factor Survey, is shown in the column in the middle. The consensus binding motif of the transcription factor inferred from the position weight matrix and used as input for the Sequence Manipulation Suite DNA Pattern Find program is listed in the column on the right.

d5778 850bp Wild type enhancer with Scro binding sites highlighted

Sequence

CATTAACTCGAGTCTGGTTTCCGATTCCGATTTCGCTTCCTCCTGCCAACTTATTTCTATATCTTC
TCCCTTTGTGCCCTGTGTGTGTGAAACAAAAACGTTTGTTTCAATACGTTGGCTTCGTGCATTTTA
CGGTGTTGGGAAACAGACGAAATGGACTCATTGATTCCAATTGACTGATTTCAATTGATGTTAAG
TGTCTGCCACAGTCGCAGCCGCAAATTCAGTGGCACAACTCCGTCGCAGCCAAATGCCATTTGC
TTTTCACATCCAGGTCGAACGGCGTTGCCTTGTTGACTTTGTTTTTGCTACTCATTGCCGCGATTT
GGGTTAGGCATGGGGTATGTGCGCACTGTGGGAACTTTGGATTACTCAGATGAAACAGCATTTA
GGACACTATGCAGCTGGAAAGATAAACTAGTTGATAGCTACTCATTTACTCATTTACTACTTACTA
CTAATTTAATGCATTTTTAACAACTTTAAGCTACACAAGCCAAAACTAATGGGTATTTTATAGTCCT
ATTTAACCCCTTTAACGAATGCATCCTTTTACCTTTTTTGGTCACGGCAGCTGAACTCTGCCCTTT
CGTTGGGGGTGACTCCTCCCTCCCGTACTCCCTCCCTCCCTCCCCTCCCTCTCCGCGCCACAGT
CGACCTTGTCAAGTACCTTGTTAGCTGTTGGGCAAATGTGCCACACAAGTGGCTCACATCAGCG
GGATCGAAAATAAAAAGCGAAACGCATCGAGAACTTCCCAAGAAAACGGCGAGTCAAAGTTGAG
AAAACGCTGCTTCCGTTTAATTGACAATTGAACCCGAACCCGGACCGAACTCCTGGAGAATATGT
ACG

Figure 2.19. Most commonly occurring sites for NK-2 transcription factors' binding were shortlisted as likely Scro binding sites in the d5778 850bp enhancer. Potential Scro binding sites in the d5778 enhancer were identified based on the most commonly occurring binding sites of related NK-2 family transcription factors (see main text for method details) highlighted in magenta.

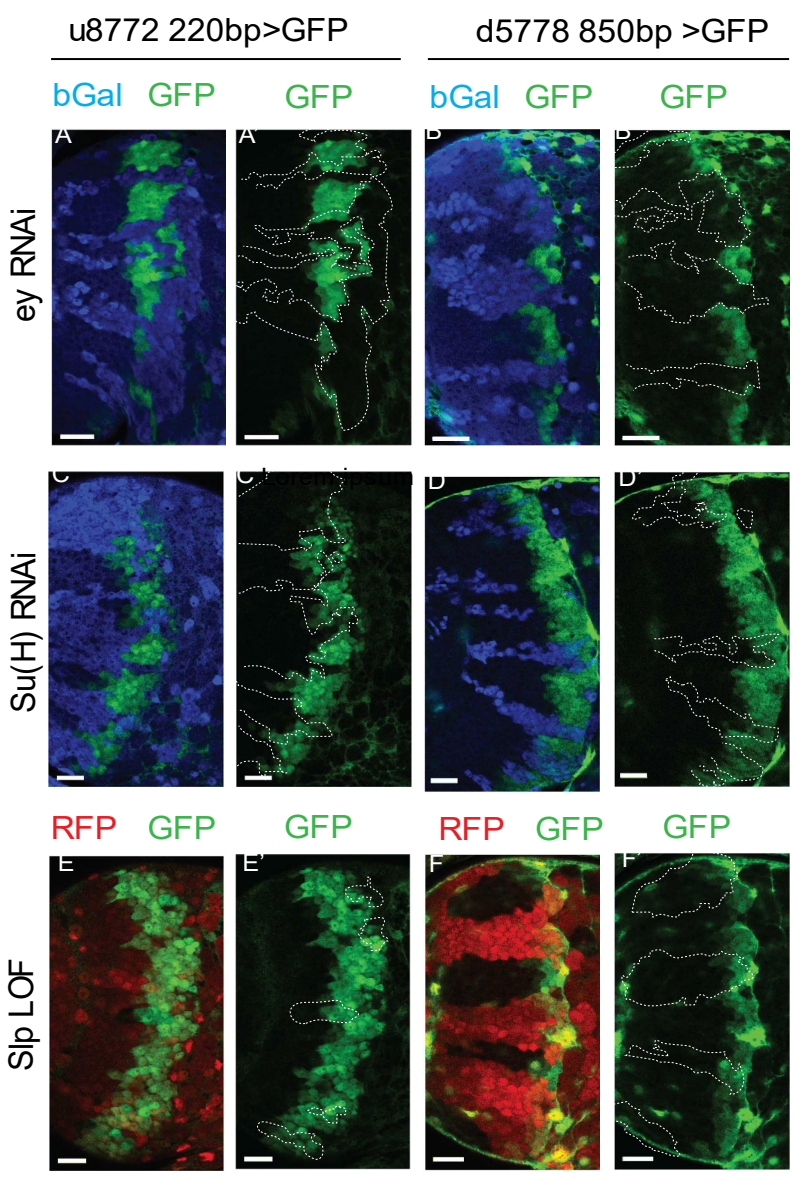

Figure 2.20 Eyeless and the Notch pathway act through the 220 bp and 850 bp enhancers to regulate the expression of *slp* genes. (A-D') RNAi clones in which Ey or Su(H) is knocked down are marked by *Beta-galactosidase* (*bGal*) in blue, while regions unmarked by *bGal* are populated by wild type neuroblasts. (A, A') Observed expression of a GFP reporter driven by the 220 bp enhancer element in *Ey RNAi* clones and wild-

Figure 2.20 (cont.) type neuroblasts. (B, B') Observed expression of a GFP reporter driven by the 850 bp enhancer element in *Ey RNAi* knockdown clones and wild-type neuroblasts. In the case of both enhancers, knockdown of Ey leads to a loss of GFP reporter expression. (C, C') The expression of the GFP reporter driven by the 220bp enhancer in Su(H) RNAi clones and wild-type neuroblasts. (D, D') The expression of the GFP reporter driven by the 850bp enhancer in Su(H) RNAi clones and wild-type neuroblasts. In the case of both enhancers, the expression of the GFP reporter is lost or delayed. (E, E') The 220 bp GFP reporter was expressed in *slp1* and *slp2* loss of function mitotic clones ('dark' regions) and wild-type neuroblasts (marked by RFP). (F, F') Expression of the 850 bp enhancer GFP reporter in *slp* LOF clones and wild-type neuroblasts similar to (E, E'). Slp1 binding sites were identified in both enhancer elements, which indicate that Slp1 may auto-regulate its expression. However, GFP reporter expression driven by these two enhancers is not significantly affected within *slp* LOF neuroblasts, suggesting that Slp1/2 are not required to initiate their expression in neuroblasts. Scale bar 20 microns.

A. u8772 220bp wild type enhancer sequence with Ey sites highlighted

Sequence

GAATCGAGTGGTGAGCGATAGTTTTCACATGTTTTGTTCGAGCATTAATTCCGTTTAAATGATTTC
CGCAACAGATTTGAGCTTTGCACGTAATCAAGTGGAAATGAATTTGACCAACACAAGAGGTTTAT
ACACACATCACATTTTCTGCCTTTATGTTTTTGCGGTGTCCCATTAGTTTGATTGTTTCGAAGGCC
ACTGAGCCGTGAAAAATATCAGA

B. Ey binding site sequence	Strand	Mutated to
TAATTCCGTTTAAATGATT	+	Deleted
TTCGAAGGCCACTGAGCCGTGAA	+	TTCGAAGGCCACATAGCCGTGAA

C. u8772 220bp wild type enhancer sequence with Ey sites mutated

Sequence

GAATCGAGTGGTGAGCGATAGTTTTCACATGTTTTGTTCGAGCATTCCGCAACAGATTTGAGCTTT
GCACGTAATCAAGTGGAAATGAATTTGACCAACACAAGAGGTTTATACACACATCACATTTTCTGC
CTTTATGTTTTTGCGGTGTCCCATTAGTTTGATTGTTTCGAAGGCCACATAGCCGTGAAAAATATC
AGA

Figure 2.21 Mutagenesis of potential Ey binding sites in the u8772 220bp enhancer.

A. Potential Ey binding sites identified within u8772 220bp enhancer highlighted. B. Table shows the mutations made to the identified Ey binding sites in the final DNA gene block. C. Sequence of the Ey mutation gBlock used for transgenesis and mutagenesis studies.

A. d5778 wild type enhancer with Ey sites highlighted

Sequence

CATTAACTCGAGTCTGGTTTCCGATTCCGATTTCGCTTCCTCCTGCCAACTTATTTCTATATCTTC
TCCCTTTGTGCCCTGTGTGTGTGAAACAAAAACGTTTGTTTCAATACGTTGGCTTCGTGCATTTTA
CGGTGTTGGGAAACAGACGAAATGGACTCATTGATTCCAATTGACTGATTTCAATTGATGTTAAG
TGTCTGCCACAGTCGCAGCCGCAAATTCAGTGGCACAACTCCGTCGCAGCCAAATGCCATTTGC
TTTTCACATCCAGGTCGAACGGCGTTGCCTTGTTGACTTTGTTTTTGCTACTCATTGCCGCGATTT
GGGTTAGGCATGGGGTATGTGCGCACTGTGGGAACTTTGGATTACTCAGATGAAACAGCATTTA
GGACACTATGCAGCTGGAAAGATAAACTAGTTGATAGCTACTCATTTACTCATTTACTACTTACTA
CTAATTTAATGCATTTTTAACAACTTTAAGCTACACAAGCCAAAACTAATGGGTATTTTATAGTCCT
ATTTAACCCCTTTAACGAATGCATCCTTTTACCTTTTTTGGTCACGGCAGCTGAACTCTGCCCTTT
CGTTGGGGGTGACTCCTCCCTCCCGTACTCCCTCCCTCCCTCCCCTCCCTCTCCGCGCCACAGT
CGACCTTGTCAAGTACCTTGTTAGCTGTTGGGCAAATGTGCCACACAAGTGGCTCACATCAGCG
GGATCGAAAATAAAAAGCGAAACGCATCGAGAACTTCCCAAGAAAACGGCGAGTCAAAGTTGAG
AAAACGCTGCTTCCGTTTAATTGACAATTGAACCCGAACCCGGACCGAACTCCTGGAGAATATGT
ACG

B. Ey binding site sequence	Strand	Mutated to
TTTGTGCCCTGTGTGTG	+	TATGTGGCTTGTGTGTG
TGATTCCAATTGACTGATTTC	+	deleted
TGCCACACAAGTGGCTCACAT	-	deleted

Figure 2.22

C. d5778 gBlock with Ey sites mutated

Sequence

CATTAACTCGAGTCTGGTTTCCGATTCCGATTTCGCTTCCTCCTGCCAACTTATTTCTATATCTTC
TCCCTATGTGGCTTGTGTGTGTGAAACAAAAACGTTTGTTTCAATACGTTGGCTTCGTGCATTTT
ACGGTGTTGGGAAACAGACGAAATGGACTCATAATTGATGTTAAGTGTCTGCCACAGTCGCAGC
CGCAAATTCAGTGGCACAACTCCGTCGCAGCCAAATGCCATTTGCTTTTCACATCCAGGTCGAA
CGGCGTTGCCTTGTTGACTTTGTTTTTGCTACTCATTGCCGCGATTTGGGTTAGGCATGGGGTA
TGTGCGCACTGTGGGAACTTTGGATTACTCAGATGAAACAGCATTTAGGACACTATGCAGCTGG
AAAGATAAACTAGTTGATAGCTACTCATTTACTCATTTACTACTTACTACTAATTTAATGCATTTTT
AACAACTTTAAGCTACACAAGCCAAAACTAATGGGTATTTTATAGTCCTATTTAACCCCTTTAACG
AATGCATCCTTTTACCTTTTTTGGTCACGGCAGCTGAACTCTGCCCTTTCGTTGGGGGTGACTC
CTCCCTCCCGTACTCCCTCCCTCCCTCCCCTCCCTCTCCGCGCCACAGTCGACCTTGTCAAGTA
CCTTGTTAGCTGTTGGGCAAATGCAGCGGGATCGAAAATAAAAAGCGAAACGCATCGAGAACTT
CCCAAGAAAACGGCGAGTCAAAGTTGAGAAAACGCTGCTTCCGTTTAATTGACAATTGAACCCG
AACCCGGACCGAACTCCTGGAGAATATGTACG

Figure 2.22 (cont.) Mutagenesis of potential Ey binding sites in the d5778 850bp enhancer. A. Potential Ey binding sites identified within d5778 850bp enhancer highlighted. B. Table shows the mutations made to the identified Ey binding sites in the final DNA gene block. C. Sequence of gene block with Ey sites mutated, used for transgenesis and mutagenesis studies.

A. u8772 220bp wild type enhancer sequence with Su(H) sites highlighted

Sequence

GAATCGAGTGGTGAGCGATAGTTTTCACATGTTTTGTTCGAGCATTAATTCCGTTTAAATGATTTC
CGCAACAGATTTGAGCTTTGCACGTAATCAAGTGGAAATGAATTTGACCAACACAAGAGGTTTATA
CACACATCACATTTTCTGCCTTTATGTTTTTGCGGTGTCCCATTAGTTTGATTGTTTCGAAGGCCA
CTGAGCCGTGAAAAATATCAGA

B. Su(H) binding site	Strand	Mutated to
TAGTTTTCACATGT	+	CTAGGAGACGATGT
AGCTTTGCACGTAA	+	AGCTTAGACTGTAA
TCAAGTGGAAaTGAATTT	-	TCAAGCGTAAGTGGATTT
GCCGTGAAAAATA	-	GCCGTAAAGCGAG

C. u8772 220bp enhancer with Su(H) sites mutated

Sequence

GAATCGAGTGGTGAGCGACTAGGAGACGATGTTTTGTTCGAGCATTAATTCCGTTTAAATGATTT
CCGCAACAGATTTGAGCTTAGACTGTAATCAAGCGTAAGTGGATTTGACCAACACAAGAGGTTTA
TACACACATCACATTTTCTGCCTTTATGTTTTTGCGGTGTCCCATTAGTTTGATTGTTTCGAAGGC
CACTGAGCCGTAAAGCGAGTCAGA

Figure 2.23 Mutagenesis of potential Su(H) binding sites in the u8772 220bp enhancer. A. Potential Su(H) binding sites identified within u8772 220bp enhancer highlighted. B. Table shows the mutations made to the identified Su(H) binding sites in the final gBlock DNA fragment. C. Sequence of the Su(H) mutation gene block used for transgenesis and mutagenesis studies.

A. d5778 850bp wild type enhancer with Su(H) sites highlighted

Sequence

CATTAACTCGAGTCTGGTTTCCGATTCCGATTTCGCTTCCTCCTGCCAACTTATTTCTATATCTTC
TCCCTTTGTGCCCTGTGTGTGTGAAACAAAAACGTTTGTTTCAATACGTTGGCTTCGTGCATTTTA
CGGTGTTGGGAAACAGACGAAATGGACTCATTGATTCCAATTGACTGATTTCAATTGATGTTAAG
TGTCTGCCACAGTCGCAGCCGCAAATTCAGTGGCACAACTCCGTCGCAGCCAAATGCCATTTGC
TTTTCACATCCAGGTCGAACGGCGTTGCCTTGTTGACTTTGTTTTTGCTACTCATTGCCGCGATTT
GGGTTAGGCATGGGGTATGTGCGCACTGTGGGAACTTTGGATTACTCAGATGAAACAGCATTTA
GGACACTATGCAGCTGGAAAGATAAACTAGTTGATAGCTACTCATTTACTCATTTACTACTTACTA
CTAATTTAATGCATTTTTAACAACTTTAAGCTACACAAGCCAAAACTAATGGGTATTTTATAGTCCT
ATTTAACCCCTTTAACGAATGCATCCTTTTACCTTTTTTGGTCACGGCAGCTGAACTCTGCCCTTT
CGTTGGGGGTGACTCCTCCCTCCCGTACTCCCTCCCTCCCTCCCCTCCCTCTCCGCGCCACAGT
CGACCTTGTCAAGTACCTTGTTAGCTGTTGGGCAAATGTGCCACACAAGTGGCTCACATCAGCG
GGATCGAAAATAAAAAGCGAAACGCATCGAGAACTTCCCAAGAAAACGGCGAGTCAAAGTTGAG
AAAACGCTGCTTCCGTTTAATTGACAATTGAACCCGAACCCGGACCGAACTCCTGGAGAATATGT
ACG

B. Su(H) binding site	Strand	Mutated to
TGTGTGTGTGAAACAAAAACG	-	TGTGTGTGTGCGTATCCAGCG
GCGCACTGTGGGAACTTTGGA	-	deleted
GCATTTTTAACAACTTTAAGC	+	deleted
CAAAGTTGAGAAAACGCTGCT	+	deleted

Figure 2.24

C. d5778 gBlock with Su(H) sites mutated

Sequence

CATTAACTCGAGTCTGGTTTCCGATTCCGATTTCGCTTCCTCCTGCCAACTTATTTCTATATCTTC
TCCCTTTGTGCCCTGTGTGTGTGCGTATCCAGCGTTTGTTTCAATACGTTGGCTTCGTGCATTTT
ACGGTGTTGGGAAACAGACGAAATGGACTCATTGATTCCAATTGACTGATTTCAATTGATGTTAA
GTGTCTGCCACAGTCGCAGCCGCAAATTCAGTGGCACAACTCCGTCGCAGCCAAATGCCATTTG
CTTTTCACATCCAGGTCGAACGGCGTTGCCTTGTTGACTTTGTTTTTGCTACTCATTGCCGCGAT
TTGGGTTAGGCATGGGGTATGTTTACTCAGATGAAACAGCATTTAGGACACTATGCAGCTGGAA
AGATAAACTAGTTGATAGCTACTCATTTACTCATTTACTACTTACTACTAATTTAATTACACAAGCC
AAAACTAATGGGTATTTTATAGTCCTATTTAACCCCTTTAACGAATGCATCCTTTTACCTTTTTTGG
TCACGGCAGCTGAACTCTGCCCTTTCGTTGGGGGTGACTCCTCCCTCCCGTACTCCCTCCCTCC
CTCCCCTCCCTCTCCGCGCCACAGTCGACCTTGTCAAGTACCTTGTTAGCTGTTGGGCAAATGT
GCCACACAAGTGGCTCACATCAGCGGGATCGAAAATAAAAAGCGAAACGCATCGAGAACTTCCC
AAGAAAACGGCGAGTTCCGTTTAATTGACAATTGAACCCGAACCCGGACCGAACTCCTGGAGAA
TATGTACG

Figure 2.24 (cont.) Mutagenesis of potential Su(H) binding sites in the d5778 850bp enhancer. A. Potential Su(H) binding sites identified within the d5778 850bp enhancer highlighted. B. Table showing the mutations made to the identified Su(H) binding sites in the final gBlock DNA fragment. C. Sequence of gene block with Su(H) sites mutated, used for transgenesis and mutagenesis studies.

A. u8772 220bp wild type enhancer sequence with Slp1 sites highlighted

Sequence

GAATCGAGTGGTGAGCGATAGTTTTCACATGTTTTGTTCGAGCATTAATTCCGTTTAAATGATTTC
CGCAACAGATTTGAGCTTTGCACGTAATCAAGTGGAAATGAATTTGACCAACACAAGAGGTTTAT
ACACACATCACATTTTCTGCCTTTATGTTTTTGCGGTGTCCCATTAGTTTGATTGTTTCGAAGGCC
ACTGAGCCGTGAAAAATATCAGA

B. Slp1 binding site	Strand	Mutated to
TGTTTTGTT	**+**	**TGTACCAAG**
TGACCAACA	**_**	**GATCGACTC**

C. u8772 220bp enhancer with Slp1 sites mutated

Sequence

GAATCGAGTGGTGAGCGATAGTTTTCACATGTACCAAGCGAGCATTAATTCCGTTTAAATGATTT
CCGCAACAGATTTGAGCTTTGCACGTAATCAAGTGGAAATGAATTGATCGACTCCAAGAGGTTTA
TACACACATCACATTTTCTGCCTTTATGTTTTTGCGGTGTCCCATTAGTTTGATTGTTTCGAAGGC
CACTGAGCCGTGAAAAATATCAGA

Figure 2.25 Mutagenesis of potential Slp1 binding sites in the u8772 220bp enhancer. A. Potential Slp1 binding sites identified within u8772 220bp enhancer highlighted. B. Table shows the mutations made to the identified Slp1 binding sites in the final gBlock DNA fragment. C. Sequence of gene block with Slp1 sites mutated, used for transgenesis and mutagenesis studies.

A. d5778 850 bp wild type enhancer with Slp1 site highlighted

Sequences

CATTAACTCGAGTCTGGTTTCCGATTCCGATTTCGCTTCCTCCTGCCAACTTATTTCTATATCTTC
TCCCTTTGTGCCCTGTGTGTGTGAAACAAAAACGTTTGTTTCAATACGTTGGCTTCGTGCATTTTA
CGGTGTTGGGAAACAGACGAAATGGACTCATTGATTCCAATTGACTGATTTCAATTGATGTTAAG
TGTCTGCCACAGTCGCAGCCGCAAATTCAGTGGCACAACTCCGTCGCAGCCAAATGCCATTTGC
TTTTCACATCCAGGTCGAACGGCGTTGCCTTGTTGACTTTGTTTTTGCTACTCATTGCCGCGATTT
GGGTTAGGCATGGGGTATGTGCGCACTGTGGGAACTTTGGATTACTCAGATGAAACAGCATTTA
GGACACTATGCAGCTGGAAAGATAAACTAGTTGATAGCTACTCATTTACTCATTTACTACTTACTA
CTAATTTAATGCATTTTTAACAACTTTAAGCTACACAAGCCAAAACTAATGGGTATTTTATAGTCCT
ATTTAACCCCTTTAACGAATGCATCCTTTTACCTTTTTTGGTCACGGCAGCTGAACTCTGCCCTTT
CGTTGGGGGTGACTCCTCCCTCCCGTACTCCCTCCCTCCCTCCCCTCCCTCTCCGCGCCACAGT
CGACCTTGTCAAGTACCTTGTTAGCTGTTGGGCAAATGTGCCACACAAGTGGCTCACATCAGCG
GGATCGAAAATAAAAAGCGAAACGCATCGAGAACTTCCCAAGAAAACGGCGAGTCAAAGTTGAG
AAAACGCTGCTTCCGTTTAATTGACAATTGAACCCGAACCCGGACCGAACTCCTGGAGAATATGT
ACG

B. Slp1 binding site	Strand	Mutated to
TGACTTTGTTTTTGCTACTCA	+	deleted

Figure 2.26

C. d5778 850 bp gBlock with Slp1 site mutated

Sequence

CATTAACTCGAGTCTGGTTTCCGATTCCGATTTCGCTTCCTCCTGCCAACTTATTTCTATATCTTC
TCCCTTTGTGCCCTGTGTGTGTGAAACAAAAACGTTTGTTTCAATACGTTGGCTTCGTGCATTTTA
CGGTGTTGGGAAACAGACGAAATGGACTCATTGATTCCAATTGACTGATTTCAATTGATGTTAAG
TGTCTGCCACAGTCGCAGCCGCAAATTCAGTGGCACAACTCCGTCGCAGCCAAATGCCATTTGC
TTTTCACATCCAGGTCGAACGGCGTTGCCTTGTTTGCCGCGATTTGGGTTAGGCATGGGGTATG
TGCGCACTGTGGGAACTTTGGATTACTCAGATGAAACAGCATTTAGGACACTATGCAGCTGGAAA
GATAAACTAGTTGATAGCTACTCATTTACTCATTTACTACTTACTACTAATTTAATGCATTTTTAACA
ACTTTAAGCTACACAAGCCAAAACTAATGGGTATTTTATAGTCCTATTTAACCCCTTTAACGAATG
CATCCTTTTACCTTTTTTGGTCACGGCAGCTGAACTCTGCCCTTTCGTTGGGGGTGACTCCTCCC
TCCCGTACTCCCTCCCTCCCTCCCCTCCCTCTCCGCGCCACAGTCGACCTTGTCAAGTACCTTG
TTAGCTGTTGGGCAAATGTGCCACACAAGTGGCTCACATCAGCGGGATCGAAAATAAAAAGCGA
AACGCATCGAGAACTTCCCAAGAAAACGGCGAGTCAAAGTTGAGAAAACGCTGCTTCCGTTTAAT
TGACAATTGAACCCGAACCCGGACCGAACTCCTGGAGAATATGTACG

Figure 2.26 (cont.) Mutagenesis of potential Slp1 binding sites in the d5778 850bp enhancer. A. Potential Slp1 binding sites identified within d5778 850bp enhancer highlighted. B. Table shows the mutations made to the identified Slp1 binding site in the final gBlock DNA fragment. C. Sequence of the gene block with Slp1 sites mutated, used for transgenesis and mutagenesis studies.

A. u8772 220bp wild type enhancer sequence with vnd/Scro site highlighted

Sequence

GAATCGAGTGGTGAGCGATAGTTTTCACATGTTTTGTTCGAGCATTAATTCCGTTTAAATGATTTC
CGCAACAGATTTGAGCTTTGCACGTAATCAAGTGGAAATGAATTTGACCAACACAAGAGGTTTAT
ACACACATCACATTTTCTGCCTTTATGTTTTTGCGGTGTCCCATTAGTTTGATTGTTTCGAAGGCC
ACTGAGCCGTGAAAAATATCAGA

B. Vnd/Scro binding site	Strand	Mutated to
TGCACGTAATCAAGTGGAAAT	+	Deleted

C. u8772 220bp enhancer with vnd/Scro site mutated

Sequence

GAATCGAGTGGTGAGCGATAGTTTTCACATGTTTTGTTCGAGCATTAATTCCGTTTAAATGATTTC
CGCAACAGATTTGAGCTTGAATTTGACCAACACAAGAGGTTTATACACACATCACATTTTCTGCCT
TTATGTTTTTGCGGTGTCCCATTAGTTTGATTGTTTCGAAGGCCACTGAGCCGTGAAAAATATCA
GA

Figure 2.27 Mutagenesis of potential vnd/Scro binding sites in the u8772 220bp enhancer. A. Potential vnd binding sites identified within u8772 220bp enhancer highlighted. B. Table shows the mutations made to the identified vnd binding site in the final gBlock DNA fragment. C. Sequence of the vnd/Scro site mutated gene block used for transgenesis and mutagenesis studies. Given the short length of the u8772 220bp enhancer and the relatedness of vnd and Scro proteins, the vnd binding site was assumed

Figure 2.27 (cont.) to be the most likely Scro binding. Scro binding consensus motifs were unavailable, necessitating an indirect identification method.

A. d5778 850bp Wild type enhancer with Scro binding sites highlighted

Sequence

CATTAACTCGAGTCTGGTTTCCGATTCCGATTTCGCTTCCTCCTGCCAACTTATTTCTATATCTTC
TCCCTTTGTGCCCTGTGTGTGTGAAACAAAAACGTTTGTTTCAATACGTTGGCTTCGTGCATTTTA
CGGTGTTGGGAAACAGACGAAATGGACTCATTGATTCCAATTGACTGATTTCAATTGATGTTAAG
TGTCTGCCACAGTCGCAGCCGCAAATTCAGTGGCACAACTCCGTCGCAGCCAAATGCCATTTGC
TTTTCACATCCAGGTCGAACGGCGTTGCCTTGTTGACTTTGTTTTTGCTACTCATTGCCGCGATTT
GGGTTAGGCATGGGGTATGTGCGCACTGTGGGAACTTTGGATTACTCAGATGAAACAGCATTTA
GGACACTATGCAGCTGGAAAGATAAACTAGTTGATAGCTACTCATTTACTCATTTACTACTTACTA
CTAATTTAATGCATTTTTAACAACTTTAAGCTACACAAGCCAAAACTAATGGGTATTTTATAGTCCT
ATTTAACCCCTTTAACGAATGCATCCTTTTACCTTTTTTGGTCACGGCAGCTGAACTCTGCCCTTT
CGTTGGGGGTGACTCCTCCCTCCCGTACTCCCTCCCTCCCTCCCCTCCCTCTCCGCGCCACAGT
CGACCTTGTCAAGTACCTTGTTAGCTGTTGGGCAAATGTGCCACACAAGTGGCTCACATCAGCG
GGATCGAAAATAAAAAGCGAAACGCATCGAGAACTTCCCAAGAAAACGGCGAGTCAAAGTTGAG
AAAACGCTGCTTCCGTTTAATTGACAATTGAACCCGAACCCGGACCGAACTCCTGGAGAATATGT
ACG

B. Putative Scro binding sites based on binding sites of NK7 transcription factors

Sequence	Strand	Mutated to
TTGATGTTAAGTGTCTGCCAC	+	Deleted
AACAGCATTTAGGACACTATG	_	Deleted
CAAGCCAAAACTAATGGGTAT	+	Deleted
CCTATTTAACCCCTTTAACGA	_	Deleted
TTGTCAAGTACCTTGTTAGCT	_	Deleted
CGTTTAATTGACAATTGAACC	_	Deleted

Figure 2.28

C. d5778 850bp enhancer with Scro sites mutated

Sequence

CATTAACTCGAGTCTGGTTTCCGATTCCGATTTCGCTTCCTCCTGCCAACTTATTTCTATATCTTC
TCCCTTGTGCCCTGTGTGTGTGAAACAAAAACGTTTGTTTCAATACGTTGGCTTCGTGCATTTTAC
GGTGTTGGGAAACAGACGAAATGGACTCATTGATTCCAATTGACTGATTTCAAAGTCGCAGCCG
CAAATTCAGTGGCACAACTCCGTCGCAGCCAAATGCCATTTGCTTTTCACATCCAGGTCGAACG
GCGTTGCCTTGTTGACTTTGTTTTTGCTACTCATTGCCGCGATTTGGGTTAGGCATGGGGTATGT
GCGCACTGTGGGAACTTTGGATTACTCAGATGACAGCTGGAAAGATAAACTAGTTGATAGCTACT
CATTTACTCATTTACTACTTACTACTAATTTAATGCATTTTTAACAACTTTAAGCTACATTTATAGTA
TGCATCCTTTTACCTTTTTTGGTCACGGCAGCTGAACTCTGCCCTTTCGTTGGGGGTGACTCCTC
CCTCCCGTACTCCCTCCCTCCCTCCCCTCCCTCTCCGCGCCACAGTCGACCGTTGGGCAAATGT
GCCACACAAGTGGCTCACATCAGCGGGATCGAAAATAAAAAGCGAAACGCATCGAGAACTTCCC
AAGAAAACGGCGAGTCAAAGTTGAGAAAACGCTGCTTCCGAACCCGGACCGAACTCCTGGAGAA
TATGTACG

Figure 2.28 (cont.) Mutagenesis of potential Scro binding sites in the d5778 850bp enhancer. A. Potential Scro binding sites identified within d5778 850bp enhancer highlighted. B. Table shows the mutations made to the identified Scro binding sites in the final gBlock DNA fragment. C. Sequence of the Scro binding site mutation gBlock used for transgenesis and mutagenesis studies. Scro binding consensus motifs were unavailable. Most common binding sites of related NK-2 family transcription factors were used as most likely Scro binding sites (see methods for details).

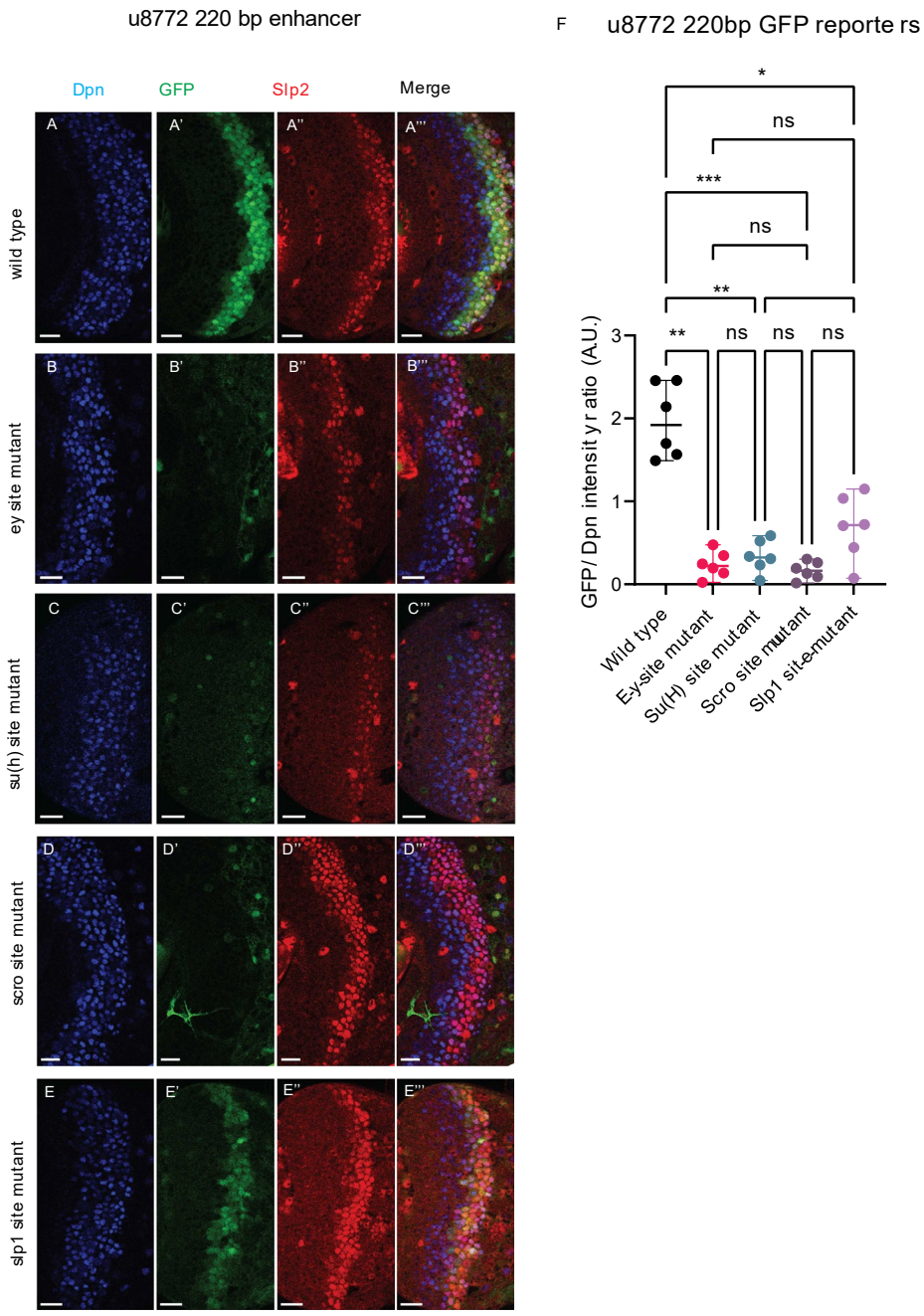

Figure 2.29 Mutations of putative binding sites for Ey, Su(H), and Scro in u8772 220 bp enhancer confirm their requirement for activating expressions of Slp1/2 genes.

The expression of GFP reporter driven by the wild-type 220 bp enhancer (A-A''') was compared against GFP reporters driven by mutated versions of the 220 bp enhancer.

Figure 2. 29 (cont.) Predicted binding sites for specific transcription factors were mutated. (B-B’’’) 220 bp enhancer with predicted ey binding sites mutated, (C-C’’’) with predicted Su(H) binding sites mutated, (D-D’’) with predicted Scro binding sites mutated, (E-E’’’) with predicted Slp1 binding sites mutated. Mutation of binding sites for Ey, Su(H), and Scro in the 220 bp enhancer led to a loss of GFP reporter expression. Scale bar: 20 microns. F. Intensity comparisons of mutated and wild type GFP reporters of the u8772 220bp enhancer. The intensities of GFP expression from mutated variants of the 220bp enhancer are significantly less relative to the wild-type enhancer. One-way ANOVA Tukey’s multiple comparison test, adjusted p-value for Ey mutant = 0.0013, for Su(H) mutant=0.0032, for Scro site mutant =0.0007, for Slp1 site mutant = 0.0225, n=6). Graphs indicate the mean and 95% CI and distributions of each data point about the mean.

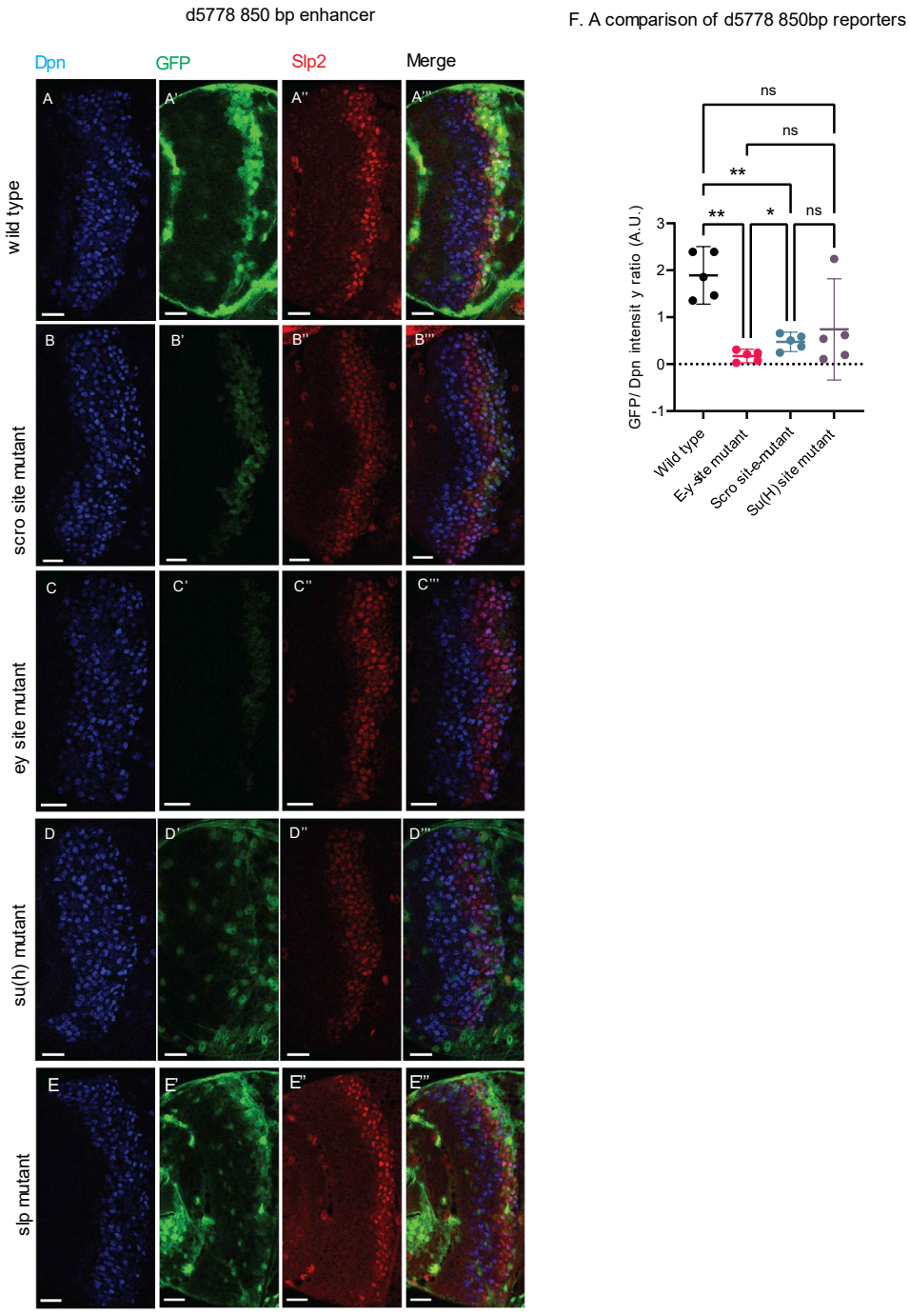

Figure 2.30 Mutations of putative binding sites for Ey, Su(H), and Scro in d5778 850 bp enhancer confirm their requirement for activating expressions of *slp1.2* genes. A parallel comparison was made for GFP reporter expression driven by the wild type 850 bp enhancer (A-A'') to the same GFP reporter expression driven by versions of the 850

Figure 2.30 (cont.) bp enhancer with binding sites for specific transcription factors Scro, Ey, and Su(H) mutated (B-B’’’, C-C’’’ and D-D’’’ respectively). Loss of binding sites for Ey nearly obliterated GFP reporter expression in neuroblasts, as did the loss of Su(H) binding sites. Additionally, in Su(H) binding site mutant, the expression of GFP reporter has intensified in surface glial cells. Loss of potential Scro binding sites also greatly reduced GFP reporter expression. Loss of Slp1 binding sites had a much less pronounced effect on GFP reporter intensity and did not significantly reduce the intensity (E-E’’’). Scale bars: 20 microns. F. Quantitation of d5778 850bp reporter intensities of the wild type and the factor binding site mutated variants shows that the reduction of GFP intensity compared to wild type for Ey binding site and Scro binding site mutated reporters is statistically significant (one-way ANOVA and Tukey’s multiple comparison test performed, adjusted p-value for Ey mutant= 0.0027, the adjusted p-value for Scro mutant = 0.0087). For the Su(H) site mutated variant, though GFP expression was visibly reduced in neuroblasts, the unavoidable contributions of GFP signals from surface glial cells have confounded our measurements of GFP reporter intensity, making GFP signals from neuroblasts appear stronger than they are, and the intensity reduction relative to wild type statistically insignificant.

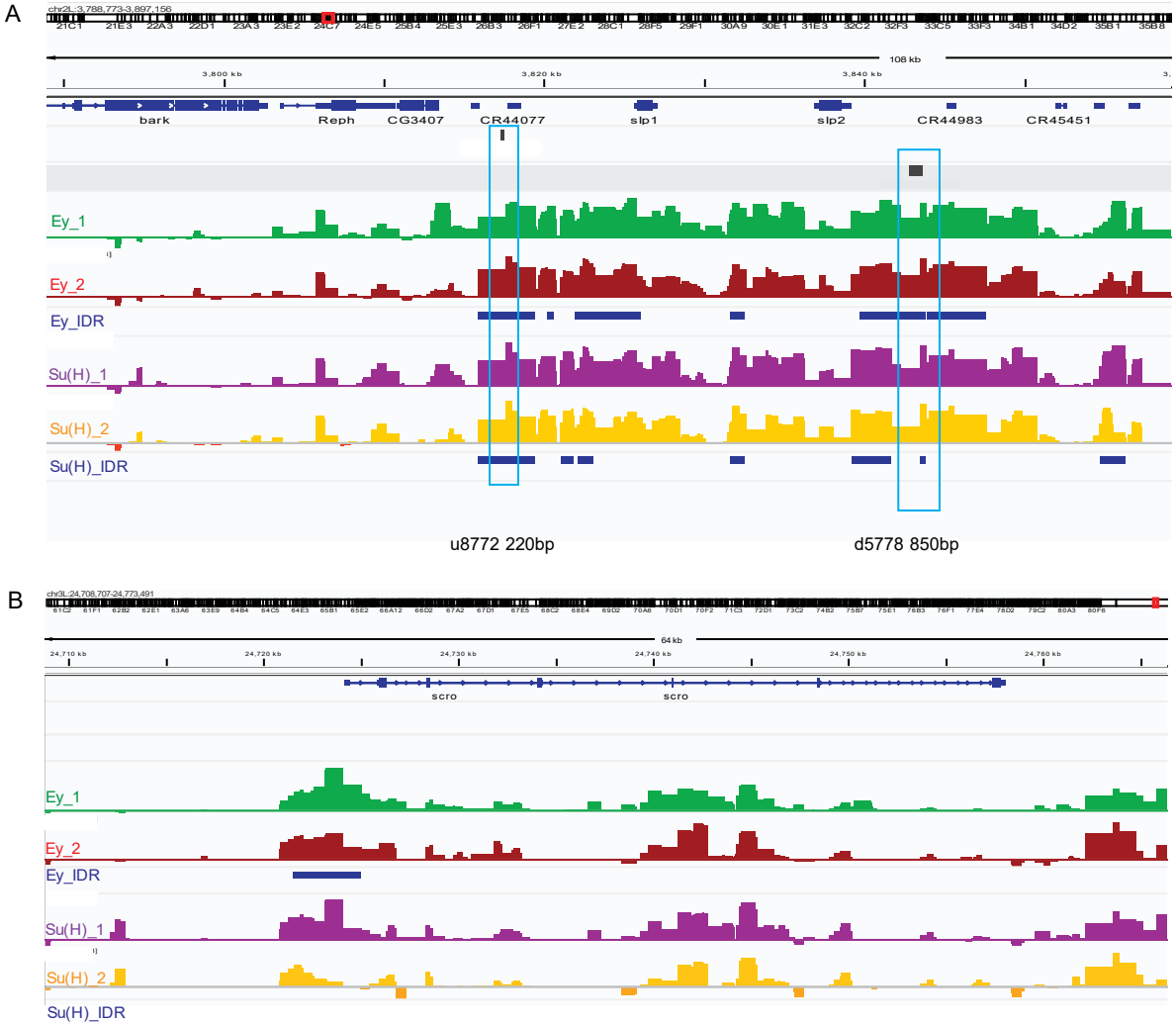

Figure 2.31 Genome-wide binding of Ey and Su(H) observed by DamID-seq. A. Prominent peaks of Ey and Su(H) binding are seen in the neighborhood of the *slp1* and *slp2* gene loci, including at the genomic locations of identified 220bp and 850 bp enhancers in both replicates of Ey-Dam and Su(H)-Dam experiments. Peaks at the u8772 220bp and the d5778 850bp enhancers have passed IDR< 0.05 cut-off, supporting their reproducibility. B. Peaks for Ey and Su(H) binding are also observed in the vicinity of the

Figure 2.31 (cont.) *scarecrow* gene locus. However, IDR reproducible peaks were seen only for Ey binding at this position, suggesting that Ey may be more important for the activation of Scro expression.

A.

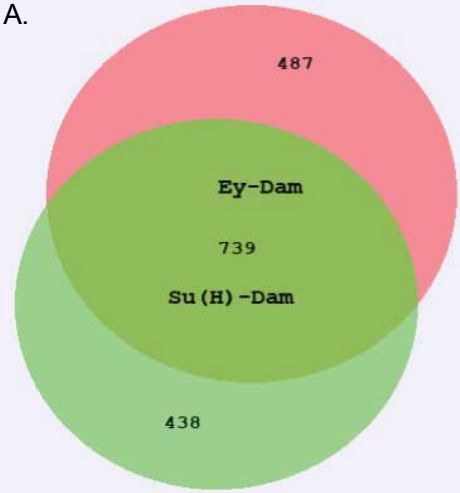

B. GO Term: Cell Division

Cyclin A (Cyc A)
Cyclin G (Cyc G)
Cyclin E (Cyc E)
diaphanous (dia)
pontin (pont)
peanut (pnut)
string (stg)

C. GO Term: Asymmetric Cell Division

CG3779-RB (numb)
G protein α i subunit
Notch (N)
brain tumor (brat)
frizzled (fz)
neuralized (neur)
prospero (pros)

D. GO Term: Apical Cell Polarity

Abl tyrosine kinase (Abl)
CG42684- RB
G protein α i subunit
TNF- receptor associated factor 4 (Traf4)
brain tumor (brat)

Figure 2.32 Many genes are bound by Dam-Ey and Dam-Su(H) in the medulla. A Venn diagram showing the overlap of genes bound by Dam-Ey (in green) and Dam-Su(H) (in pink) in the medulla is shown in (A). 739 of the 1177 genes bound by Dam-Ey and 739 of the 1226 genes bound by Su(H) are bound by both transcription factors. GO terms and associated biological processes that genes co-bound by both Dam-Ey and Dam-Su(H) participate in are shown in (B), (C), and (D).

Figure 2.33

Experiment	Forward Primer (5’ -> 3’)	Reverse Primer (5’ -> 3’)
Enhancer bashing GMR35H02		
Cloning R2.2	TTAGGCGCGCCAGTGCGTGTCTGCCCTTTCATTTTG	ATATATGCGGCCGCCCCAGCTAGCTCCCTTCACTCTTCT
Cloning L1.5	TTAGGCGCGCCGAATCGAAATGCTTCCCCGCCTCG	ATATATGCGGCCGCTGAACGTGCAACATCAAAGGCCGC
Cloning M1.0	TTAGGCGCGCCGCGGCCTTTGATGTTGCACGTTCA	ATATATGCGGCCGCGGACAGTTCGGAATGTGCCTCGA
Cloning slpf1	TTAGGCGCGCCGAATCGAGTGGTGAGCGATAG	ATATATGCGGCCGCTCTGATATTTTTCACGGCTCA
Cloning slpf2	TTAGGCGCGCCTTCGACCTTGTAGTGGCAAG	ATATATGCGGCCGCCGGAGATCGGAAGGTTAGTG
Cloning slpf3	TTAGGCGCGCCTCTCCTTGTTGCTCCTCACA	ATATATGCGGCCGCTGAACGTGCAACATCAAAGG
Enhancer bashing d5778 enhancer		
d5778 cloning	TTAGGCGCGCCTGGTCTTTTACGTTAATCTGGGCAGCT	ATATATGCGGCCGCACATTACGCATTGCATTCCTCCTCCTT
d5778f08	TTAGGCGCGCCCATTAACTCGAGTCTGGTTTCCGAT	ATATATGCGGCCGCCGTACATATTCTCCAGGAGTTCGGTC
Su(H) cloning in pUAST-attB-Dam	ATATATGCGGCCGCAAATGAAGAGCTACAGCCAATTTAATTTAAACGCCGCC	AAAATACTCGAGTCAGGATAAGCCGCTACCATGACTATTCCATTGC
CRISPR deletion of u8772 enhancer		
u8772 gRNA pCFD5		
Fragment 1	GCGGCCCGGGTTCGATTCCCGGCCGATGCATCGAAATTTCCTGGTATTCGGTTTTAGAGCTAGAAATAGCAAG	CGCCTCGCCCAAATGCATTTTGCACCAGCCGGGAATCGAACCC
Fragment 2	AAATGCATTTGGGCGAGGCGGTTTTAGAGCTAGAAATAGCAAG	TTAGTTTGATTGTTTCGAAGTGCACCAGCCGGGAATCGAACCC
Fragment 3	CTTCGAAACAATCAAACTAAGTTTTAGAGCTAGAAATAGCAAG	ATTTTAACTTGCTATTTCTAGCTCTAAAACAAACTGGAAGTCATTGACCCTGCACCAGCCGGGAATCGAACCC

Experiment	Forward Primer (5’ -> 3’)	Reverse Primer (5’ -> 3’)
Verifying u8772 deletion	TTGCAAATACTTTTTATTCAAGGAATCGAC	AATCTCAAGTTTGGTGTTTGTAATTTTTGG
CRISPR deletion of d5778 enhancer		
d5778 gRNA pCFD5		
Fragment 1	GCGGCCCGGGTTCGATTCCCGGCCGATGCAATAAGTCCTTGGGTAATACGGTTTTAGAGCTAGAAATAGCAAG	AACATTTATCTAGGACATCTTGCACCAGCCGGGAATCGAACCC
Fragment 2	AGATGTCCTAGATAAATGTTGTTTTAGAGCTAGAAATAGCAAG	TGTTGGCAAGCGGCGCTTCATGCACCAGCCGGGAATCGAACCC
Fragment 3	TGAAGCGCCGCTTGCCAACAGTTTTAGAGCTAGAAATAGCAAG	ATTTTAACTTGCTATTTCTAGCTCTAAAACTTTCGATATCCCAGCTCCTTTGCACCAGCCGGGAATCGAACCC
Verifying d5778 deletion	CTATTGAAGGGCGGACATATTAGACAACAATTGGATCGCTTG	CTGCATTCCATCCCGTCGCATCCTTGTC

Figure 2.33 (cont.) Sequences of primers used for the experiments described in the Methods section.

Eyeless gBlock for cloning into pUAST-attB-Dam

AGATCTGCGGCCGCAAATGTTTACATTGCAACCAACTCCAACTGCTATAGGCACCGTGGTTCCCC
CATGGTCAGCGGGAACATTGATAGAGCGCCTGCCGTCTTTAGAAGACATGGCTCACAAGGGTCA
CAGTGGAGTAAATCAGCTGGGTGGCGTTTTTGTTGGAGGAAGGCCTTTGCCAGATTCAACACGG
CAAAAAATTGTCGAACTGGCACATTCTGGAGCTCGGCCATGTGATATTTCTCGAATTCTGCAAGT
ATCAAATGGATGTGTGAGCAAAATTCTCGGGAGGTATTATGAAACAGGAAGCATACGACCACGTG
CTATCGGAGGATCCAAGCCACGTGTGGCCACAGCCGAAGTCGTTAGCAAAATTTCGCAGTACAA
ACGCGAGTGTCCTAGCATATTTGCTTGGGAAATTCGGGATAGATTACTTCAGGAGAACGTTTGTA
CTAACGATAATATACCAAGTGTGTCCTCAATAAACCGTGTATTGAGAAACTTGGCTGCGCAAAAG
GAGCAGCAAAGCACGGGATCCGGGAGCTCCAGCACATCCGCCGGCAACTCAATCAGCGCAAAA
GTGTCTGTCAGCATCGGTGGCAACGTGAGCAATGTGGCAAGCGGATCGAGAGGCACGTTGAGC
TCTTCCACCGATCTTATGCAGACAGCCACTCCTCTTAACTCTTCGGAAAGCGGTGGCGCAAGCAA
CTCCGGGGAGGGTAGTGAACAGGAGGCGATTTACGAGAAGCTTCGGCTGTTAAATACTCAGCAC
GCTGCAGGACCAGGACCACTGGAGCCTGCCAGAGCAGCGCCCTTGGTAGGTCAATCACCCAAC
CACCTAGGAACCCGATCCAGCCACCCCCAGCTGGTGCACGGTAACCATCAGGCACTACAGCAG
CATCAACAGCAGAGCTGGCCGCCCCGTCACTATTCCGGATCTTGGTACCCCACCTCTCTTAGCG
AAATACCCATCTCATCGGCTCCCAATATCGCATCCGTTACGGCGTATGCATCAGGACCTTCACTT
GCTCACTCACTGAGTCCACCCAACGACATCGAAAGCCTGGCCAGTATCGGTCACCAGAGAAACT
GCCCCGTTGCAACGGAGGACATACATTTAAAAAAAGAACTTGATGGTCATCAGTCCGATGAAACG
GGCTCCGGTGAAGGTGAAAACTCCAATGGTGGCGCTTCAAATATAGGAAACACTGAGGATGATC
AAGCTCGGCTCATACTAAAAAGAAAGTTGCAACGCAATCGAACATCTTTCACGAACGACCAGATA
GACAGTCTTGAAAAAGAGTTTGAACGAACACACTATCCAGATGTTTTTGCCCGCGAACGTTTGGC
TGGAAAGATTGGGTTGCCAGAGGCAAGAATTCAGGTTTGGTTCTCAAACCGTCGAGCAAAATGG
CGTCGCGAGGAGAAGCTGCGAAACCAGCGAAGAACACCAAATTCCACAGGAGCTAGTGCAACTT
CTTCCTCTACATCGGCAACCGCCTCTTTGACTGACAGCCCTAACAGCCTAAGTGCTTGTTCCTCG
CTGCTGTCCGGATCAGCTGGGGGTCCCTCAGTCAGTACCATTAATGGCTTATCGTCTCCAAGCA

Figure 2.34

CATTGTCTACTAATGTCAATGCTCCAACGCTTGGCGCTGGGATCGATAGCTCTGAAAGCCCAAC
ACCAATCCCGCACATTCGGCCTAGCTGCACCTCTGACAATGACAATGGTCGTCAAAGTGAAGAT
TGCAGAAGAGTTTGTTCTCCATGCCCACTTGGCGTTGGCGGGCATCAAAATACTCATCATATCC
AGAGCAATGGTCACGCCCAAGGTCATGCACTTGTTCCTGCCATTTCGCCACGACTCAATTTTAA
TAGTGGTAGTTTCGGCGCGATGTACTCCAACATGCATCATACGGCGTTATCCATGAGCGATTCA
TATGGGGCGGTTACGCCGATTCCGAGCTTTAACCACTCAGCTGTCGGTCCGCTGGCTCCGCCA
TCGCCAATACCGCAACAGGGCGATCTTACCCCTTCCTCGTTATATCCGTGCCACATGACCCTAC
GACCCCCTCCGATGGCTCCCGCTCACCATCACATCGTGCCGGGTGACGGTGGCAGACCTGCG
GGCGTTGGCCTAGGCAGTGGCCAATCTGCGAATTTGGGAGCAAGCTGCAGCGGATCGGGATA
CGAAGTGCTATCTGCCTACGCGTTGCCACCGCCCCCTATGGCGTCGAGCTCTGCTGCTGATTC
AAGCTTCTCAGCCGCGTCCAGTGCCAGCGCTAATGTGACCCCACATCACACCATAGCCCAAGA
ATCATGCCCCTCTCCGTGTTCAAGCGCGAGCCACTTTGGAGTTGCTCACAGTTCTGGGTTTTCG
TCCGACCCGATTTCACCGGCTGTATCTTCGTATGCACATATGAGCTACAATTACGCGTCGTCCG
CTAACACCATGACGCCTTCCTCCGCCAGCGGCACATCAGCACACGTGGCCCCGGGAAAACAAC
AGTTCTTCGCCTCCTGTTTCTACTCACCGTGGGTCTAGCTCGAGGGTACC

Figure 2.34 (cont.) Sequence of gene Block with *eyeless* coding sequences used for cloning into pUAST-attB-Dam vector (sequence continued from the previous page)

gRNA	Sequence (5’ -> 3’)
gRNA1	TCGAAATTTCCTGGTATTCGTGG
gRNA2	AAATGCATTTGGGCGAGGCGGGG
gRNA3	CTTCGAAACAATCAAACTAATGG
gRNA4	GGGTCAATGACTTCCAGTTTGGG

A. Sequences of gRNAs used for deleting the u8772 220bp enhancer.

gRNAs	Sequence (5’ -> 3’)
gRNA1	ATAAGTCCTTGGGTAATACG
gRNA2	AGATGTCCTAGATAAATGTT
gRNA3	TGAAGCGCCGCTTGCCAACA
gRNA4	AAGGAGCTGGGATATCGAAA

B. Sequences of gRNAs used for deleting the d5778 enhancer.

Figure 2.35 Sequences of gRNAs used to delete the two enhancers of *slp1/2* transcription in the medulla using CRISPR-Cas9.

A. Oligonucleotide injected with u8772 CRISPR injections
ATCCAAAATCAAAAGGAAATATATATACATATATTTACTTGAATCGAAATGCTTCCCCGCCTGGAA GTCATTGACCCAGTTACTTTTCAACTATATATTGAATTTATATATTTATGTATT

B. Oligonucleotide injected with d5778 CRISPR injections
TGGTCTTTTACGTTAATCTGGGCAGCTGGCCAGAAGTTGGCCAATAAGTCCTTGGGTAATAAAAG GAGGAGGAATGCAATGCGTAATGTATTAATTTCATTTATGGCCATATTTATTCTC

Figure 2.36 Oligonucleotides injected in embryos with gRNA expressing pCFD5 vectors for CRISPR deletion experiments.

A. Sequence containing the u8772-220bp enhancer deleted by CRISPR

CGCCTCGCCCAAATGCATTTGAATCGAGTGGTGAGCGATAGTTTTCACATGTTTTGTTCGAGCAT
TAATTCCGTTTAAATGATTTCCGCAACAGATTTGAGCTTTGCACGTAATCAAGTGGAAATGAATTT
GACCAACACAAGAGGTTTATACACACATCACATTTTCTGCCTTTATGTTTTTGCGGTGTCCCATTA
GTTTGATTGTTTCGAAGGCCACTGAGCCGTGAAAAATATCAGAGAAATAAAAATCGAAATACCGA
AATGAGCTGGTTTTTTGTTAGCGAAAGTGCAGATTTTTCAGGACTCGCAAAGGGATGTGATTGAA
GATCTTCAGGATATTTCAGCACATGCATCGATATTTGTCCCAAACTGGAAGTCATTGACCCAGTT
ACTTTT

B. Sequence containing the d5778-850bp enhancer deleted by CRISPR

GCAGCAGAAAAGGTCAAGGTATCTGAAAGTCTACACCTCGCATTTTCAATGGTCTTTTACGTTAA
TCTGGGCAGCTGGCCAGAAGTTGGCCAATAAGTCCTTGGGTAATACGAGGAGAACAAAAACAAG
TAAGGATAATATTTTCATAGGCAAAACAATTGTGGTTGTGCAAGGAAGTGACTTTTGGGAACGGG
AGGCACTTGCAGCTGCCCAAGTATATCCACCATATCCCATATCCTTTTTCCGAGTCCCTAATTTC
CTGGGAAAGCTTTCGGTGCAGTTCGCCAGCCAAAACACTTGAGCACTTAAAAAGGCGCATTAAC
TCGAGTCTGGTTTCCGATTCCGATTTCGCTTCCTCCTGCCAACTTATTTCTATATCTTCTCCCTTT
GTGCCCTGTGTGTGTGAAACAAAAACGTTTGTTTCAATACGTTGGCTTCGTGCATTTTACGGTGT
TGGGAAACAGACGAAATGGACTCATTGATTCCAATTGACTGATTTCAATTGATGTTAAGTGTCTG
CCACAGTCGCAGCCGCAAATTCAGTGGCACAACTCCGTCGCAGCCAAATGCCATTTGCTTTTCA
CATCCAGGTCGAACGGCGTTGCCTTGTTGACTTTGTTTTTGCTACTCATTGCCGCGATTTGGGTT
AGGCATGGGGTATGTGCGCACTGTGGGAACTTTGGATTACTCAGATGAAACAGCATTTAGGACA
CTATGCAGCTGGAAAGATAAACTAGTTGATAGCTACTCATTTACTCATTTACTACTTACTACTAATT
TAATGCATTTTTAACAACTTTAAGCTACACAAGCCAAAACTAATGGGTATTTTATAGTCCTATTTAA

Figure 2.37

B. Sequence containing the d5778-850bp enhancer deleted by CRISPR (cont.)

CCCCTTTAACGAATGCATCCTTTTACCTTTTTTGGTCACGGCAGCTGAACTCTGCCCTTTCGTTG
GGGGTGACTCCTCCCTCCCGTACTCCCTCCCTCCCTCCCCTCCCTCTCCGCGCCACAGTCGAC
CTTGTCAAGTACCTTGTTAGCTGTTGGGCAAATGTGCCACACAAGTGGCTCACATCAGCGGGAT
CGAAAATAAAAAGCGAAACGCATCGAGAACTTCCCAAGAAAACGGCGAGTCAAAGTTGAGAAAA
CGCTGCTTCCGTTTAATTGACAATTGAACCCGAACCCGGACCGAACTCCTGGAGAATATGTACG
CTGCTATCCGGCATAGTCGAGTCATCCCAAGTCATGCGCTTAATTTCCCGTTTAAAACGCCATTC
ATTCAATTAAGCGAATGAATTTGTGGCACGGCAGACGACAGCAGAAGTTTTTTTTTCCTGAAAGA
AGACTATCATCATTGAGATGCCCCGAGATCTCTCGGCTGGAGCTCCAGATCCGATGCGATCCAA
TCGGATGAGATGAGATCGTATGGAATAGGATGGAGCATGCGGGTCTCTGGGGTCTGTGGTCTT
TCGATCTTTTTGTCTGCCCCCGGGGGCTTTCTTCAGTAATCAGACGCGGGTCAAAATATTTACCA
CTTGACCCTATTGATTTAATTAAATAGTTTCAAGACATTCAACTGTTTGTTGGCCGCGCAAAATGA
ATTTCGTGTGCGAGATAACTCAGATACAGTAGCTGCAGTAGCTGATCAACTATCTTTCAGATATG
CGCACATTTCTCTCTCGTTTTGTCTCCGAGCTGTCAACACAGATTCCAAACTGCAGACGTGTTAA
TTAACGACAGAGTTAACTAATTGTTGTTAGCAAAATATTTTCGTAATTCGATACTAAATTCGAGTT
CCGCTCAACTTGCTTGCTTGTGGGCTTTTGTGTTGAACAGCACAAGACCTCAAGGAACAGTGGA
ACAGTGCTTCAAAGTGGGGAAAAACATCTTATAATCTAGATCATTTTTAAATTTCATAAAGTCTTT
GATTGAAATAAAACGTTTAAGTGAGGCAAGTTCGTATTATTATTAGAGAAAGATAACTAACCTTTT
TGGTTTATATTTAGGTCTTGAAGCACTGTTCCTGCTGTTTTCGCTGTTGACTGCCCATGAAACGC
TTAACTGCGAGTGGCAATTGGATACCTGGCTGAATCCAAATACGAATCTTAATCTGAATCTGCGA
GTCTTTGTGGCCAATGAACACGGCAGCGGCACAACACAAAAACTTAGCAGATACTCATGTTTTAT
TTGTGCATTTCGCGCGCGCGTTCCACTTGGAAATGCTCTGTGGCACCAAAAGGAGCCACTGATG
TCCAAAATCAAAATGGTTTCAGTTCGCCGGGGCAATGCCTAAAATGTTTCTTTGTTTTTGTGTTC
CCTGTTGGCAAGCGGCGCTTCA

Figure 2.37 (cont.) Genomic DNA sequences deleted in CRISPR experiments. A. Sequence surrounding u8772 220bp deleted. B. Sequence containing the d5778 enhancer deleted by CRISPR.

Chapter 3. The Notch pathway and the cell cycle regulate the expressions of Slp1 and Slp2 in medulla neuroblasts

Introduction

Neural progenitors divide mitotically simultaneously as they are temporally patterned and produce a definite number of progeny neurons during each temporal patterning transcription factor (TTF) expression window. It has thus been speculated whether the cell cycle in neuroblasts represents an inherent timing mechanism determining the duration over which a particular TTF is expressed (Grosskortenhaus, Pearson et al. 2005). If true, this implies that loss of function of cell cycle regulators should impair temporal patterning. In the embryonic fly ventral nerve cord (VNC) temporal program, cytokinesis is required for transitioning from Hunchback (Hb) to Kruppel (Kr) expression. This observed dependence is because the mRNA of a switching factor Seven-up (Svp), which facilitates this transition (Grosskortenhaus, Pearson et al. 2005), is exported outside of the nucleus for translation in a cytokinesis-dependent manner. Except for this early transition in larval VNC neuroblasts (NBs), the expression of later TTFs proceeds normally in G2 arrested neuroblasts (Mettler, Vogler et al. 2006). In larval VNC NBs, a timely transition from the Imp /Castor/Chinmo to Syncrip/Broad stage (van den Ameele and Brand 2019) is also cell-cycle dependent though the cause for this dependence isn't clear. These results suggest that the requirement of cell-cycle progression varies depending on the specific temporal transition. In temporally patterned vertebrate cortical progenitors, however, the transition from generating deep layer neurons to generating upper layer neurons is unaffected by blocking cell cycle progression in progenitors with

constitutively active Notch signaling (Okamoto, Miyata et al. 2016). While suggesting that the cell cycle does not regulate temporal patterning in vertebrates, this observation does not rule out that active Notch signaling may enable temporal transitions even in the absence of cell cycle progression.

Notch signaling plays critical pleiotropic roles in neurogenesis and neural development in both vertebrates and invertebrates (reviewed in (Moore and Alexandre 2020)). The Notch pathway (Figure 3.1A), comprising only a one-step signal transduction event without intermediate amplification steps, is as follows (Bray 2006). On binding to a ligand from a neighboring cell, the transmembrane Notch receptor is cleaved intracellularly at the cell surface to release the Notch intracellular domain (NICD). The NICD enters the nucleus and associates with the DNA-binding protein CSL (CBF1/RBPjκ/Su(H)/Lag-1), known as Suppressor-of- Hairless (Su(H)) in *Drosophila*. The complex formed between Notch extracellular domain (NECD) and its associated ligand is recycled by endocytosis. The NICD-CSL then recruits transcriptional co-activator Mastermind (MAM) to activate transcription of Notch target genes, mainly the bHLH transcriptional repressors of the HES (Hairy and Enhancer of split) families (Bray 2006, Fortini 2009, Kopan and Ilagan 2009). As *Drosophila* neuroblasts divide asymmetrically, they generate at each division a self-renewed neuroblast and a more differentiated progeny that is either an intermediate progenitor (such as a Ganglion Mother Cell (GMC) for Type I neuroblasts, or an Intermediate Neural Progenitor (INP) for a Type II neuroblast) or a post-mitotic neuron (Type 0 neuroblasts) (reviewed in (Walsh and Doe 2017)). Of the two progenies born from an asymmetric neuroblast division, Notch signaling is active in only the neuroblast. The

reason for this asymmetry lies in that a negative regulator of Notch signaling, called Numb, which in the parent neuroblast is tethered to the basal cortex, is preferentially partitioned during asymmetric division to the daughter intermediate progenitor cell such as GMCs in Type I neuroblasts (Rhyu 1994, Knoblich 1995) (Figure 3.1C). In GMCs, Numb is active in the cytoplasm and inhibits Notch signaling, possibly by preventing translocation of the NICD inside the nucleus (Figure 3.1B). However, other potential models for Numbs antagonism of Notch signaling have been proposed (Reichardt and Knoblich 2013, Flores, McDermott et al. 2014). The limitation of Notch activity to the neuroblast results in unidirectional Delta-Notch signaling from the intermediate progenitor to the neuroblast (Roegiers and Jan 2004). Ectopic activation of Notch signaling in the progeny causes them to revert into neuroblasts and over-proliferate, while inhibition of Notch signaling in type II NBs eliminates the whole lineage (Wang, Somers et al. 2006, Bowman, Rolland et al. 2008, Weng, Golden et al. 2010). In most type I NB lineages, however, loss of N signaling does not affect neuroblast maintenance (Almeida and Bray 2005, Magadi, Voutyraki et al. 2020). The reason for this may lie in the partially redundant actions of the Enhancer-of-Split (E(spl)) complex proteins and Deadpan (Dpn) in maintaining the stemness of neuroblasts by repressing differentiation genes (Babaoglan, Housden et al. 2013). Notch signaling also controls the daughter cell proliferation modes, precisely the type I to type 0 switch in neuroblasts of the embryonic ventral nerve cord (Ulvklo, MacDonald et al. 2012, Bivik, MacDonald et al. 2016).

In the central nervous systems of vertebrates, after the asymmetric division of neural progenitors, the more differentiated progeny expresses Delta (Dl) and activates Notch

signaling in the sister cell to maintain the neural progenitor fate (reviewed in (Moore and Alexandre 2020)). The expression of Notch target Hes genes oscillates during the cell cycle in vertebrate neural progenitors (reviewed in (Kageyama, Ohtsuka et al. 2009)). Thus, Notch signaling has several vital roles in neural lineage development across diverse animal species.

In the fly optic lobe medulla, Notch activity has been shown to regulate a binary fate choice in neurons, which adds to the diversity of neurons in the system (Li, Erclik et al. 2013). However, whether Notch signaling facilitates temporal transitions in fly medulla neuroblasts is unknown.

As described in the previous chapter, we identified the Notch co-factor Suppressor of Hairless (Su(H)) as a new regulator of Slp1/2 expression in medulla neuroblasts. The work described in this chapter details our efforts toward verifying the role of Notch signaling in regulating Slp1/2 and assessing the contributions of the cell cycle in controlling the temporal patterning program in this system.

Results

The Notch pathway regulates Slp1 and Slp2 expression in medulla neuroblasts

We observed Slp1 and Slp2 in RNAi knockdown clones of key Notch pathway components induced by *ayGal4* (*actin>FRT-y^{+}-STOP-FRT-Gal4*; the *actin* promoter

drives Gal4 expression only after the action of heat shock excises a STOP cassette activated Flippase (Flp) (Ito 1997)). Slp1 and Slp2 are both regulated similarly and expressed at about the same time in medulla neuroblasts; hence expression patterns of one protein reflect that of the other. On inducing RNAi knockdowns of the critical Notch pathway components- the Notch receptor and Su(H), it is seen that Slp2 expression is delayed within the GFP-labeled RNAi knockdown clones (Figure 3.2A-A''' and 3.2B-B''' respectively) compared to wild type neuroblasts of the same age outside the clones (in the same vertical 'stripe'). A similar effect is seen when a dominant-negative variant of the third core component of the Notch transcriptional complex, mastermind (mam), is expressed under the control ayGal4 (Figure 3.2C-C'''). These data suggest that the Notch pathway regulates the timing of Slp1/2 expression in medulla neuroblasts.

To identify the ligands of Notch that function in activating Notch signaling in medulla neuroblasts, we examined the expression of known Notch ligands- Delta (Dl) (Campos-Ortega 1988) (Figure 3.3), Serrate (Ser) (Fleming 1990, Rebay 1991), and Weary (Wry) (Kim, Wolf et al. 2010) in the medulla (Figure 3.4). Several available RNAi lines were tested for their impact on Slp1/2 expression on medulla neuroblasts for each Notch ligand. Also, we crossed *UAS-GFP* reporter lines to Dl-Gal4 and Ser-Gal4 fusion lines to observe if they could express UAS-GFP in medulla neuroblasts. Only UAS-GFP driven by Delta-Gal4 was expressed in medulla neuroblasts and in their progeny GMCs (Figure 3.3A-A'''). We then examined whether loss of Dl recapitulates the effects we observe on Slp1/2 expression with loss of function of core Notch transcription complex components if Dl is required for activating Notch signaling in these cells. RNAi knockdown of Dl resulted in a

similar delay in initiating Slp2 expression as observed with the loss of function of other key actors in the Notch pathway (Fig. 3.2D-D'"), confirming this expectation.

Notch signaling is dependent on cell-cycle progression.

It is well-established that GMCs generated by the asymmetric division of neuroblasts signal to their sister neuroblasts to provide the Notch signaling (Rhyu 1994, Knoblich 1995). However, it is unknown if Notch signaling is lost in cell-cycle arrested medulla neuroblasts since these neuroblasts fail to generate GMCs due to impaired cell division. Using a regional Gal4 (vsxGal4), we expressed *UAS-DCR2* and an RNAi knockdown against Proliferating Cell Nuclear Antigen (PCNA), which is essential for DNA replication and S phase progression (Moldovan, Pfander et al. 2006). The *vsxGal4* (Erclik, Li et al. 2017) is expressed in the central domain of the medulla crescent, starting in the neuroepithelium. Blocking cell cycle progression caused a precocious transformation of neuroepithelial cells to neuroblasts. These cell cycle arrested neuroblasts express the normal neuroblast marker Deadpan (Dpn) (Figure 3.5A', C') but produce no progeny (Figure 3.5B'', D' and D''). Some neuroblasts are also present in the deep layers that neural progenies typically occupy (Figure 3.5B, C). Most of the cell cycle defective neuroblasts in the expression domain of *vsx-Gal4* do not express the Notch activity reporter E(spl)mγGFP (Figure 3.5 A', A'', A''', labeled by arrowheads) (Campos-Ortega 1988), while all neuroblasts in the control regions do (Figure 3.5 A', A'', A'''). Thus, Notch signaling is largely lost in cell-cycle arrested neuroblasts.

A normal progression through the cell cycle is required for the Ey to Slp1/2 transition

Next, we tested whether blocking cell-cycle progression affected the medulla temporal patterning factor sequence progression. In *vsxGal4>PCNA RNAi* brains, neuroblasts in the affected region do not express either Ey or Slp1/2 (Figure 3.5 C''-C''') but maintain Sox Neuro (SoxN) expression (Figure 3.6 C-C''). This suggests that an earlier temporal transition step required for Ey expression is blocked in cell cycle arrested neuroblasts, preventing us from examining whether the Ey to Slp transition also requires cell cycle progression. To circumvent this problem, we used the *ay*Gal4 to drive *UAS-DCR2* and *PCNA RNAi*. We obtained a condition where Ey expression is minimally affected by adjusting heat shock timing to induce clones. Slp2 expression is still severely delayed in cell cycle arrested clones with intact Ey expression (Figure 3.7C-C'''). In addition to the timing of clone induction, the *ayGal4* is also likely weaker than VsxGal4 at inducing RNAi. The cell cycle is possibly slowed down rather than wholly blocked when *ayGal4* is used to drive *PCNA* RNAi, as we still observe some neural progenies in *ayGal4* clones (Figure 3.7 C''). Also, Slp1/2 expression is delayed rather than lost when we knock down String /Cdc25 required for the G2 to M phase transition (Edgar 1989) and when we overexpress Dacapo (Dap), a Cyclin-dependent kinase inhibitor of the CIP/KIP family (Lane, Sauer et al. 1996) using *ayGal4* (Figure 3.6A-A''' and Figure 3.6B-B''', respectively). Thus, cell cycle progression is required for the precise timing of Ey to Slp1/2 transition.

Notch signaling can rescue the Slp1/2 expression delay caused by cell cycle defects.

Finally, we tested if supplying Notch signaling to cell-cycle arrested or delayed neuroblasts can rescue the timing of Slp1/2 expression initiation. We provided active Notch in neuroblasts using a *dpn>FRT-stop-FRT3-FRT-NICD* transgene (which drives the expression of NICD from the *dpn* enhancer in the presence of heat shock activated Flippase; see Methods) while simultaneously inducing knockdown of *PCNA* using *vsx*Gal4 (Figure 3.7 A-A'''). Ectopic expression of NICD led to a proliferation in the number of neuroblasts relative to wild type brains (Figure 3.7 A', B) but had a negligible effect on rescuing expression of Slp2 in the spatial region where *PCNA* knockdown was induced by *vsxGal4* (Figure 3.7 A''', B''). This is perhaps because ectopic NICD expression fails to rescue Ey expression, and Ey is necessary for Slp1/2 expression (Figure 3.7 A'', B'). To test the consequences of supplying active Notch signaling in the presence of Ey, we expressed NICD in brains while driving PCNA knockdown using ayGal4, utilizing the same heat shock condition optimized earlier that leaves Ey expression largely unaffected. In this circumstance, supplying NICD was sufficient to rescue Slp2 expression in *PCNA RNAi* clones (Figure 3.7 D-D'''). These results suggest that for the Ey to Slp transition, active Notch signaling can substitute for the requirement for the cell-cycle progression.

Discussion

Notch signaling directly regulates the transcription of a temporal patterning factor

Although Ey is necessary for activating Slp1/2 expressions, previous studies demonstrated that it is insufficient (Li, Erclik et al. 2013). There is always a time delay from the start of Ey expression to the beginning of Slp expression to ensure the sufficient duration of the Ey window. How is the timing controlled? In the previous chapter, from our analyses of the *slp1/2* enhancer sequences, we found several binding sites for the CSL transcription factor Su(H), an essential co-factor of Notch and the main DNA-binding component of the Notch transcription complex. To confirm the involvement of the Notch pathway in regulating Slp1/2, we observed the effects of knocking down key Notch pathway components on endogenous Slp1/2 expression. In all cases, we observed a delay in the expression of Slp1/2 in neuroblasts expressing the cell cycle regulator gene RNAi knockdowns compared to the time of Slp1/2 initiation in wild-type neuroblasts. Together with results from experiments described in Chapter 2, these findings strengthen the idea that Notch signaling regulates Slp1/2 transcription. Ey may still play a more central role in activating Slp1/2 expression than the Notch pathway since Slp1/2 are still expressed, albeit later in the absence of Su(H) and other Notch components, but are lost in the absence of Ey. In Chapter 2, we confirmed Su(H) binding *in vivo* to our enhancers of interest using DamID-sequencing (Marshall, Southall et al. 2016). Thus, our work provides evidence that Notch signaling, a general signaling pathway involved in the asymmetric division of neuroblasts, functions to speed up the activation of a temporal patterning transcription factor. This might be one of the mechanisms to promote the

temporal cascade progression, specifically in neuroblasts, where Notch signaling is active.

Cooperative regulation of target genes, including *slp1 and slp2,* by the TTF Ey and Notch signaling

What might explain the delay in Slp1/2 expression in the absence of a functional Notch pathway? Recent developments in single-molecule Fluorescence In Situ Hybridization (smFISH) technology and live imaging techniques using the MS2-MCP system have enabled the studying of transcriptional processes in molecular detail. Imaging transcription driven by Notch responsive enhancers in native contexts has shown this process to be inherently 'bursty,' i.e., episodes of transcription (enhancer 'On' state) are punctuated with gaps in activity (enhancer in 'Off' state) (Falo-Sanjuan, Lammers et al. 2019, Lee, Shin et al. 2019). The dosage of NICD modulates the duration of the 'On' phase in one context studied by live imaging (Lee, Shin et al. 2019). Additionally, binding of tissue-specific regional factors to these Notch responsive enhancers may prime these enhancers and help synchronize transcription and sustain a steady transcriptional output upon Notch binding to enhancers; this helps integrate important positional cues and the perception of context (Falo-Sanjuan, Lammers et al. 2019). Applying these insights to our system, we suggest that the delay observed may correspond to an increased number of abortive transcription events in the absence of Su(H) and Notch and in the presence of Ey alone. Ey may also act by priming our Notch responsive enhancers providing crucial contextual information before robust levels of Slp1/2 can be transcribed, in addition to helping initiate Slp1/2 expression. The possible role of Ey in providing specificity to Notch-

mediated regulation is supported by observations from our DamID data that 62.78% of genes bound by Su(H) and 60.3% of genes bound by Ey were also bound by the other transcription factor. Enriched GO terms within genes bound by both Ey and Su(H) included ‘Notch signaling,’ ‘asymmetric cell division,’ ‘cell division,’ ‘apical cell polarity, etc. These are processes crucial to neuron development.

The cell cycle interacts with Notch signaling to achieve temporal progression in medulla neuroblasts

Notch target genes of the E(spl) family and Dpn are transcriptional repressors with partially redundant functions in maintaining neuroblast identity (Babaoglan, Housden et al. 2013). In type II NBs, Dpn is dependent on Notch signaling, and loss of Dpn causes premature differentiation into neurons (Bowman, Rolland et al. 2008, San Juan, Andrade-Zapata et al. 2012). However, in type I NBs, Dpn is not lost if Notch signaling is lost, and Notch signaling is dispensable for the self-renewing abilities of NBs (Almeida and Bray 2005, Zacharioudaki, Magadi et al. 2012, Magadi, Voutyraki et al. 2020). In the medulla neuroblasts, we observe that the clone size is not significantly affected in Su(H) mutant clones, indicating Notch signaling is not required for cell growth and division, consistent with data from other Type I neuroblasts. We also observe that Notch signaling in medulla neuroblasts requires cell-cycle progression, and the expression of Notch target genes is lost when cell cycle progression is blocked.

In the medulla, blocking cell cycle progression in neuroepithelial cells transforms them prematurely into neuroblasts, and these neuroblasts are arrested in the TTF cascade at the SoxN stage. The expressions of Ey and Slp1/2 are never activated in such neuroblasts. When we stopped or slowed down the cell cycle in neuroblasts later to preserve Ey expression, Slp expression was still delayed. Therefore, cell cycle progression also has a role in the Ey to Slp transition. Further, we showed that supplying Notch signaling is sufficient to rescue the Ey to Slp transition delay caused by cell cycle defects. These results suggest that at the Ey to Slp transition, the cell cycle effect is mediated through the direct regulation of Slp transcription by Notch signaling. This Notch pathway-mediated connection between temporal patterning progression and the cell cycle in neuroblasts can be a mechanism to coordinate the TTF transition with the cell cycle progression and generate an appropriate number of neural progenies at a given temporal stage.

Abbreviations commonly used in text

TTF- Temporal-patterning Transcription Factor

VNC- Ventral Nerve Cord

NB- neuroblast

Imp- IGF II mRNA-binding protein

GMC- Ganglion Mother Cells (intermediate progenitors produced by TypeI neuroblasts)

IP- Intermediate Progenitor

Dpn- Deadpan (a transcription factor and a neuroblast marker)

Ey- Eyeless

Slp1/2- Sloppy-paired 1 and 2

Su(H)- Suppressor of Hairless

NICD- Notch Intracellular Domain

Dl- Delta

Materials and methods

Fly Stocks used

UAS -N-RNAi (BDSC 7078)

UAS-Su(H)-RNAi (VDRC 103597)

UAS-Dl-RNAi (VDRC 32788)

UAS-PCNA-RNAi (VDRC 51253)

UAS-mamDN (from Dr. Justin Kumar (Kumar 2001))

Stock numbers of fly strains used for screening Notch ligands are indicated in Figure 3.3. Flies were reared on yeast food at 25°C unless otherwise stated.

RNAi experiments

ayGal4 (*actin*>FRT-y^+-STOP-FRT-Gal4, in which *actin* promoter drives Gal4 expression after a STOP cassette is excised by the action of heat shock activated Flippase) was used to drive RNAi of N, Su(H), Dl. *ayGal4* was also used to induce expression of *UAS-mamDN*. Flies of genotype *ywhsFlp; ayGal4>UAS GFP; UAS Dcr2/Tm6B* were crossed to the RNAi lines. Larvae were heat-shocked at 37°C for 10 minutes 48 hours after egg laying and then raised at 29°C until the brains of third instar larvae were dissected and stained.

Cell cycle arrest experiments

For some experiments examining the effect of cell cycle arrest on Slp1/2 expression and the Notch reporter E(spl)-mγ::GFP, *vsxGal4* was used to drive the expression of *UAS PCNA RNAi* and *UAS Dcr2* in neuroblasts. Flies of genotype *VsxG4; E(spl)-mγGFP; UAS Dcr2/Tm6B* were crossed to those with genotype *ywhsFlp; UAS-PCNA RNAi/CyO; T2/Tm6B*. Larvae were shifted to 29°C 48 hours after egg-laying. The brains of third instar larvae were observed. For other experiments, flies of genotype *ywhsFlp; UAS-PCNA RNAi* were crossed to *ywhsFlp; ayGal4>UAS GFP; UAS Dcr2/Tm6B* flies. Larvae with genotype *ywhsFLP; ayGal4UASGFP /UAS-PCNARNAi; UASDCR2/+* were heat-shocked for 8 minutes at 37°C 50 hours after egg laying (70 hours before they develop into climbing third instar larvae) and were then dissected. For rescuing Notch expression in cell cycle arrested neuroblasts flies of genotype *ywhsFlp; ayGal4>UAS GFP; UAS Dcr2/Tm6B* were crossed to those with genotype *ywhsFlp; UAS PCNA RNAi; dpn>hsNICD*. Larvae of genotype *ywhsFLP; ayGal4UASGFP /UAS-PCNARNAi; UASDCR2/dpn>hsNICD* were heat-shocked for 8 minutes at 37°C 50 hours after egg laying (70 hours before the third instar stage) as before and then dissected.

Plasmid constructs and transgenic stocks

Primer sequences for all cloning are provided separately in Figure 3.8.

For making all constructs, DNA was amplified from a BAC template using Expand High-Fidelity Polymerase (Roche) unless stated otherwise, and all constructs were verified by

sequencing. All fly embryo injections for making transgenic flies were carried out by Bestgene Inc, Chino Hills, CA.

To generate the heat shock inducible NICD expression plasmid, we modified the pJR12 vector used in enhancer bashing experiments in Chapter 2 to replace the GFP coding sequence with the Notch intracellular domain (NICD) coding sequence. First, we generated by PCR splicing a DNA fragment that had the sequences of the pJR12 vector flanking the eGFP coding sequence, but that did not contain the eGFP sequence. Then, using restriction enzymes *NsiI* and *XhoI*, we excised the eGFP coding sequence from the pJR12 vector and replaced it with our eGFP deleted fragment generated at the previous step. Next, we PCR-amplified an *FRT-stop-FRT3-FRT* encoding segment from the CoinFlp plasmid (Bosch, Tran et al. 2015) (Addgene plasmid # 52889, a kind gift from Dr. Iswar Hariharan) and spliced it with a fragment of Notch Intracellular Domain (NICD) by PCR. Sequences corresponding to the Notch Intracellular Domain were amplified from the Notch cDNA LD34134 (DGRC). We cloned the *FRT-stop-FRT3-FRT-NICD* fragment into the modified pJR12 vector (the one lacking the eGFP coding sequence, as described earlier) between the *PmeI* and *AgeI* restriction sites. We then cloned the *deadpan* (*dpn*) enhancer sequence amplified from the BAC clone CH321-86A18 (BACPAC resources) into the modified pJR12 vector. This created a heat-shock inducible NICD expression construct that is expressible in all neuroblasts in the same pattern as Dpn (abbreviated as *dpn> hsNICD* or hsNICD). The *dpn>hsNICD* construct was inserted at the VK00027 landing site (BL 9744) by φC31 integrase-mediated transgenesis. The w+ eye color

marker expression identified positive transformants, and stocks were created by crossing to a double balancer of genotype *ywhsFlp; Sp/CyO; Tm2/Tm6B*.

Figures

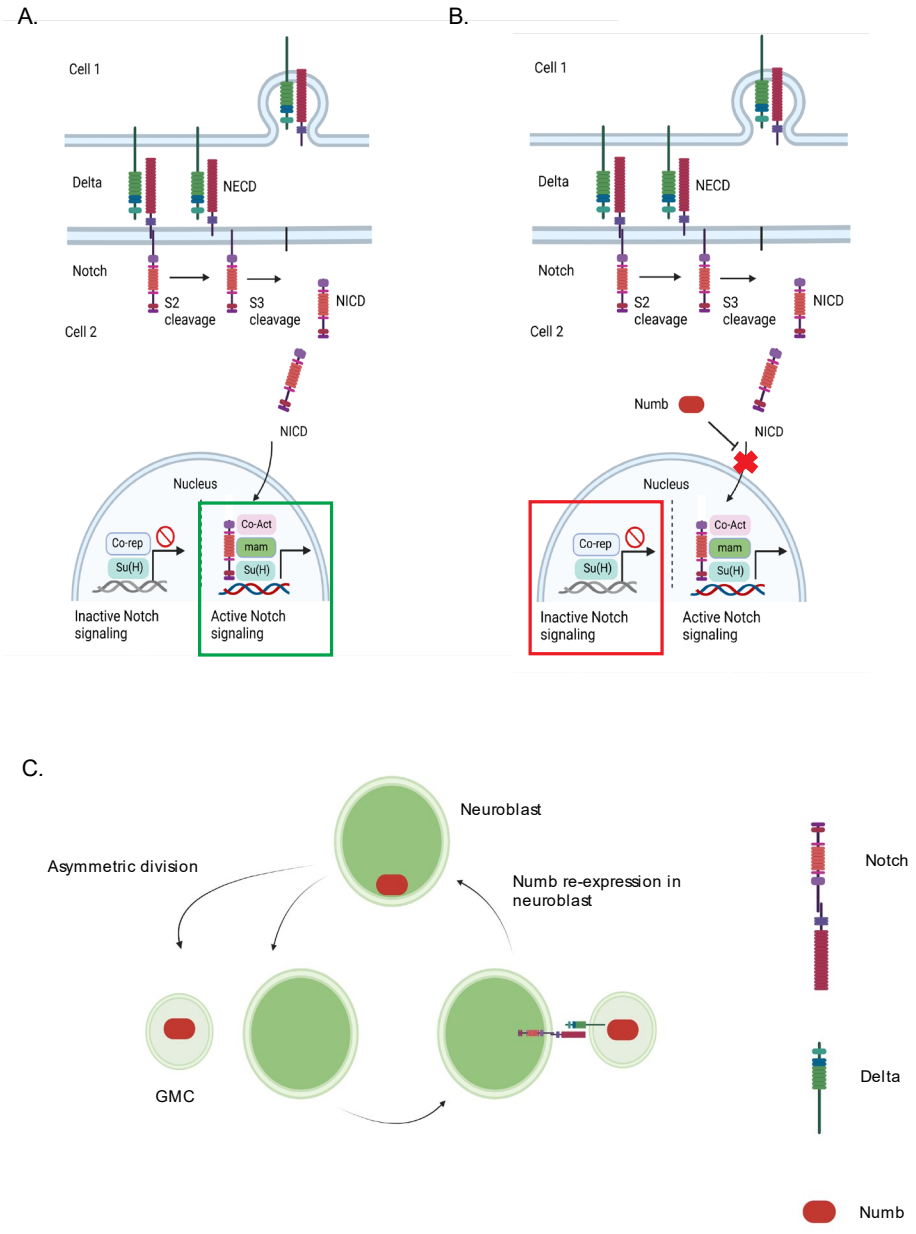

Figure 3.1. The Notch signaling pathway in neuroblasts and intermediate progenitors. A. In cells with active Notch signaling, Notch receptors expressed on a cell's surface (here Cell 2) engage with Notch ligands such as Delta expressed on the surface

Figure 3.1 (cont.) of a neighboring cell (here Cell 1). This receptor-ligand interaction activates downstream processes that involve two successive proteolytic cleavages of the Notch receptor at the membrane. As a result, a fragment of the Notch receptor called the Notch Intracellular Domain (NICD) is released. This fragment is the transcriptionally active part of the Notch receptor. It enters the nucleus, and associates with the proteins Suppressor of Hairless (Su(H)), a CSL family transcription factor, and the co-activator Mastermind (mam). The three-protein complex begins transcribing Notch target genes such as the Enhancer of Split (E(spl))- helix-loop-helix family of genes. B. In cells with inactive Notch signaling, such as the Ganglion Mother Cell intermediate progenitors, a negative regulator of Notch, called Numb, is active. Numb itself is an adaptor protein and may interact with other adaptor proteins. Numb prevents NICD translocation into the nucleus. Alternative models to explain Numb's mode of action suggest that Numb may block the recycling of Notch receptors to the cell surface by inhibiting its endocytosis into vesicles. However, all evidence agrees on Numb downregulating Notch signaling in cells where it is present in the cytoplasm. In the absence of NICD in the nucleus, the Su(H) protein usually acts as a transcriptional repressor. Notch target genes are not expressed without the tripartite Notch transcriptional complex. C. Self-renewing asymmetric divisions of neuroblasts impact Notch signaling in their progeny. In neuroblasts, the Numb protein is present in the basal cortex tethered away from the cytoplasm and hence unable to inhibit Notch-dependent transcription. After asymmetric division, Numb is partitioned into the daughter intermediate progenitor (Ganglion Mother Cell or GMC). Being cytoplasmic, Numb inhibits (Figure 3.1 cont.) Notch signaling in GMCs. GMCs thus do not express Notch receptors but express Notch ligands like Delta (Dl), thereby potentiating Notch

Figure 3.1 (cont.) signaling in its neighboring sister neuroblast. The daughter neuroblast subsequently re-expresses Numb, which is again cortically tethered and inactive, continuing the cycle. Figure created with BioRender.

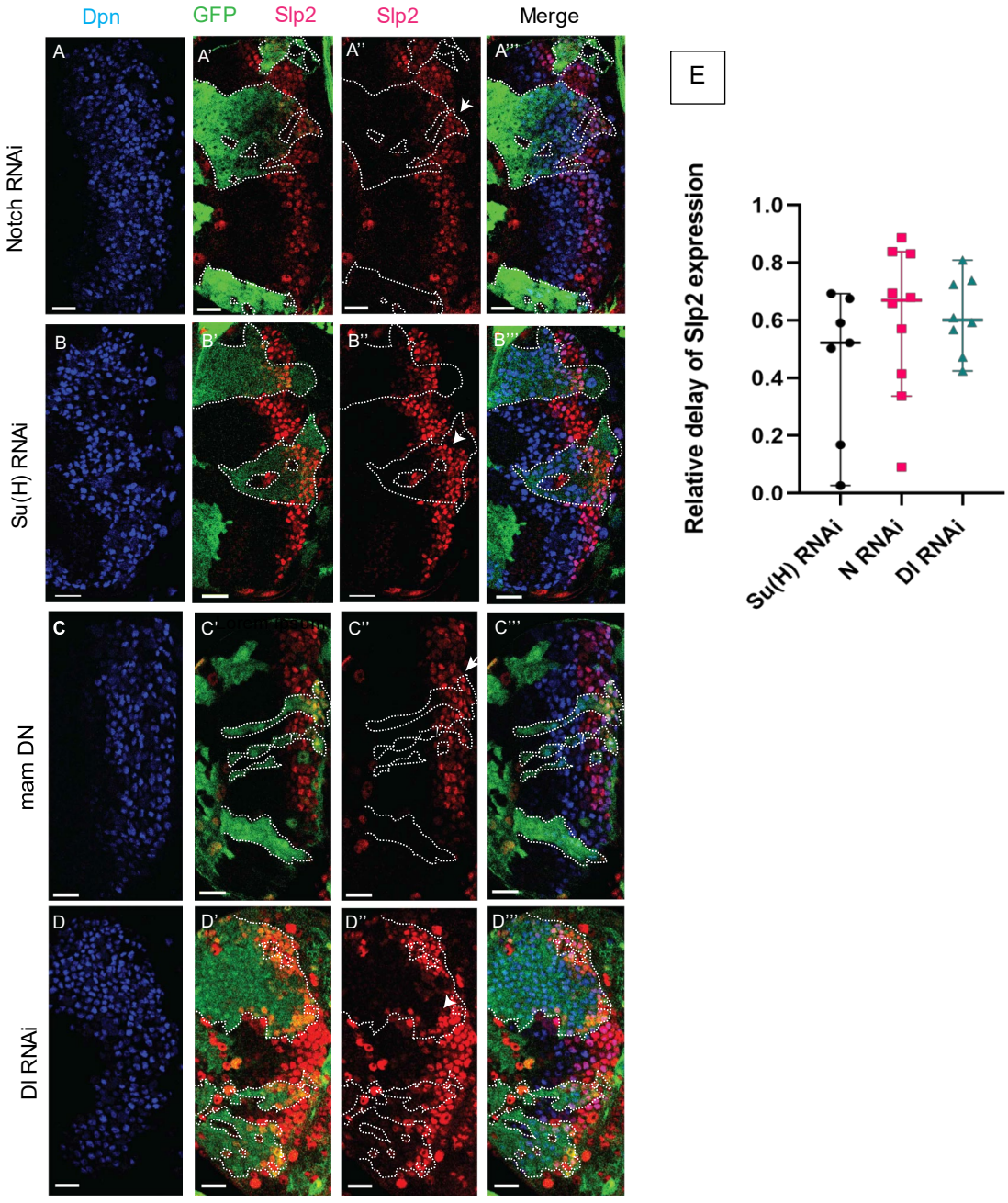

Figure 3.2 The Notch pathway regulates the expression of *slp* genes in medulla neuroblasts. 2A. RNAi knockdown of Notch leads to a delay in the expressions of *slp* genes compared to contemporaneous wild-type neuroblasts outside the GFP marked clones within which Notch RNAi is induced. 2B. Knockdown of *su(h)* shows a similar delay

Figure 3.2 (cont.) in Slp1/2 expression as for Notch-RNAi. 2C. The expression of a dominant-negative variant of *mastermind*, the third component of the Notch transcription complex, shows a similar phenotype as *NRNAi* and *Su(H) RNAi* and delays Slp1/2 expression. 2D. Knockdown of *Dl*, a Notch ligand, has a similar delay in expressing *slp1/2* genes indicating that Dl is the ligand that the Notch signal is transduced through in medulla neuroblasts. Scale bar 20 microns. *ayGal4 UAS GFP* clone boundaries are shown in dotted lines, and arrows indicate neuroblasts within knockdown clones expressing Slp2 later than wild type. Scale bar: 20 microns. E. Quantification of delay phenotype in Notch pathway mutants. The ratio of the width of the Slp2 expression band within an RNAi clone to the width of the Dpn expression band at the same location was computed. As a control, the ratio of Slp2 expression width to Dpn expression width in wild type cells outside an RNAi clone was calculated. The relative delay in Slp2 expression due to knockdown of a Notch pathway component was calculated as the difference in ratios of Slp2 band width to Dpn band width in wild type cells and in RNAi clones divided by the ratio in wild type cells. This number may be interpreted as the fraction of Slp2 expression lost in Notch pathway component mutant clones relative to wild type cells. Descriptive statistics for RNAi knockdown clones of *Su(H) RNAi*, *N RNAi* and *Dl RNAi* are shown. Graphs show the scatter of individual values, the median and 95% confidence intervals for each knockdown. For quantifying the *Su(H) RNAi* phenotype, 7 clones from 5 brains were analyzed. Mean of delay for *Su(H) RNAi* knockdown relative to wild type = 0.4540, S.D.= 0.2571, median= 0.5220. For quantifying the *N RNAi* phenotype 10 clones from 7 brains (Figure 3.2 cont.) were analyzed. Mean of delay for *N RNAi* knockdown relative to wild type = 0.6., S.D.= 0.2529, median= 0.6693. For quantifying the *Dl RNAi*

Figure 3.2 (cont.) phenotype 8 clones from 3 brains were analyzed. Mean of delay for *Dl RNAi* knockdown relative to wild type = 0.6172., S.D.= 0.1333, median= 0.6010.

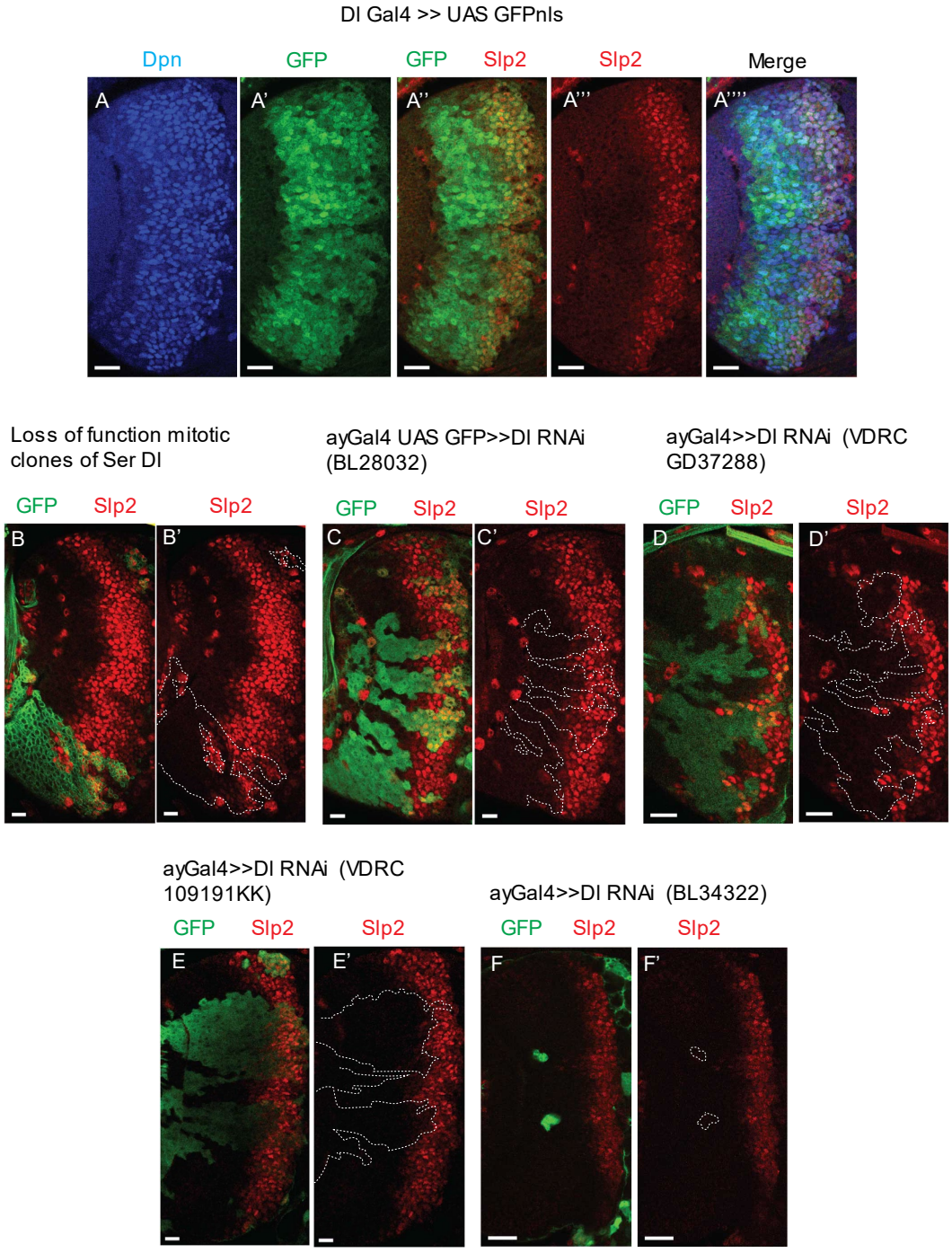

Figure 3.3 Delta is the Notch ligand expressed in medulla neuroblasts. (A-A''''). *UAS-GFP* driven by a Dl-Gal4 line (A') is expressed in Dpn expressing medulla neuroblasts. Many UAS-GFP expressing cells overlap with those expressing Slp2 (A'-A''''). (B-B').

Figure 3.3 (cont.) Mitotic clones with two copies of a loss of function mutant of Ser and Dl (i.e., functionally lacking both Ser and Dl) show a delayed expression of Slp2, indicating that either Dl or Ser or both mediate Notch signaling in medulla neuroblasts. To determine whether Dl is the Notch ligand in medulla neuroblasts and GMCs, several available *Dl-RNAi* lines were screened to find one that could emulate the Ser-Dl loss of function phenotype in (B-B'). *Dl-RNAi* expressing lines were crossed with flies of genotype *y w hsFlp; ayGal4 UAS GFP; UAS Dcr2.* Third instar larvae of their offspring were screened to observe the effect of *Dl* knockdown on Slp2 expression. Results of the screen for *Dl-RNAi* lines :(C-C') BL28032, (D-D') VDRC GD 37288, (E-E') VDRC 109191KK, (F-F') BL 34322. Of the screened lines, VDRC GD 37288 (D-D') and VDRC 109191KK (E-E') displayed the most noticeable effects on Slp2 expression. The line VDRC GD 37288 was used for further experiments. Scale bars are 20 microns for (A-A''''), (D-D') and (F-F'), and 10 microns for the rest.

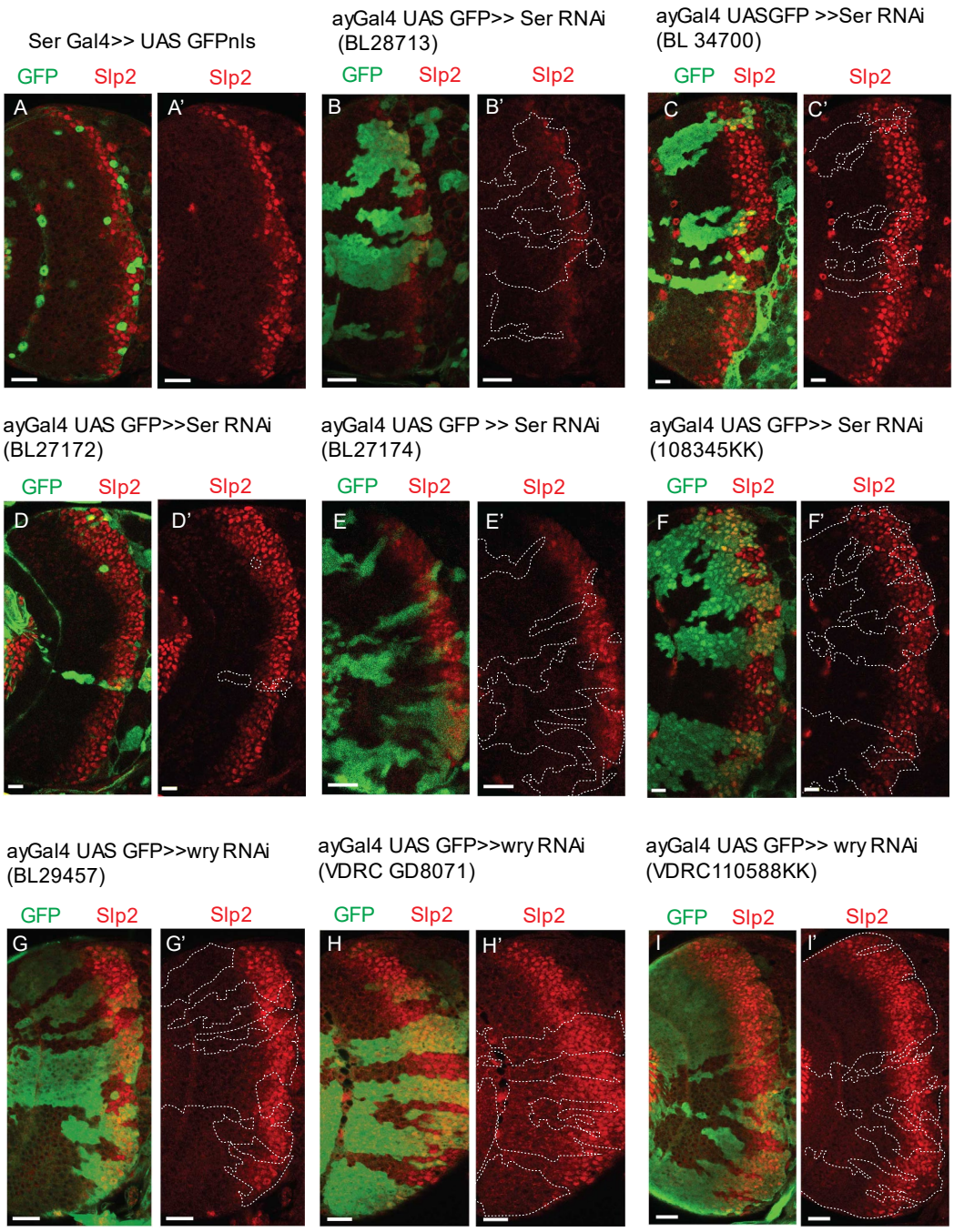

Figure 3.4 The Notch ligands Serrate (Ser) and Weary (wry) are not expressed in medulla neuroblasts. (A-A') *UAS-GFP* expressed by a *Ser-Gal4* shows GFP expression in surface glial cells but not in neuroblasts. As with *Dl*, available *ser-RNAi* lines were screened for any effect of *Ser* knockdown on endogenous Slp2 expression by crossing

Figure 3.4 (cont.) the RNAi lines to flies of genotype *y w hsFlp; ayGal4 UAS GFP; UAS Dcr2.* Results of the screen for *Ser RNAi* lines: (B-B') BL28713, (C-C') BL 34700, (D-D') BL 27172 (E-E') BL 27174, and (F-F') VDRC 108345KK. None of the lines screened showed any effect on endogenous Slp2 expression. RNAi lines for the gene *wry*, a more recently reported Notch ligand, were screened as shown in (G-G'), (H-H'), and (I-I'). The stocks used are indicated above the images. None of the *wry RNAi* lines affected Slp2 expression either. Scale bars for (C-C'), (D-D'), (F-F'), and (I-I') are 10 microns, and scale bars for the rest of the images are 20 microns.

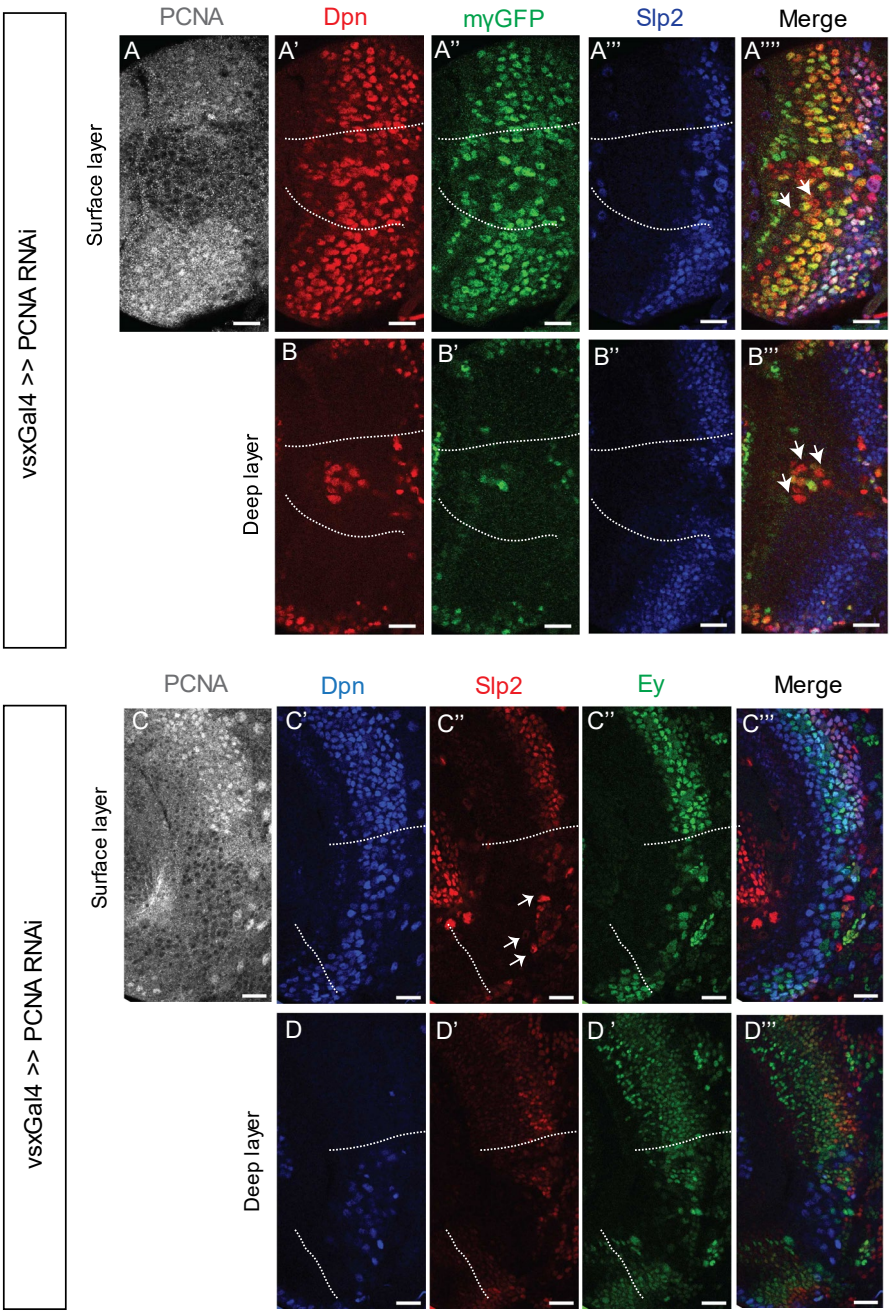

Figure 3.5 Cell cycle arrest at the G1/S phase leads to loss of expressions of the Notch reporter E(spl)mγGFP and temporal transcription factors. When the critical G1/S regulator PCNA is knocked down (A, C), neuroepithelial cells are prematurely transformed into neuroblasts (A', C'). Also, fewer Dpn expressing neuroblasts express

Figure 3.5 (cont.) the Notch reporter E(spl) mγGFP in cells expressing PCNA knockdown (A’’’’). Since these cell-cycle arrested neuroblasts do not divide and produce progeny, deeper brain layers continue to express Dpn (B). Like neuroblasts at the brain surface, these deep brain neuroblasts also don’t express E(spl) mγGFP (B’’’), indicating that neuroblast division is essential for maintaining active Notch signaling in neuroblasts. (C-C’’’’) Cell cycle arrest also leads to an interruption of temporal patterning transcription factor expression in medulla neuroblasts. *PCNA RNAi* expressing neuroblasts do not express Slp2 (C’’) and Ey (C’’’). The Slp2 signal in (C’’ marked by arrows) seems to originate in surface glial cells than in neuroblasts since these Slp2 expressing cells don’t express Dpn. The lack of neurons expressing Slp2 and Ey in deep brain layers is also evident (D’ and D’’, respectively). Dpn expressing neuroblasts in deep layers do not express either Ey or Slp2 (D), indicating that cell cycle arrest blocks temporal patterning at a step before Ey expression. Scale bars 20 microns.

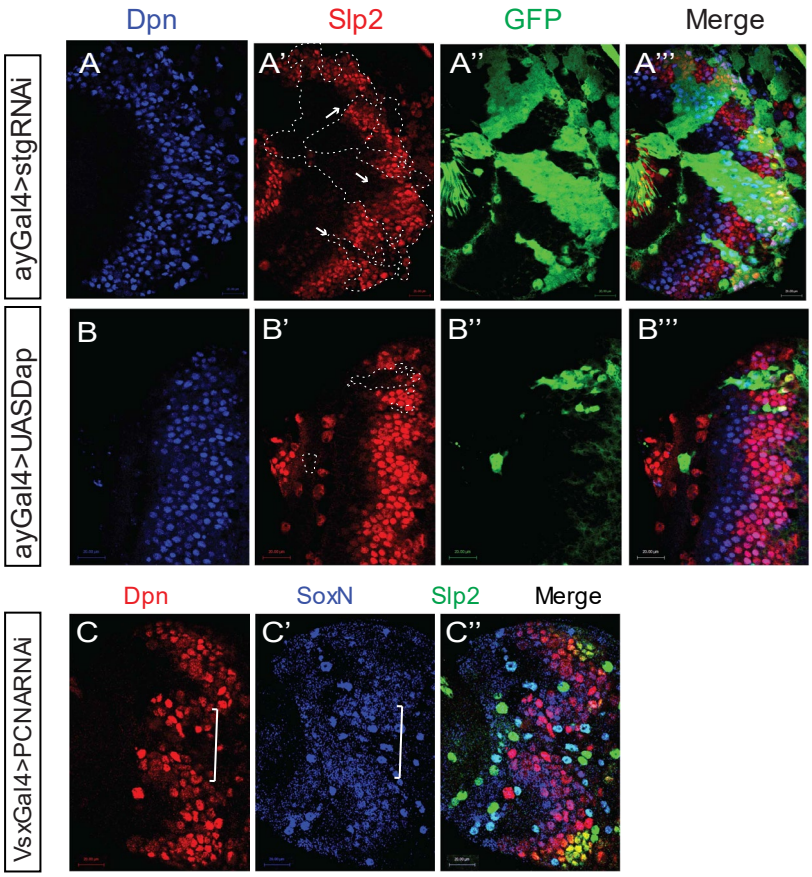

Figure 3.6 Cell cycle arrest in neuroblast blocks temporal patterning at a stage preceding Ey expression. Blocking the cell cycle in neuroblasts at stages other than G1/S recapitulates phenotypes observed with *PCNA RNAi*-induced cell cycle arrest. When the neuroblast cell divisions were blocked at cytokinesis using *UAS- stg-RNAi* driven by *ayGal4 UAS-GFP* (A-A'''), Slp2 expression was delayed in GFP marked cells expressing *UAS-stg-RNAi* (indicated by arrows in A'). Similarly, if the cell cycle is blocked at G1 by overexpressing the p27-CIP family CDK inhibitor *Dacapo* (*UAS-Dap*) using *ayGal4 UAS GFP*, GFP marked cells expressing UAS-Dap show delayed expression of

Figure 3.6 (cont.) Slp2 (showed within dotted lines in B'). When the cell cycle is arrested by driving *PCNA RNAi* using *vsxGal4* (the spatial region of *vsxGal4* expression indicated by a bracket in C, C'), neuroepithelial cells are prematurely converted to neuroblasts. This premature transformation to neuroblasts accounts for the earlier occurrence of Dpn expressing neuroblasts in the domain of *PCNA RNAi* expression (C). *PCNA* knockdown neuroblasts express an early temporal patterning factor SoxN (C'), suggesting that cell cycle arrest blocks temporal patterning at a step in between SoxN expression and Ey expression. Scale bars 20 microns.

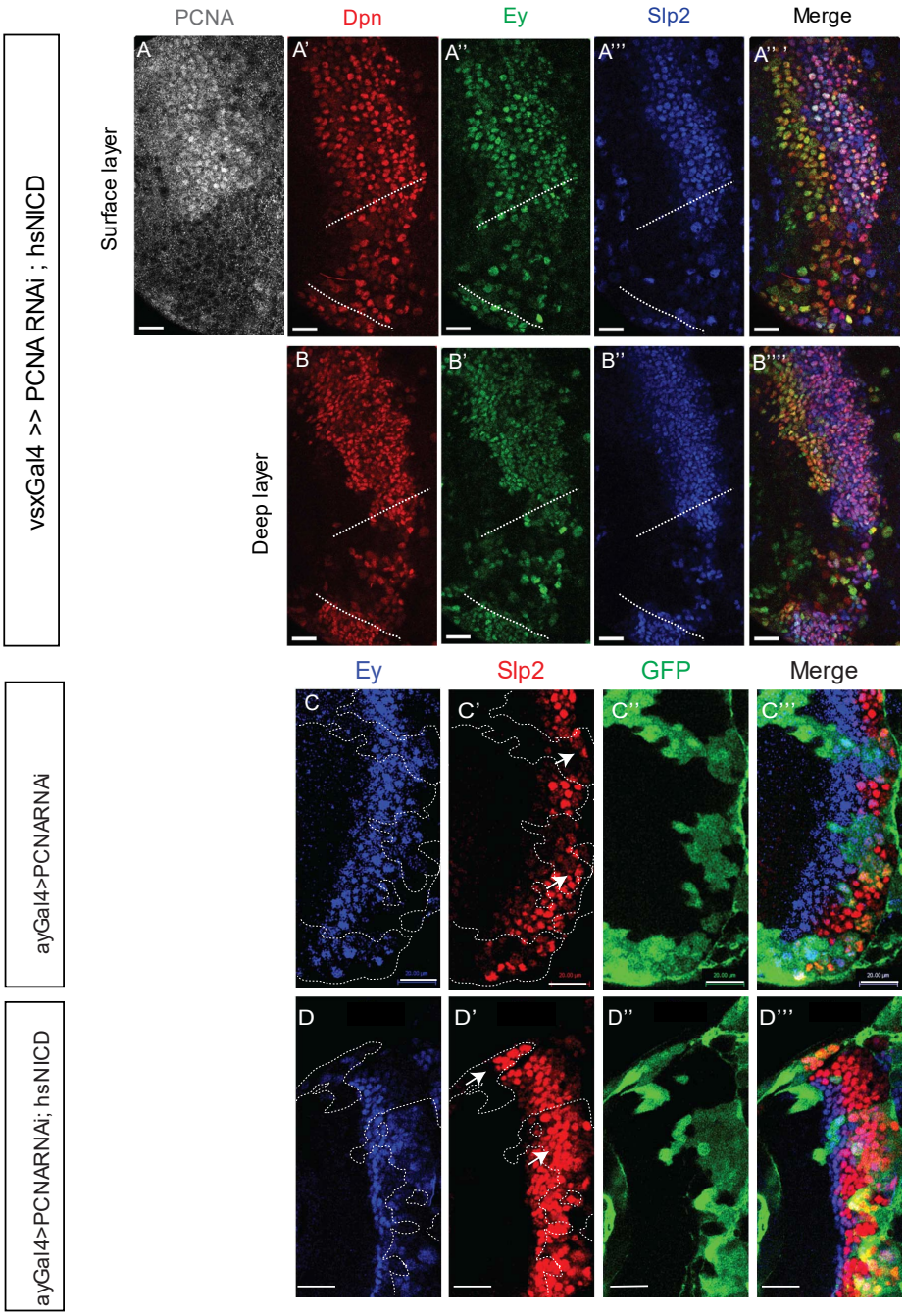

Figure 3.7 Ectopic expression of Notch in cell cycle arrested neuroblasts rescues the delay in Slp2 expression. When a heat-shock inducible NICD transgene is expressed in *vsxGal4>> UAS PCNA RNAi* expressing neuroblasts (A-A'''', B-B'''), we see supernumerary neuroblasts (in the entire medulla, since the transgene expression pattern

Figure 3.7 (cont.) is controlled by the *dpn* enhancer) (A'). However, Slp2 expression is not appreciably rescued by NICD expression alone in *PCNA* knockdown neuroblasts (A'''), *vsxGal4* expressing region indicated within dotted lines). The number of sub-surface neuroblasts is expanded in the *PCNA* knockdown expressing region (B'-B''', PCNA knockdown region shown within dotted lines). Since cell cycle arrest also reduces the number of Ey expressing cells and as Ey is necessary for Slp1/2 expression, we observed Slp2 expression in a condition where Ey levels are preserved. (C-C''') Ey expression is near normal when 3rd instar larvae expressing *UAS PCNA RNAi* are heat shocked using an optimized protocol. *PCNA* knockdown clones marked by GFP expression (C'') have normal levels of Ey as wild type cells outside the GFP clones (C) but show delayed Slp2 expression (C', the beginning of Slp2 expression indicated by arrowheads). (D-D''') When NICD is ectopically supplied to *PCNA RNAi* neuroblasts using the optimized heat shock protocol that preserves Ey (D''), the timing and expression levels of Slp2 are restored to that of wild-type cells (D', initiation of Slp2 expression indicated by arrowheads). Scale bars 20 microns.

Experiment	Forward Primer	Reverse Primer
GFP deletion from pJR12		
Fragment 1	TTAGAGATGCATCTCAAAAAA ATGGTGGGCATAATAGTGTTG TTTATATATATCAAAAATAACA AC	CCACCGGTCGCCACCGACGTCA GCGGCCGGCCGC
Fragment 2	GTCGCGGCCGGCCGCTGACG TCGGTGGCGACCGGTGGATC GTTTAAACAGGCC	CAATAACTCGAGGAGCGCCGGA GTATAAATAGAGGCGCTTCGTCT ACG
Verifying GFP deletion	CCATTATAAGCTGCAATAAAC AAGTTAACAAC	GTCGCTAAGCGAAAGCTAAGC
***dpn* enhancer cloning**	TTAGGCGCGCCCTTCGCTTTT GCCTGGTCGGCTCATCGG	ATATATGCGGCCGCACGCCTCGT CCTGGCACCCTC
NICD cloning	TATTTAACCGGTTATTATCAAA TGTAGATGGCCTCGGAACCCT TG	ATAATAGTTTAAACATGAGTACGC AAAGAAAGCGGGCAC
PCR splicing 'Stop' cassette with NICD		
Fragment 1	TATTTAACCGGTTATTATCAAA TGTAGATGGCCTCGGAACCCT TG	GGAAGTTCCTATTCTCTAGAAAGT ATAGGAACTTCGAATTCCAAAATG AGTACGCAAAGAAAGCGGGCAC
Fragment 2	GTGCCCGCTTTCTTTGCGTAC TCATTTTGGAATTCGAAGTTC CTATACTTTCTAGAGAATAGG AACTTCC	ATAATAGTTTAAACGAAGTTCCTA TTCTCTAGAAAGTATAGGAACTTC CCCGC

Figure 3.8 Sequences of primers used for cloning experiments described in the Methods section.

Chapter 4. Conclusions and future directions

Regulation of developmental gene expression is an important and exciting area of research. Nervous systems of tractable genetic model systems such as the fruit fly *Drosophila melanogaster* present an immense opportunity for interrogating development and differentiation processes because many neurons with subtly different properties must be differentiated from an initial pool of neural stem cell progenitors in these systems. At the same time, their numbers must be strictly controlled to ensure functional connectivity of neuron circuits. Temporal patterning has been described in several regions of the developing fly nervous system as a mechanism to expand neural diversity (reviewed in (Doe 2017)). Since its early descriptions, parallel mechanisms have been reported in mammals, thereby establishing the generality of this developmental process (reviewed in (Lodato and Arlotta 2015)).

My graduate work focused on understanding mechanisms underlying successive expressions of temporal patterning factors in Type I neuroblasts of the optic lobe medulla shortly after temporal patterning had been described in this system (Li, Erclik et al. 2013). Specifically, I focused on deciphering the mechanistic basis of the switch in expression from Eyeless (Ey) to Sloppy-paired (Slp) in medulla neuroblasts. We focused on this transition because, at the time, Ey was considered the first bonafide temporal patterning factor in the medulla temporal sequence that followed the 'activate the next and repress the previous' model of temporal patterning transcription factor (TTF) regulation (Li, Erclik

et al. 2013, Doe 2017). My work established that expressions of Slp1 and Slp2 are regulated at transcription. Furthermore, I identified two enhancers that function additively and redundantly in driving Slp1/2 expression in the spatiotemporal pattern we observe in medulla neuroblasts, as described in Chapter 2, and provided further evidence of transcriptional regulation. I also identified the Notch pathway as a regulator of Slp1/2 transcription alongside other temporal patterning transcription factors Ey and Scarecrow (Scro). I also demonstrated that the cell cycle has a specific role in regulating Notch target genes, including *slp1/2*.

However, many questions remain yet to be explored. For example, we consistently observe binding sites for Slp1 in the enhancers we identified. This may indicate that Slp1 auto-up-regulates its expression in neuroblasts where *slp1* transcripts have accumulated past a critical threshold. This hypothesis is supported by the observed reduction in GFP reporter intensity that is driven by both enhancers when Slp1 binding sites are mutated. In the future, Slp1 auto-upregulation can be tested using a combination of single-molecule fluorescence *in situ* hybridization (smFISH) and super-resolution microscopy. Alternatively, this question can be addressed using an MS2-containing reporter driving the expression of the *yellow* gene from the *slp* enhancers identified in a genetic background where MCP-GFP is also made available. Also, it is unclear at present how the cell cycle in neuroblasts influences Notch signaling. An analysis of gene ontology terms enriched in genes bound by Ey and Suppressor of Hairless (Su(H)) revealed several genes with cell cycle-related functions. Among these are *cyclin A, cyclin G*, *cyclin E*, *diaphanous* (encodes a protein related to mammalian formins), and *peanut* (encodes

a protein related to septins). It remains to be seen whether transcripts for the same genes are down-regulated on inducing cell cycle block. Comparison of single-cell transcriptomes of wild type and cell cycle arrested neuroblasts may reveal what processes are involved in cell cycle regulation of Notch. Both Ey and Su(H) also bind a large complement of genes, including several TTFs. This raises the possibility that regulation of TTFs by Notch signaling may be more pervasive than we currently believe. As discussed at the end of chapter 3, Ey binding may help provide a context-specific signal to recruit the Notch transcription complex to enhancers of Notch target genes in neuroblasts. A smFISH or MS2-MCP and live imaging-based experimental approach as used in (Falo-Sanjuan, Lammers et al. 2019, Lee, Shin et al. 2019) may help resolve the behavior of Notch responsive enhancers in the absence of Ey, thereby verifying or refuting this idea.

On a larger scale, regulatory elements driving the expression of temporal genes in medulla neuroblasts are still largely uncharted. Recent advances in single-cell sequencing technologies and computing have enabled the creation of gene expression atlases of the fly-brain across several developmental stages (Konstantinides, Rossi et al. 2021, Ozel, Simon et al. 2021). Single-cell mRNA sequencing has already expanded the existing network of TTFs in the medulla (Zhu, Zhao et al. 2022). Recent studies have also attempted to combine single-cell transcriptome data from RNA sequencing with single-cell epigenomic data from ATAC-seq to create a multi-omics-based description of the fly brain developmental history (Janssens, Aibar et al. 2022). These developments will now help answer questions such as whether changes in epigenetic landscape precede or follow changes in transcription output in cells. They will also help understand how multiple

enhancers of a single developmental gene collaborate to achieve the observed expression by constructing *cis*-regulatory element interaction maps or 'cistromes'.(Janssens, Aibar et al. 2022) Possibilities presented by interfacing single-cell omics with high-resolution microscopy seem nearly endless (for recent reviews, see (Kelsey 2017, Agbleke, Amitai et al. 2020)); we may soon be able to map out the development of animal brains as in a recent study that mapped the history of every cell in an ascidian embryo (Sladitschek, Fiuza et al. 2020). Ultimately what we can achieve in organismal development may only be limited by our imaginations.

Figures

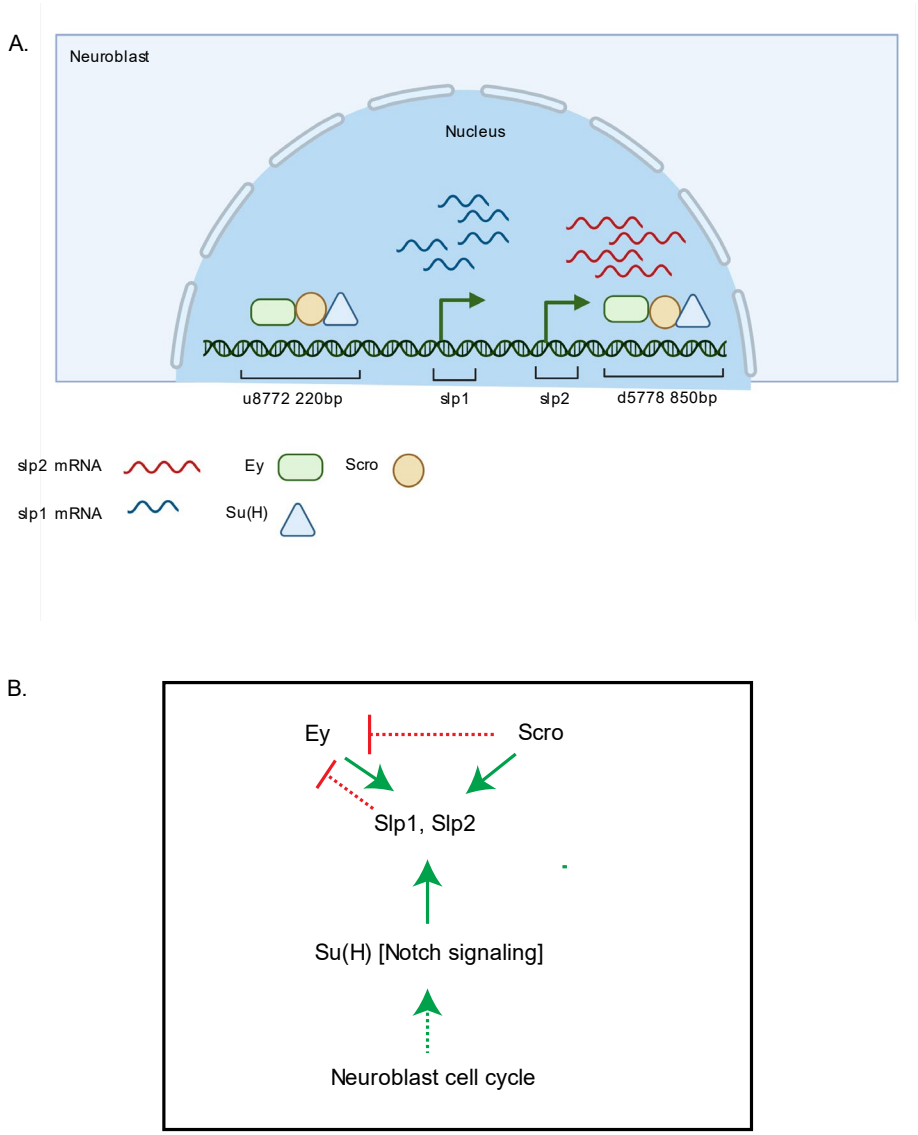

Figure 4.1 A coordinated action of temporal patterning factors Eyeless (Ey) and Scarecrow (Scro) and the Notch signaling pathway regulates the expressions of Slp1 and Slp2 in medulla neuroblasts. A. A schematic summarizing the main conclusions of my thesis work. In medulla neuroblasts, expressions of slp1 and slp2 are transcriptionally regulated by previous temporal patterning factors Ey and Scro and by

Figure 4.1 (cont.) the Notch signaling pathway. Ey, Scro, and the Notch pathway transcription factor Suppressor of Hairless (Su(H)) regulate slp1 and slp2 transcription by binding to enhancers identified u8772 220bp and d5778 850bp. B. A summary of genetic interactions regulating Slp1/2 expression in medulla neuroblasts. Green arrows indicate activation. Solid green arrows indicate activation by direct enhancer-binding. Dotted green arrows indicate activation for which direct transcriptional regulation has not been established. Red marks inhibition and dotted red lines indicate inhibitory interactions inferred from genetics the mechanistic basis of which is unknown. Ey, Scro, and Su(H) activate slp1 and slp2 transcription by binding to their enhancers u8772 220bp and d5778 850bp. Other studies have shown that Slp1 and Slp2 repress Ey expression, as does Scro. A functioning cell cycle in medulla neuroblasts is also necessary for expressing Slp1/2. Ectopic expression of active Notch in neuroblasts partially compensates for the requirement of cell division for Slp1/2 expression, indicating that the cell cycle may act via the Notch signaling pathway to influence temporal patterning of medulla neuroblasts.

Appendix A. Identification of an enhancer of *eyeless* transcription in optic lobe medulla neuroblasts

Introduction

When neuroepithelial cells of the medulla are converted to neuroblasts, Eyeless (Ey) is among the earliest neuroblast-specific temporal patterning transcription factors expressed. The pioneering study that established temporal patterning of medulla neuroblasts showed that the first temporal patterning factor Homothorax (Hth), was required to activate Ey but was not sufficient (Li, Erclik et al. 2013). Further studies that have since expanded the repertoire of temporal patterning factors in medulla neuroblasts have shown using genetic interaction experiments that Ey may be activated by Odd-paired (Opa) and Doublesex-Mab related 99B (Dmrt99B) (Zhu, Zhao et al. 2022). However, whether these factors regulate ey gene expression at transcription remains unknown. Identifying enhancers of *ey* transcription by screening potential enhancer-Gal4 encoding fly lines and narrowing down putative transcriptional enhancers by enhancer bashing experiments, as demonstrated for *slp1* and *slp2* in Chapter 2, could fill this knowledge gap.

The *ey* gene was first identified as homologous to the *Pax6 (Small eye)* gene of mice and the *Aniridia* gene in humans (Quiring 1994). Like its counterpart in other species, it was essential for compound eye formation in *Drosophila*. The *ey* gene function is highly conserved across taxa, with the expression of *ey* homologs from other species inducing

eye formation in flies (Halder 1995, Callaerts 1997, Tomarev 1997). However, that *Pax6* has roles beyond eye development was suggested by observations that mice with homozygous mutations of the *Pax6* gene were lethal (Quiring 1994). Subsequent studies showed that *Pax6* mutant mice exhibited defects in forebrain development (Stoykova 1996), reminiscent of the roles of Ey in optic lobe patterning in flies. Early studies of *ey* gene regulation in flies primarily focused on *ey* function in the eye imaginal disc and the embryonic eye precursor region. In the context of eye development, a 212 bp enhancer element sufficient for driving *ey* gene expression in the eye imaginal disc was identified in the second intron of the *ey* gene (Hauck 1999). Also, analyses of hypomorphic mutant alleles of the *ey* gene revealed an enhancer of *ey* within intron 1 of the *ey* gene (Quiring 1994). Identifying potential Pax6 binding motifs within the second intronic *ey* enhancer also provided early evidence of direct transcriptional regulation of *ey* expression by a second *Pax6* gene in *Drosophila* called the *twin of eyeless* (*toy*) (Hauck 1999).

In contrast to an extensive body of literature on the transcriptional regulation of the *ey* gene and its interactions with other vital players of eye development, relatively little is known about Ey expression in the *Drosophila* central nervous system (CNS). A study of *ey* regulation in the fly CNS, especially in the mushroom bodies of the central brain, revealed the functioning of two *ey* enhancers in this context. One of these enhancers is located within an intron of the *ey* gene and the other upstream of it. These enhancers were distinct from those driving *ey* expression in eye discs (Adachi, Hauck et al. 2003). Moreover, the same study concluded that enhancers of *ey* active in the eye discs failed to drive robust Ey protein expression in the CNS. These studies suggest that the

transcriptional regulation of the *ey* gene has been observed across many systems and processes and therefore is a plausible mechanism of *ey* expression regulation in medulla neuroblasts. Ey appears to act as a temporal patterning factor in Type I medulla neuroblasts (Li, Erclik, et al. 2013) and intermediate progenitors of Type II neuroblasts in the fly ventral nerve cord (Bayraktar and Doe 2013). In both situations, interactions of Ey with other patterning factors have been inferred from genetic experiments, but transcriptional regulation has not been demonstrated. The *Pax6* gene is also expressed in early-born radial glia (Gotz 1998, Molyneaux, Arlotta et al. 2007), where it may play a role in the temporal patterning of the mammalian cortex (Li, Erclik et al. 2013), a system analogous to the fruit-fly optic lobe medulla in some respects. However, upstream regulators of *Pax6* expression in radial glia are not well established. Identifying *cis*-regulatory enhancers of *ey* in the fly medulla and transcription factors that bind them may help inform discoveries about *Pax6* regulation in radial glia of mammals. This is because gene networks controlling *ey* expression in the CNS likely differ from those regulating Ey expression in eye discs (Adachi, Hauck et al. 2003). Still, like in eye imaginal discs, these networks may be conserved across taxa.

In this study, we have identified an enhancer driving *ey* gene expression specifically in medulla neuroblasts, using an approach similar to that adopted for identifying enhancers of *slp* activation (Chapter 2). Besides furthering our understanding of the regulation of temporal patterning in fly medulla neuroblasts, identifying cis-regulatory enhancers of *ey* in the fly medulla and transcription factors that bind them may help inform discoveries about Pax6 regulation in the mammalian cortex as well.

Results

The GMR16F10 line expresses UAS-GFP in a pattern like endogenous ey in medulla neuroblasts.

We identified the GMR16F10-Gal4 for further testing from the FlyLight database, as it showed prominent expression in the fly optic lobe medulla in third instar larvae. When we crossed the *GMR16F10-Gal4* flies to *UAS GFPnls* flies, the pattern of GFP expressed closely coincided with endogenous Ey (Figure A1.1, A'-A'''').

Enhancer bashing experiments identified a 922bp segment within the GMR16F10 sequence that contains the ey enhancer

The 3034 bp sequence encoded by the GMR16F10-Gal4 line was divided into three smaller segments, EyL1, EyM1, and EyR2- each of lengths 1084 bp, 922bp, and 1986 bp, respectively. We cloned these elements into the pJR12 reporter vector (Rister 2015). As earlier, we generated transgenic flies expressing these enhancer-GFP reporters and compared the expression of GFP driven by the enhancers to patterns of endogenous Ey (Figure A1.1 B-B", C-C", D-D").

Of the three enhancer fragments tested, only the fragment named EyM1 of size 922 bp resulted in prominent GFP expression. This indicated that the active enhancer influencing Ey expression in medulla neuroblasts is located within the 922 bp fragment encoded by EyM1. The chromosomal location of the enhancer element (4: 698825-699651) coincides

with the first intron of the *ey* gene, so this enhancer element also has an intronic location but is distinct from the other intronic enhancers reported in the eye discs (Quiring 1994, Hauck 1999).

Preliminary bioinformatics analyses identified sites for binding temporal-patterning transcription factors in the 922 bp ey enhancer

Preliminary analysis using FIMO identified transcription factor binding sites for transcription factors that function as temporal patterning factors in medulla neuroblasts. A binding site for the temporal patterning transcription factor Odd-paired (Opa) expressed before Ey is found on this enhancer, indicating a strong possibility that Opa may initiate *ey* gene transcription in medulla neuroblasts. Additionally, sites for binding temporal patterning factors expressed later in the cascade, such as Sloppy-paired 1 and 2 (Slp1, Slp2) and Dichaete (D), are also present, indicating that the termination of Ey expression may also be regulated by these later temporal factors functioning as repressors. Sites for the transcription factor Glial cells missing (Gcm) expressed in old medulla neuroblasts that terminally differentiate into glia are also seen in the 922bp ey enhancer, as are sites for a transcription factor Lola. Future experiments will help verify the practical significance of these sites.

Discussion

This chapter describes our search for and discovering an enhancer that drives Ey expression, specifically in medulla neuroblasts. We screened putative enhancer-Gal4

lines from Janelia (Pfeiffer 2008, Jenett, Rubin et al. 2012) and identified that one Gal4 driver line- the GMR16F10 expresses UAS-GFP in a pattern like endogenous ey in medulla neuroblasts. Through enhancer bashing experiments, we have narrowed down the location of this enhancer element to a 922 bp segment inside the first intron of the *ey* gene. A search of other enhancers reported to direct Ey expression from the REDfly database (Gallo, Li et al. 2006) suggests that this 922bp enhancer is possibly one whose activity has not been reported in other developmental contexts. The presence of transcription binding sites for factors whose expressions and activity in medulla neuroblasts have been demonstrated in independent studies (Zhu, Zhao et al. 2022) is also a promising sign that this enhancer may indeed be active *in vivo*. Apart from temporal patterning factors, the *ey* enhancer also contains general binding sites for the transcription factor *longitudinals lacking* (*lola*). Lola factors have been shown to regulate the speed of temporal patterning cascade progression in medulla neuroblasts, with the early steps of the cascade, including Ey expression, being significantly slowed down in its absence ((Zhu, Zhao et al. 2022). Lola sites on the *ey* enhancer suggest that Lola may function in this capacity by transcriptional regulation of *ey* gene expression. In conclusion, identifying the 922bp *ey* enhancer and transcription factor binding sites for temporal patterning factors that constitute the medulla temporal cascade presents a promising opportunity to explore the mechanistic basis for *ey* transcription regulation.

Materials and methods

Fly Stocks used

GMR16F10-Gal4 (BDSC 48737)

w[1118]; P{w[+mC]=UAS-GFP.nls}14 (BDSC 4755)

y[1] w[1118]; PBac{y[+]-attP-9A}VK00027 (BDSC 9744)

ywhsFlp; Sp/CyO; T2/Tm6B

ywhsFlp; Sp/CyO; EyL1>GFP/Tm6B (this study)

ywhsFlp; Sp/CyO; EyM1/Tm6B (this study)

ywhsFlp; Sp/CyO; EyR2/Tm6B (this study)

Antibodies used

guinea-pig anti-Dpn (1:500) (a kind gift from Dr. Chris Doe).

sheep anti-GFP (1:500, AbD Serotec, 4745-1051)

mouse anti-eyeless (1:10, Developmental Studies Hybridoma Bank (DSHB))

Secondary antibodies are from Jackson or Invitrogen.

Experimental Methods

Methods used in enhancer identification, cloning, and making transgenic flies expressing putative enhancer segments and bioinformatic identification of transcription factor binding sites are the same as described in Chapter 2

Plasmids constructs and the making of transgenic fly stocks

Primer sequences for all cloning are provided separately (Figure A1.4). For all constructs, DNA was amplified from a BAC template using Expand High-Fidelity Polymerase (Roche) unless stated otherwise, and all constructs were verified by sequencing. All fly embryo injections for making transgenic flies were carried out by Bestgene Inc, Chino Hills, CA.

Generating constructs for reporter assays and enhancer bashing and making transgenic reporter expressing stocks

Sequences corresponding to the fragments of regulatory DNA encoded in GMR16F10 were cloned from the BAC clone CH322-15A2 (Venken, Carlson et al. 2009) (BACPAC resources). Sequences were PCR amplified from this BAC and cloned into the pJR12 vector (a kind gift from Dr. Jens Rister) between *EcoRI* and *BamHI* sites. Transgenes were inserted at the landing site VK00027 on the third chromosome (BL9744) by φC31 integrase mediated transgenesis (Groth 2004), and positive transformants were selected using the w+ marker originally present in the pJR12 plasmid.

Bioinformatic identification of transcription factor binding sites

To identify candidate transcription factors with binding sites within the 922 bp EyM1 enhancer, we analyzed the EyM1 sequence using an analytic tool developed at EPFL (https://biss.epfl.ch) that uses FIMO (Grant, Bailey et al. 2011) to identify motifs in a DNA sequence (Michael Frochaux, Dr.Bart Deplancke personal communication). The sites for binding transcription factors that have been shown experimentally to be active in temporal patterning medulla neuroblasts are highlighted in Figure A1.3.

Immunofluorescence staining

Antibody staining was carried out as described in (Li, Erclik et al. 2013) with a few modifications. The protocol is described as follows: brains from climbing third instar larvae were dissected in 1XPBS and fixed in 4% Formaldehyde solution in 1X PBS for 30 minutes on ice. Brains were then incubated in primary antibody solution overnight at 4^{o}C, washed three times for 30 minutes each at 4^{o}C, then incubated in fluor conjugated-secondary antibody solution overnight at 4^{o}C, and then washed thrice at room temperature each time for 30 minutes. Samples were mounted in Slowfade Gold antifade reagent (Invitrogen). Images are acquired using a Zeiss LSM500 Confocal Microscope.

Figures

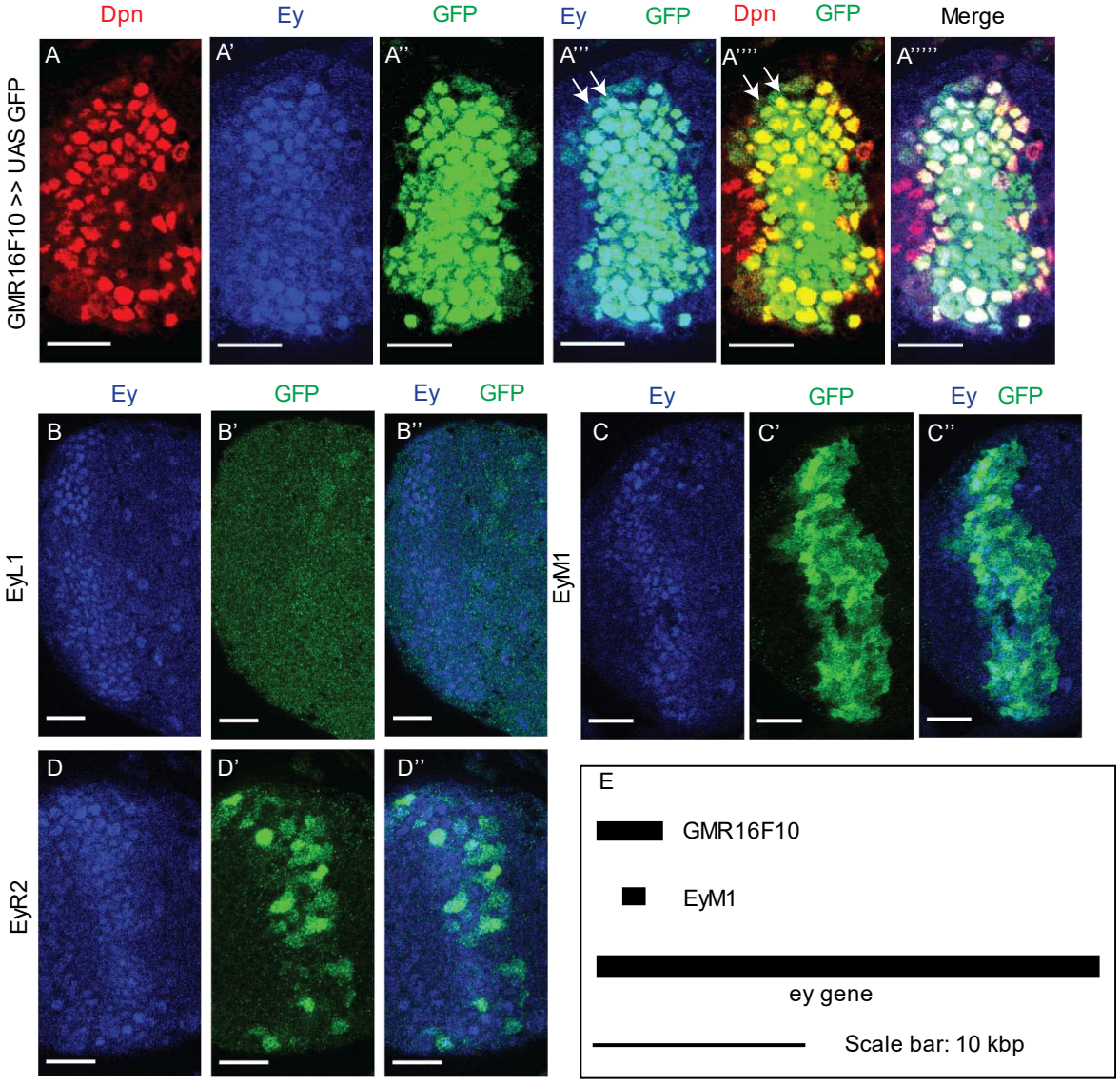

Figure A.1 A 922bp DNA element within the ey gene functions as an enhancer of ey expression in medulla neuroblasts. (A-A'''') The GMR16F10 Gal4 contains an enhancer element that drives *UAS-GFP* expression in a pattern that overlaps endogenous Ey (A''', neuroblasts co-expressing Ey and GFP marked by arrows) in

Figure A.1 (cont.) medulla neuroblasts marked by Dpn expression (A, A""). Sub-segments of sequence encoded in the GMR16F10 Gal4 were cloned in the pJR12 GFP reporter vector. Transgenic flies were observed for GFP expression (B-D). Of these smaller DNA fragments, the EyM1 fragment (C-C") expressed GFP in a pattern overlapping endogenous Ey (C"). The EyR2 fragment showed GFP expression in small cell clusters in some neuroblasts and deeper neural layers but did not overlap uniformly with Ey expression (D-D"). The EyL1 fragment did not show any GFP expression (B-B"). Scale bars 20 microns. E. A schematic drawing to scale shows the ey gene's relative genomic positions to the GMR16F10 Gal4 and the smaller EyM1 enhancer within the GMR16F10 sequence. The 5' end of the GMR16F10 encoded sequence is 18bp from the 5' terminus of the *ey* gene, and the GMR16F10 element is of length 3kbp. The 922 bp EyM1 element is located 1854bp from the 5' end of the GMR16F10 element.

A. EyL1

Chromosomal location 4:697672-698755

Size: 1084bp

Sequence

GCAGATGCGTGCTGAAGTCCAATCGATACTACAAAATACCAAAATACACAGAAAATATAAACAAT
ATTGCATAAACAATATTGTACGAACGTTCGTTTTAGTGTTTAATCACATACTGTTTTTCCCCCATCC
GAAAATCGAAGAAAATGTGTGACAATCAATATCTAATAAAAGAATCAGGATACATGTGCGACCATT
CGTAATATAAATATGTATGTATATTTTGTAAATATTATTCCCTACTAACTAAACCCATCTGTGTGAA
TTTTTCCCAAAAGCCCTCTTATTATTGCAGGTAGTACATATATTAGTCGAAATAATTATGATCCGAA
AGTTTTTTAATAAGGCTTTTGACCGTAATTAATTTCGAATTGGTTTAACCAAAAAGTGACGACGGT
CATTTAAAAGGTCAGAAATTTAATTTAAAATATTAGAAGAGAAACTCTAATATTTTTATTTTGTGTCA
TACATTGCACCCATTCGGAATATACCGTTTTTTTTTAAAATTATATGTAATGCCCTTTGGCTTGCCA
CTCACTCGGTGAGGCCATAAGATGTTCTCCGATCGCCACCGTGTTTAAGAGAGAAAGTTGCAGA
ATGAAGTCTTACAAGCACATTTCTAAAAAAGGGACAACGCTCTTAAAAGGAAATAGTTATATATAC
CGAGTAATGACATCTGTGATTAGTCTATGATTTATATTATAATATAGCTACGCAGATCGTAACTAA
CAGATACCCCTTACATTGCTGGTAGGAGTTTTTACTCCTACTCTCTTTTGAGAGATGGAGAAAAAA
TAAAAAGAAAAACACTCTTCGATATTGGTCGATAGCTTAAGCTGGTGGCGGTTAGATTAATTGCC
ATTGTAATTTGCGGGCGTTACTCATTTGGCACTCTTAAAATCAAAGTGGAAAGAAAGGTGGATAA
GTAAAAAAGGGTGCGGAATGAGTACCGTTTATATAGTGTGTTTATCAAGTAAATGACAATTTTTTC
GTCACTAAAGTTGATATTACAACTTTTTATGTTGGAGGTTCGATCTGAAAATAGCAACAGCAATAA
AACATCGACTCTCAGAAACCAGTTACC

Figure A.2

B. EyM1

Chromosomal location 4: 698825-699651

Size: 922bp

Sequence

ACATCGACTCTCAGAAACCAGTTACCAGAAACCATCGACAAAAATTGGCCCGAAAAACATTAAAA
AACTAAACAAAAACAATTCAAATTTCAAAAGTGCGGGCGTGGGGTTATGGGTTATGGGGTTATGT
TGACATGGGTAAACAAACTTGAGCTGCGTCTATGTCTCTGGAATCTGCAAGTCAACTCTATAGCT
TTATTAGTTCCTGAGATCGCGGCGTTCATATGGTTAGACGGACGAACAGACGAACATGTTCATAT
TGACTCGGCTATTGATACTGATCAATAATATATATACTTTATATGGTCGGAAACGCTCTCTTCTATT
TGCTACATAATCTTCAAAGCATAAAATAATAATAATGGGTGTAATAATGGTTTTTTATTTTGGCAAG
CCAATTTATAGTGAATTATTAAAAATTATAAACTGCAGTCAATAAAGTAACATTGCTTGTTATTTAA
GAAATCGCAGGCCTTATGACTAGTCAAGAATTTAATATATTTAAAGGTCTCAACCCCAGGATTCA
GGAACTTCTCCCAGTGAACCCCACTAGTTTGGTACTAAAGGCATTACCGTAAGACGCTTATATCG
ACTCCTCTTTGTTATTTCCAGTTTGGGCAGATCGAACACTTTGATCTTCCTTGTTGGGCCTCACAG
CGGGAAAAAAAAAGTTGCTTTGCATGGGTTTAGGGAACTTTACAACTGTTCGATCACGATCTTTG
CAGTGCAACCCCTAGGAGCCAAGTCGGGAAGCGGGTTAGCCGGTCTGCTATCGATTCTCGTGT
GAACACATGCAATTATGGTTTTATTTGTATTATTCGTAGTTTGCATTTACAAGTTTTTGTTTGTTTTC
AAAATAGAACCTTAAGTTTGAAATTTTCATGATCATGAGAAGCTATTGTTCGTGAAAGCCCAACAG
CGT

Figure A.2 (cont.)

C. EyR2

Chromosomal location 4: 698825-700705

Size: 1960bp

Sequence

ACCAGTTACCAGAAACCATCGACAAAAATTGGCCCGAAAAACATTAAAAAACTAAACAAAAACAAT
TCAAATTTCAAAAGTGCGGGCGTGGGGTTATGGGTTATGGGGTTATGTTGACATGGGTAAACAA
ACTTGAGCTGCGTCTATGTCTCTGGAATCTGCAAGTCAACTCTATAGCTTTATTAGTTCCTGAGAT
CGCGGCGTTCATATGGTTAGACGGACGAACAGACGAACATGTTCATATTGACTCGGCTATTGATA
CTGATCAATAATATATATACTTTATATGGTCGGAAACGCTCTCTTCTATTTGCTACATAATCTTCAA
AGCATAAAATAATAATAATGGGTGTAATAATGGTTTTTTATTTTGGCAAGCCAATTTATAGTGAATT
ATTAAAAATTATAAACTGCAGTCAATAAAGTAACATTGCTTGTTATTTAAGAAATCGCAGGCCTTAT
GACTAGTCAAGAATTTAATATATTTAAAGGTCTCAACCCCAGGATTCAGGAACTTCTCCCAGTGAA
CCCCACTAGTTTGGTACTAAAGGCATTACCGTAAGACGCTTATATCGACTCCTCTTTGTTATTTCC
AGTTTGGGCAGATCGAACACTTTGATCTTCCTTGTTGGGCCTCACAGCGGGAAAAAAAAAGTTGC
TTTGCATGGGTTTAGGGAACTTTACAACTGTTCGATCACGATCTTTGCAGTGCAACCCCTAGGAG
CCAAGTCGGGAAGCGGGTTAGCCGGTCTGCTATCGATTCTCGTGTGAACACATGCAATTATGGT
TTTATTTGTATTATTCGTAGTTTGCATTTACAAGTTTTTGTTTGTTTTCAAAATAGAACCTTAAGTTT
GAAATTTTCATGATCATGAGAAGCTATTGTTCGTGAAAGCCCAACAGCGTGGCAACCCTAATTGT
TTTGTAAAAAGAAATATAAAACATTTAAAGGCATGTGAATGTTGGAAGAAACCACTATTCATTTTG
ATACCGAATAAGTACATTTTATATAGTTCAAATAAATATAAAACAACGTCCTGTATCAAACCAAAAT
TCACAAAAAGTTTTAATTTTATGATCCCCAAAAATGTATATTTGGGAATGTCTTCTTATGAAACCCC
ATCAGCCACAATTGTCTAAACTTGTACTTCAGTTGAGCTCCTAGTGGGAGTTCAAAGCAGAAATT
TCCATATTTCTTTTTGTCAAATCGATAGAAAGCAGCTAGACAATAAGGAAATACGTTTTAATATTTT
TAAAAAGTGTACGTATGCATGCTTTGTCTCAAATTTCTGGCCTTGATAGTTAGTTACTGAAATCTC

Figure A.2 (cont.)

C. EyR2 (sequence continued from previous page)

AAAGTTTACACGGCTGGACTGACATAAGTACGGATAGGCGGACGTGGCCTAGTAGACTCGTTTT
GTGATCGTGAAATATGTGAATAAAAAGAAAAAATCGCTTTTTTTTATCTATTGCGAACTTAAAGAAT
ATAGTCTAGCTGGGCACTCTACGGGTAAGGGGCTTACATTTATCGCTGTTAAGGACGCAGTTATT
TCAAGTTTTATAATTGTGCTATATTTACGCTCGGGATGGATGAGAAGCACTTGATATGGCTGAGC
AAGGCCACTGGGCACTAGCAAAAACTTCCAACCACTTTACTTTGTTAAATTTGATTTTAATCCGCT
GATAATATTTTAAGACTTTCTCTTTCGCTCGGTTGAATTTAATGCGATTTAATCACACCGTATACAA
AGAGTGTACATCAATTTTCGTTCCAGGAGGAAAAAGGTGGCGTGCTAAAAAATAACTTAAATCGT
AAAGGCGATATCGTAACCAATTTAAATGTTTAACCTTTTATGAAATACTTTAAGAAATATCAAAAAT
TAAACTTTACGAGTAACGGGTATAAAGCAAAAGGAACACACTCCACATTGCGTATTGTATAGATAT
TCTGATTATACGCATTAGATTGGTTGAACTGTCTGCAACAGGAAGAAGG

Figure A.2 (cont.) The GMR16F10 sequence was divided into three smaller segments whose enhancer functions were tested in GFP reporter assays. Sequence, chromosomal location, and size of A. EyL1, B. EyM1, and C.EyR2 are shown.

A. Transcription factor binding sites in EyM1

Sequence

ACATCGACTCTCAGAAACCAGTTACCAGAAACCATCGACAAAAATTGGCCCGAAAAACATTAAAA
AACTAAACAAAAACAATTCAAATTTCAAAAGTGCGGGCGTGGGGTTATGGGTTATGGGGTTATGT
TGACATGGGTAAACAAACTTGAGCTGCGTCTATGTCTCTGGAATCTGCAAGTCAACTCTATAGCT
TTATTAGTTCCTGAGATCGCGGCGTTCATATGGTTAGACGGACGAACAGACGAACATGTTCATAT
TGACTCGGCTATTGATACTGATCAATAATATATATACTTTATATGGTCGGAAACGCTCTCTTCTATT
TGCTACATAATCTTCAAAGCATAAAATAATAATAATGGGTGTAATAATGGTTTTTTATTTTGGCAAG
CCAATTTATAGTGAATTATTAAAAATTATAAACTGCAGTCAATAAAGTAACATTGCTTGTTATTTAA
GAAATCGCAGGCCTTATGACTAGTCAAGAATTTAATATATTTAAAGGTCTCAACCCCAGGATTCA
GGAACTTCTCCCAGTGAACCCCACTAGTTTGGTACTAAAGGCATTACCGTAAGACGCTTATATCG
ACTCCTCTTTGTTATTTCCAGTTTGGGCAGATCGAACACTTTGATCTTCCTTGTTGGGCCTCACAG
CGGGAAAAAAAAAGTTGCTTTGCATGGGTTTAGGGAACTTTACAACTGTTCGATCACGATCTTTG
CAGTGCAACCCCTAGGAGCCAAGTCGGGAAGCGGGTTAGCCGGTCTGCTATCGATTCTCGTGT
GAACACATGCAATTATGGTTTTATTTGTATTATTCGTAGTTTGCATTTACAAGTTTTTGTTTGTTTTC
AAAATAGAACCTTAAGTTTGAAATTTTCATGATCATGAGAAGCTATTGTTCGTGAAAGCCCAACAG
CGT

B. Transcription Factor	Strand	Sequence
Slp1	-	TTGTTTACCCA
Slp1	-	TTGTTTTTGTT
Gcm	-	ACGCCCGCACTTT
Lola	+	AGCATAA
D	+	GCTATTGTTCG
Opa	+	GTGAACCCCACTA

Figure A.3 Sites for binding transcription factors that participate in the temporal patterning of medulla neuroblasts were identified in the EyM1 sequence. A. Sequence of EyM1 with transcription factor binding sites for medulla temporal patterning

Figure A.3 (cont.) transcription factors highlighted. Yellow marks sites for Slp1 binding, magenta indicates sites for Lola binding, green for D binding, red for Opa binding, and blue for Gcm binding. B. A table showing the strand and the locations of transcription factor binding sites in A.

Experiment	Forward Primer	Reverse primer
Cloning EyL1	AATGAATTCGCAGATGCGTGCTGAAGTCCAATC	TATGGATCCGGTAACTGGTTTCTGAGAGTCGATGT
Cloning EyM1	AATGAATTCACATCGACTCTCAGAAACCAGTTACC	TATGGATCCACGCTGTTGGGCTTTCACGAACAA
Cloning EyR2	AATGAATTCACCAGTTACCAGAAACCATCGACA	TATGGATCCCCTTCTTCCTGTTGCAGACAGTTCA

Figure A.4 Sequences of primers used for cloning segments of enhancers from the GMR16F10 sequence.

References

Adachi, Y., B. Hauck, J. Clements, H. Kawauchi, M. Kurusu, Y. Totani, Y. Y. Kang, T. Eggert, U. Walldorf, K. Furukubo-Tokunaga and P. Callaerts (2003). "Conserved cis-regulatory modules mediate complex neural expression patterns of the eyeless gene in the Drosophila brain." Mech Dev **120**(10): 1113-1126.

Agbleke, A. A., A. Amitai, J. D. Buenrostro, A. Chakrabarti, L. Chu, A. S. Hansen, K. M. Koenig, A. S. Labade, S. Liu, T. Nozaki, S. Ovchinnikov, A. Seeber, H. A. Shaban, J. H. Spille, A. D. Stephens, J. H. Su and D. Wadduwage (2020). "Advances in Chromatin and Chromosome Research: Perspectives from Multiple Fields." Mol Cell **79**(6): 881-901.

Almeida, M. S. and S. J. Bray (2005). "Regulation of post-embryonic neuroblasts by Drosophila Grainyhead." Mech Dev **122**(12): 1282-1293.

Arnold, C. D., Gerlach, D.,Stelzer, C., Boryn, L.M., Rath,M. and Stark, A. (2013). "Genome-wide quantitative enhancer activity maps identified by STARR-seq." Science **339**(6123): 1074-1077.

Awasaki, T., C. F. Kao, Y. J. Lee, C. P. Yang, Y. Huang, B. D. Pfeiffer, H. Luan, X. Jing, Y. F. Huang, Y. He, M. D. Schroeder, A. Kuzin, T. Brody, C. T. Zugates, W. F. Odenwald

and T. Lee (2014). "Making Drosophila lineage-restricted drivers via patterned recombination in neuroblasts." Nat Neurosci **17**(4): 631-637.

Awgulewitsch, A., and Jacobs, D. (1992). "Deformed autoregulatory element from Drosophila functions in a conserved manner in transgenic mice " Nature **358**: 341-344.

Babaoglan, A. B., B. E. Housden, M. Furriols and S. J. Bray (2013). "Deadpan contributes to the robustness of the notch response." PLoS One **8**(9): e75632.

Bailey, T. L., J. Johnson, C. E. Grant and W. S. Noble (2015). "The MEME Suite." Nucleic Acids Res **43**(W1): W39-49.

Barolo, S. (2012). "Shadow enhancers: frequently asked questions about distributed cis-regulatory information and enhancer redundancy." Bioessays **34**(2): 135-141.

Baumgardt, M., D. Karlsson, B. Y. Salmani, C. Bivik, R. B. MacDonald, E. Gunnar and S. Thor (2014). "Global programmed switch in neural daughter cell proliferation mode triggered by a temporal gene cascade." Dev Cell **30**(2): 192-208.

Baumgardt, M., D. Karlsson, J. Terriente, F. J. Diaz-Benjumea and S. Thor (2009). "Neuronal subtype specification within a lineage by opposing temporal feed-forward loops." Cell **139**(5): 969-982.

Bayraktar, O. A. and C. Q. Doe (2013). "Combinatorial temporal patterning in progenitors expands neural diversity." Nature **498**(7455): 449-455.

Behnia, R. and C. Desplan (2015). "Visual circuits in flies: beginning to see the whole picture." Curr Opin Neurobiol **34**: 125-132.

Bello, B. C., N. Izergina, E. Caussinus and H. Reichert (2008). "Amplification of neural stem cell proliferation by intermediate progenitor cells in Drosophila brain development." Neural Dev **3**: 5.

Benito-Sipos, J., C. Ulvklo, H. Gabilondo, M. Baumgardt, A. Angel, L. Torroja and S. Thor (2011). "Seven up acts as a temporal factor during two different stages of neuroblast 5-6 development." Development **138**(24): 5311-5320.

Bertet, C., X. Li, T. Erclik, M. Cavey, B. Wells and C. Desplan (2014). "Temporal patterning of neuroblasts controls Notch-mediated cell survival through regulation of Hid or Reaper." Cell **158**(5): 1173-1186.

Bivik, C., R. B. MacDonald, E. Gunnar, K. Mazouni, F. Schweisguth and S. Thor (2016). "Control of Neural Daughter Cell Proliferation by Multi-level Notch/Su(H)/E(spl)-HLH Signaling." PLoS Genet **12**(4): e1005984.

Boone, J. Q. a. D., C.Q. (2008). "Identification of Drosophila Type II lineages containing transit amplifying ganglion mother cells." Developmental Neurobiology **68**(9).

Borst, A. and M. Helmstaedter (2015). "Common circuit design in fly and mammalian motion vision." Nat Neurosci **18**(8): 1067-1076.

Bosch, J. A., N. H. Tran and I. K. Hariharan (2015). "CoinFLP: a system for efficient mosaic screening and for visualizing clonal boundaries in Drosophila." Development **142**(3): 597-606.

Bossing, T., Udolph, G., Doe, C.Q. and Technau, G.M. (1996). "The embryonic CNS lineages of Drosophila melanogaster " Developmental Biology **179**: 41-64.

Bowman, S. K., V. Rolland, J. Betschinger, K. A. Kinsey, G. Emery and J. A. Knoblich (2008). "The tumor suppressors Brat and Numb regulate transit-amplifying neuroblast lineages in Drosophila." Dev Cell **14**(4): 535-546.

Bray, S. J. (2006). "Notch signalling: a simple pathway becomes complex." Nat Rev Mol Cell Biol **7**(9): 678-689.

Broadus, J., Skeath, J.B., Spana, E.,Bossing,T.,Technau, G. and Doe, C.Q. (1995). "New neuroblast markers and the origin of the aCC/pCC neurons in the Drosophila central nervous system " Mechanisms of Development **53**: 393-402.

Brody, T., W. Rasband, K. Baler, A. Kuzin, M. Kundu and W. F. Odenwald (2007). "cis-Decoder discovers constellations of conserved DNA sequences shared among tissue-specific enhancers." Genome Biol **8**(5): R75.

Butler, J. E. and J. T. Kadonaga (2001). "Enhancer-promoter specificity mediated by DPE or TATA core promoter motifs." Genes Dev **15**(19): 2515-2519.

Cadigan, K. M., Grossniklaus, U. and Gehring, W.J. (1994). "Functional redundancy: the respective roles of the two sloppy-paired genes in Drosophila segmentation." Proc Natl Acad Sci U S A **91**: 6324-6328.

Calegari, F. and W. B. Huttner (2003). "An inhibition of cyclin-dependent kinases that lengthens, but does not arrest, neuroepithelial cell cycle induces premature neurogenesis." J Cell Sci **116**(Pt 24): 4947-4955.

Callaerts, P., Halder, G., and, Genring, W.J. (1997). "*PAX-6* in development and evolution." Annual Reviews Neuroscience **20**: 483-532.

Campos-Ortega, J. A. (1988). "Cellular interactions during early neurogenesis of Drosophila melanogaster " Trends Neurosci **11**(9): 400-405.

Cannavo, E., P. Khoueiry, D. A. Garfield, P. Geeleher, T. Zichner, E. H. Gustafson, L. Ciglar, J. O. Korbel and E. E. Furlong (2016). "Shadow Enhancers Are Pervasive Features of Developmental Regulatory Networks." Curr Biol **26**(1): 38-51.

Chawla, G. and N. S. Sokol (2012). "Hormonal activation of let-7-C microRNAs via EcR is required for adult Drosophila melanogaster morphology and function." Development **139**(10): 1788-1797.

Chen, Z., A. Del Valle Rodriguez, X. Li, T. Erclik, V. M. Fernandes and C. Desplan (2016). "A Unique Class of Neural Progenitors in the Drosophila Optic Lobe Generates Both Migrating Neurons and Glia." Cell Rep **15**(4): 774-786.

Cleary, M. D. and C. Q. Doe (2006). "Regulation of neuroblast competence: multiple temporal identity factors specify distinct neuronal fates within a single early competence window." Genes Dev **20**(4): 429-434.

Decembrini, S., Bressan, D., Vignali, R., Pitto, L., MAriotti, S., Rainaldi, G., Wang, X., Evangelista, M., Barsachhi, G., Creminsi, F. (2009). "MicroRNAs couple cell fate and developmental timing in retina." Proc Natl Acad Sci U S A **106**(50): 21179-21184.

Doe, C. Q. (2017). "Temporal Patterning in the Drosophila CNS." Annu Rev Cell Dev Biol **33**: 219-240.

Douglass, J. K. and Strausfeld, N.J. (1995). "Visual motion detection circuits in flies: peripheral motion computation by identified small-field retinotopic neurons " The Journal of Neuroscience **15**(8): 5598-5611.

Edgar, B. A. and O' Farrell, P. (1989). "Genetic control of cell division patterns in the Drosophila embryo." Cell **57**(1): 177-187.

Egger, B., J. Q. Boone, N. R. Stevens, A. H. Brand and C. Q. Doe (2007). "Regulation of spindle orientation and neural stem cell fate in the Drosophila optic lobe." Neural Dev **2**: 1.

Elliott, J., C. Jolicoeur, V. Ramamurthy and M. Cayouette (2008). "Ikaros confers early temporal competence to mouse retinal progenitor cells." Neuron **60**(1): 26-39.

Erclik, T., V. Hartenstein, H. D. Lipshitz and R. R. McInnes (2008). "Conserved role of the Vsx genes supports a monophyletic origin for bilaterian visual systems." Curr Biol **18**(17): 1278-1287.

Erclik, T., X. Li, M. Courgeon, C. Bertet, Z. Chen, R. Baumert, J. Ng, C. Koo, U. Arain, R. Behnia, A. del Valle Rodriguez, L. Senderowicz, N. Negre, K. P. White and C. Desplan (2017). "Integration of temporal and spatial patterning generates neural diversity." Nature **541**(7637): 365-370.

Evans, C. J., J. M. Olson, K. T. Ngo, E. Kim, N. E. Lee, E. Kuoy, A. N. Patananan, D. Sitz, P. Tran, M. T. Do, K. Yackle, A. Cespedes, V. Hartenstein, G. B. Call and U. Banerjee (2009). "G-TRACE: rapid Gal4-based cell lineage analysis in Drosophila." Nat Methods **6**(8): 603-605.

Faedo, A., G. S. Tomassy, Y. Ruan, H. Teichmann, S. Krauss, S. J. Pleasure, S. Y. Tsai, M. J. Tsai, M. Studer and J. L. Rubenstein (2008). "COUP-TFI coordinates cortical patterning, neurogenesis, and laminar fate and modulates MAPK/ERK, AKT, and beta-catenin signaling." Cereb Cortex **18**(9): 2117-2131.

Falo-Sanjuan, J., N. C. Lammers, H. G. Garcia and S. J. Bray (2019). "Enhancer Priming Enables Fast and Sustained Transcriptional Responses to Notch Signaling." Dev Cell **50**(4): 411-425 e418.

Farkas, L. M. and W. B. Huttner (2008). "The cell biology of neural stem and progenitor cells and its significance for their proliferation versus differentiation during mammalian brain development." Curr Opin Cell Biol **20**(6): 707-715.

Farnsworth, D. R., O. A. Bayraktar and C. Q. Doe (2015). "Aging Neural Progenitors Lose Competence to Respond to Mitogenic Notch Signaling." Curr Biol **25**(23): 3058-3068.

Fischbach, K. F. and Dittrich., A.P.M (1989). "The optic lobe of Drosophila melanogaster. I. A Golgi analysis of wild type structure." Cell Tissue Research **258**: 441-475.

Fleming, R. J., Scottgale, T.N., Diederich, R.J., and Artavanis-Tsakonas, S. (1990). "The gene Serrate encodes a putative EGF-like transmembrane protein essential for proper ectodermal development in Drosophila melanogaster." Genes Dev **4**(12A): 2188-2201.

Flores, A. N., N. McDermott, A. Meunier and L. Marignol (2014). "NUMB inhibition of NOTCH signalling as a therapeutic target in prostate cancer." Nat Rev Urol **11**(9): 499-507.

Fornes, O., J. A. Castro-Mondragon, A. Khan, R. van der Lee, X. Zhang, P. A. Richmond, B. P. Modi, S. Correard, M. Gheorghe, D. Baranasic, W. Santana-Garcia, G. Tan, J. Cheneby, B. Ballester, F. Parcy, A. Sandelin, B. Lenhard, W. W. Wasserman and A. Mathelier (2020). "JASPAR 2020: update of the open-access database of transcription factor binding profiles." Nucleic Acids Res **48**(D1): D87-D92.

Fortini, M. E. (2009). "Notch signaling: the core pathway and its posttranslational regulation." Dev Cell **16**(5): 633-647.

Frankel, N., G. K. Davis, D. Vargas, S. Wang, F. Payre and D. L. Stern (2010). "Phenotypic robustness conferred by apparently redundant transcriptional enhancers." Nature **466**(7305): 490-493.

Fujioka, M. and J. B. Jaynes (2012). "Regulation of a duplicated locus: Drosophila sloppy paired is replete with functionally overlapping enhancers." Dev Biol **362**(2): 309-319.

Fukaya, T. and M. Levine (2017). "Transvection." Curr Biol **27**(19): R1047-R1049.

Gallo, S. M., L. Li, Z. Hu and M. S. Halfon (2006). "REDfly: a Regulatory Element Database for Drosophila." Bioinformatics **22**(3): 381-383.

Ghiasvand, N. M., D. D. Rudolph, M. Mashayekhi, J. A. t. Brzezinski, D. Goldman and T. Glaser (2011). "Deletion of a remote enhancer near ATOH7 disrupts retinal neurogenesis, causing NCRNA disease." Nat Neurosci **14**(5): 578-586.

Gold, K. S. and Brand., A.H. (2014). "Optix defines a neuroepithelial compartment in the optic lobe of the Drosophila brain." Neural Dev **9**(18).

Gomes, F. L., G. Zhang, F. Carbonell, J. A. Correa, W. A. Harris, B. D. Simons and M. Cayouette (2011). "Reconstruction of rat retinal progenitor cell lineages in vitro reveals a surprising degree of stochasticity in cell fate decisions." Development **138**(2): 227-235.

Gotz, M., Stoykova, A., and Gruss, P. (1998). "*Pax6* controls radial glia differentiation in the cerebral cortex " Neuron **21**: 1034-1044.

Grant, C. E., T. L. Bailey and W. S. Noble (2011). "FIMO: scanning for occurrences of a given motif." Bioinformatics **27**(7): 1017-1018.

Gratz, S. J., F. P. Ukken, C. D. Rubinstein, G. Thiede, L. K. Donohue, A. M. Cummings and K. M. O'Connor-Giles (2014). "Highly specific and efficient CRISPR/Cas9-catalyzed homology-directed repair in Drosophila." Genetics **196**(4): 961-971.

Green, P., Hartenstein, A.Y. and Hartenstein, V. (1993). "The embryonic development of the Drosophila visual system " Cell Tissue Research **273** 583-598.

Greig, L. C., M. B. Woodworth, M. J. Galazo, H. Padmanabhan and J. D. Macklis (2013). "Molecular logic of neocortical projection neuron specification, development and diversity." Nat Rev Neurosci **14**(11): 755-769.

Grosskortenhaus, R., B. J. Pearson, A. Marusich and C. Q. Doe (2005). "Regulation of temporal identity transitions in Drosophila neuroblasts." Dev Cell **8**(2): 193-202.

Grossniklaus, U., , Pearson, R.K. and Gehring,W.J. (1992). "The Drosophila sloppy-paired gene encodes two proteins involved in segmentation that show homology to mammalian transcription factors." Genes Dev **6**: 1030-1051.

Groth, A. C., Fish, M., Nusse, R., and Calos, M.P. (2004). "Construction of transgenic Drosophila by using the site specific integrase from Phage PhiC31 " Genetics **166**: 1775-1782.

Gupta, S., J. A. Stamatoyannopoulos, T. L. Bailey and W. S. Noble (2007). "Quantifying similarity between motifs." Genome Biol **8**(2): R24.

Halder, G., Callaerts, P., and, Genring, W.J. (1995). "Induction of ectopic eyes by targeted expression of the *eyeless* gene in Drosophila " Science **267**: 1788-1792.

Hanashima, C., Li, S.C., Shen, L.,Lai, E. and Fishell, G. (2004). "Foxg1 suppresses early cortical cell fate." Science **203**(5654): 56-59.

Hartenstein V., Younossi-Hartenstein, A. and Lekven, A. (1994). "Delamination and division in the Drosophila neurectoderm : spatiotemporal pattern, cytoskeletal dynamicsand common control by neurogenic and segment-polarity genes." Developmental Biology **165**: 480-499.

Hartenstein, V. and Campos-Ortega, J.A. (1984). "Early neurogenesis in wild type Drosophila melanogaster " Roux's archives of developmental biology **193**: 308-325.

Hauck, B., Gehring, W.J., and Walldorf, U. (1999). "Functional analysis of an eye specific enhancer of the eyeless gene in Drosophila." PNAS **96**: 564-569.

Hirono, K., J. S. Margolis, J. W. Posakony and C. Q. Doe (2012). "Identification of hunchback cis-regulatory DNA conferring temporal expression in neuroblasts and neurons." Gene Expr Patterns **12**(1-2): 11-17.

Hofbauer, A. and Campos-Ortega, J.A. (1990). "Proliferation pattern and early differentiation of the optic lobes in Drosophila melanogaster " Roux's archives of developmental biology **198**: 264-274.

Huang da, W., B. T. Sherman and R. A. Lempicki (2009). "Bioinformatics enrichment tools: paths toward the comprehensive functional analysis of large gene lists." Nucleic Acids Res **37**(1): 1-13.

Huang da, W., B. T. Sherman and R. A. Lempicki (2009). "Systematic and integrative analysis of large gene lists using DAVID bioinformatics resources." Nat Protoc **4**(1): 44-57.

Huang, Z., Shilo, B. and Kunes, S. (1998). "A retinal axon fascicle uses Spitz, an EGF receptor ligand to construct a synaptic cartridge in the brain of Drosophila " Cell **95**: 693-703.

Huang, Z. and Kunes, S. (1996). "Hedgehog, transmitted along retinal axons, triggers neurogenesis in the developing visual centers of the Drosophila brain." Cell **86**: 411-422.

Hulsen, T., J. de Vlieg and W. Alkema (2008). "BioVenn - a web application for the comparison and visualization of biological lists using area-proportional Venn diagrams." BMC Genomics **9**: 488.

Isshiki, T., Pearson, B., Holbrook, S. and Doe, C.Q. (2001). "Drosophila neuroblasts sequentially express transcription factors which specify the tmporal identity of their neuronal progeny " Cell **106**: 511-521.

Ito, K., Awano, W., Suzuki, K, Hiromi, Y., and Yamamoto, D., (1997). "The Drosophila mushroom body is a quadruple structure of clonal units each of which contains a virtually identical set of neurones and glial cells." Development **124**: 761-771.

Ito, K., Awano, W., Suzuki, K., Hiromi, Y., and Yamamoto, D. (1997). "The Drosophila mushroom body is a quadruple structure of clonal units each of which contains a virtually identical set of neurones and glial cells " Developemnt **124**: 761-771.

Ito, M., N. Masuda, K. Shinomiya, K. Endo and K. Ito (2013). "Systematic analysis of neural projections reveals clonal composition of the Drosophila brain." Curr Biol **23**(8): 644-655.

Janssens, J., S. Aibar, Taskiran, II, J. N. Ismail, A. E. Gomez, G. Aughey, K. I. Spanier, F. V. De Rop, C. B. Gonzalez-Blas, M. Dionne, K. Grimes, X. J. Quan, D. Papasokrati, G. Hulselmans, S. Makhzami, M. De Waegeneer, V. Christiaens, T. Southall and S. Aerts (2022). "Decoding gene regulation in the fly brain." Nature **601**(7894): 630-636.

Jenett, A., G. M. Rubin, T. T. Ngo, D. Shepherd, C. Murphy, H. Dionne, B. D. Pfeiffer, A. Cavallaro, D. Hall, J. Jeter, N. Iyer, D. Fetter, J. H. Hausenfluck, H. Peng, E. T. Trautman,

R. R. Svirskas, E. W. Myers, Z. R. Iwinski, Y. Aso, G. M. DePasquale, A. Enos, P. Hulamm, S. C. Lam, H. H. Li, T. R. Laverty, F. Long, L. Qu, S. D. Murphy, K. Rokicki, T. Safford, K. Shaw, J. H. Simpson, A. Sowell, S. Tae, Y. Yu and C. T. Zugates (2012). "A GAL4-driver line resource for Drosophila neurobiology." Cell Rep **2**(4): 991-1001.

Kageyama, R., T. Ohtsuka, H. Shimojo and I. Imayoshi (2009). "Dynamic regulation of Notch signaling in neural progenitor cells." Curr Opin Cell Biol **21**(6): 733-740.

Kambadur, R., Koizumi, K., Stivers, C., Nagle, J., Poole, S.J. and Odenwald, W.F. (1998). "Regulation of POU genes by castor and hunchback establishes layered compartments in the Drosophila CNS." Genes Dev **12**: 246-260.

Kanai, M. I., M. Okabe and Y. Hiromi (2005). "seven-up Controls switching of transcription factors that specify temporal identities of Drosophila neuroblasts." Dev Cell **8**(2): 203-213.
Kaphingst, K. a. K., S. (1994). "Pattern formation in the visual centers of the Drosophila brain: wingless acts via decapentaplegic to specify the dorsoventral axis " Cell **78**(437-448).

Kawaguchi, A. (2019). "Temporal patterning of neocortical progenitor cells: How do they know the right time?" Neurosci Res **138**: 3-11.

Kelsey, G., Stegle, O., and Reik, W. (2017). "Single-cell epigenomics: Recording the past and predicting the future. ." Science **358**: 69-75.

Kim, I. M., M. J. Wolf and H. A. Rockman (2010). "Gene deletion screen for cardiomyopathy in adult Drosophila identifies a new notch ligand." Circ Res **106**(7): 1233-1243.

Knoblich, J. A. (2008). "Mechanisms of asymmetric stem cell division." Cell **132**(4): 583-597.

Knoblich, J. A., Jan Lily Y., and Jan Yuh Nung (1995). "Asymmetric segregation of Numb and Prospero during cell division " Nature **377**: 624-627.

Kohwi, M. and C. Q. Doe (2013). "Temporal fate specification and neural progenitor competence during development." Nat Rev Neurosci **14**(12): 823-838.

Kohwi, M., L. S. Hiebert and C. Q. Doe (2011). "The pipsqueak-domain proteins Distal antenna and Distal antenna-related restrict Hunchback neuroblast expression and early-born neuronal identity." Development **138**(9): 1727-1735.

Kohwi, M., J. R. Lupton, S. L. Lai, M. R. Miller and C. Q. Doe (2013). "Developmentally regulated subnuclear genome reorganization restricts neural progenitor competence in Drosophila." Cell **152**(1-2): 97-108.

Konstantinides, N., A. M. Rossi, A. Escobar, L. Dudragne, Y.-C. Chen, T. Tran, A. M. Jaimes, M. N. Özel, F. Simon, Z. Shao, N. M. Tsankova, J. F. Fullard, U. Walldorf, P. Roussos and C. Desplan (2021) "A comprehensive series of temporal transcription factors in the fly visual system." Biorxiv DOI:10.1101/2021.06.13.448242 (as accessed on 10th November, 2021)

Kopan, R. and M. X. Ilagan (2009). "The canonical Notch signaling pathway: unfolding the activation mechanism." Cell **137**(2): 216-233.

Kumar, J. P. (2012). "Building an ommatidium one cell at a time." Dev Dyn **241**(1): 136-149.

Kumar, J. P., and Moses, K. (2001). "EGF receptor and Notch signaling act upstream of Eyeless/Pax6 to control eye specification." Cell **104**: 687-697.

Kvon, E. Z., T. Kazmar, G. Stampfel, J. O. Yanez-Cuna, M. Pagani, K. Schernhuber, B. J. Dickson and A. Stark (2014). "Genome-scale functional characterization of Drosophila developmental enhancers in vivo." Nature **512**(7512): 91-95.

Lagha, M., J. P. Bothma and M. Levine (2012). "Mechanisms of transcriptional precision in animal development." Trends Genet **28**(8): 409-416.

Lane, M. E., K. Sauer, K. Wallace, Y. N. Jan, C. F. Lehner and H. Vaessin (1996). "Dacapo, a Cyclin-Dependent Kinase Inhibitor, Stops Cell Proliferation during Drosophila Development." Cell **87**(7): 1225-1235.

Lee, C., H. Shin and J. Kimble (2019). "Dynamics of Notch-Dependent Transcriptional Bursting in Its Native Context." Dev Cell **50**(4): 426-435 e424.

Levine, M. (2010). "Transcriptional enhancers in animal development and evolution." Curr Biol **20**(17): R754-763.

Lewis, E. B. (1954). "The theory and application of a new method of detecting chromsomal rearrangements in Drosophila melanogaster " The American Naturalist **88**(841): 225-239.

Li, G., X. Ruan, R. K. Auerbach, K. S. Sandhu, M. Zheng, P. Wang, H. M. Poh, Y. Goh, J. Lim, J. Zhang, H. S. Sim, S. Q. Peh, F. H. Mulawadi, C. T. Ong, Y. L. Orlov, S. Hong, Z. Zhang, S. Landt, D. Raha, G. Euskirchen, C. L. Wei, W. Ge, H. Wang, C. Davis, K. I. Fisher-Aylor, A. Mortazavi, M. Gerstein, T. Gingeras, B. Wold, Y. Sun, M. J. Fullwood, E. Cheung, E. Liu, W. K. Sung, M. Snyder and Y. Ruan (2012). "Extensive promoter-centered chromatin interactions provide a topological basis for transcription regulation." Cell **148**(1-2): 84-98.

Li, X., T. Erclik, C. Bertet, Z. Chen, R. Voutev, S. Venkatesh, J. Morante, A. Celik and C. Desplan (2013). "Temporal patterning of Drosophila medulla neuroblasts controls neural fates." Nature **498**(7455): 456-462.

Liu, Z., Yang, C., Sugino, K., Fu, C., Liu, L.,Yao, X., Lee, L.P. and Lee, T. (2015). "Opposing intrinsic temporal gradients guide neural stem cell production of varied neuronal fates " Science **350**(6258): 317-320.

Lodato, S. and P. Arlotta (2015). "Generating neuronal diversity in the mammalian cerebral cortex." Annu Rev Cell Dev Biol **31**: 699-720.

Long, X., J. Colonell, A. M. Wong, R. H. Singer and T. Lionnet (2017). "Quantitative mRNA imaging throughout the entire Drosophila brain." Nat Methods **14**(7): 703-706.

Magadi, S. S., C. Voutyraki, G. Anagnostopoulos, E. Zacharioudaki, I. K. Poutakidou, C. Efraimoglou, M. Stapountzi, V. Theodorou, C. Nikolaou and C. Delidakis (2020)."Dissecting Hes-centered transcriptional neyworks in neural stem cell maintenance and tumorigenesis in *Drosophila*." Biorxiv DOI: 10.1101/2020.03.25.007187 (as accessed on 20th September 2021)

Malicki, J., Cianetti, L.C., Peschle, C., and, McGinnis, W. (1992). "A human HOX4B regulatory element provides head-specific expression in Drosophila embryos." Nature **358**: 345-347.

Marshall, O. J. and A. H. Brand (2015). "damidseq_pipeline: an automated pipeline for processing DamID sequencing datasets." Bioinformatics **31**(20): 3371-3373.

Marshall, O. J., T. D. Southall, S. W. Cheetham and A. H. Brand (2016). "Cell-type-specific profiling of protein-DNA interactions without cell isolation using targeted DamID with next-generation sequencing." Nat Protoc **11**(9): 1586-1598.

Maurange, C., L. Cheng and A. P. Gould (2008). "Temporal transcription factors and their targets schedule the end of neural proliferation in Drosophila." Cell **133**(5): 891-902.

Meinertzhagen, I. A. and Sorra, K.E. (2001). "Synaptic organization in the fly's optic lamina: few cells, many synapses and divergent microcircuits." Progress in Brain Research **131**: 53-69.

Mettler, U., G. Vogler and J. Urban (2006). "Timing of identity: spatiotemporal regulation of hunchback in neuroblast lineages of Drosophila by Seven-up and Prospero." Development **133**(3): 429-437.

Moldovan, G. L., B. Pfander and S. Jentsch (2006). "PCNA controls establishment of sister chromatid cohesion during S phase." Mol Cell **23**(5): 723-732.

Molyneaux, B. J., P. Arlotta, J. R. Menezes and J. D. Macklis (2007). "Neuronal subtype specification in the cerebral cortex." Nat Rev Neurosci **8**(6): 427-437.

Moore, R. and P. Alexandre (2020). "Delta-Notch Signaling: The Long and The Short of a Neuron's Influence on Progenitor Fates." J Dev Biol **8**(2).

Morante, J. and C. Desplan (2008). "The color-vision circuit in the medulla of Drosophila." Curr Biol **18**(8): 553-565.

Morris, J., Chen, J., Geyer, P.K. and Wu, C. (1998). "Two modes of transvection : Enhancer action in trans and bypass of a chromatin insulator in cis " Proc Natl Acad Sci U S A **95**: 10740-10745.

Morrison, S. J. and J. Kimble (2006). "Asymmetric and symmetric stem-cell divisions in development and cancer." Nature **441**(7097): 1068-1074.

Muzio, L. and A. Mallamaci (2005). "Foxg1 confines Cajal-Retzius neuronogenesis and hippocampal morphogenesis to the dorsomedial pallium." J Neurosci **25**(17): 4435-4441.

Naka, H., S. Nakamura, T. Shimazaki and H. Okano (2008). "Requirement for COUP-TFI and II in the temporal specification of neural stem cells in CNS development." Nat Neurosci **11**(9): 1014-1023.

Narbonne-Reveau, K., E. Lanet, C. Dillard, S. Foppolo, C. H. Chen, H. Parrinello, S. Rialle, N. S. Sokol and C. Maurange (2016). "Neural stem cell-encoded temporal patterning delineates an early window of malignant susceptibility in Drosophila." Elife **5**.

Nassif, C., A. Noveen and V. Hartenstein (2003). "Early development of the Drosophila brain: III. The pattern of neuropile founder tracts during the larval period." J Comp Neurol **455**(4): 417-434.

Neriec, N. and C. Desplan (2016). "From the Eye to the Brain: Development of the Drosophila Visual System." Curr Top Dev Biol **116**: 247-271.

Ngo, K. T., J. Wang, M. Junker, S. Kriz, G. Vo, B. Asem, J. M. Olson, U. Banerjee and V. Hartenstein (2010). "Concomitant requirement for Notch and Jak/Stat signaling during neuro-epithelial differentiation in the Drosophila optic lobe." Dev Biol **346**(2): 284-295.

Novotny, T. E., R. and Urban, J. (2002). "Hunchback is required for the specification of the early sublineage of neuroblast 7-3 in the Drosophila central nervous system " Development **129**: 1027-1036.

Nusslein-Volhard, C., Wieschaus, E. and Kluding, H. (1984). "Mutations affecting the pattern of larval cuticle in Drosophila melanogaster I.Zygotic loci on the second chromosome " Roux's archives of developmental biology **193**: 267-282.

Odenwald, W. F., Rasband, W., Kuzin, A., and, Brody, T. (2005). "EVOPRINTER, a multigenomic comparative tool for rapid identification of functionally important DNA." PNAS **102**(41): 14700-14705.

Okamoto, M., T. Miyata, D. Konno, H. R. Ueda, T. Kasukawa, M. Hashimoto, F. Matsuzaki and A. Kawaguchi (2016). "Cell-cycle-independent transitions in temporal identity of mammalian neural progenitor cells." Nat Commun **7**: 11349.

Ozel, M. N., F. Simon, S. Jafari, I. Holguera, Y. C. Chen, N. Benhra, R. N. El-Danaf, K. Kapuralin, J. A. Malin, N. Konstantinides and C. Desplan (2021). "Neuronal diversity and convergence in a visual system developmental atlas." Nature **589**(7840): 88-95.

Pearson, B. J. and C. Q. Doe (2004). "Specification of temporal identity in the developing nervous system." Annu Rev Cell Dev Biol **20**: 619-647.

Pfeiffer, B. D., Jenett, A., Hammonds, A.S., Ngo, T.B., Misra, S., Murphy, C., Scully, A., Carlson, J.W., Wan , K.H., Laverty, T.R., Mungall, C., Svirkas, R., KAdonaga, J.T., Doe, C.Q., Eisen, M.B., Celniker, S.E., and Rubin, G.M. (2008). "Tools for neuroanatomy and neurogenetics in Drosophila." PNAS **105**(28): 9715-9720.

Pfeiffer, B. D., T. T. Ngo, K. L. Hibbard, C. Murphy, A. Jenett, J. W. Truman and G. M. Rubin (2010). "Refinement of tools for targeted gene expression in Drosophila." Genetics **186**(2): 735-755.

Port, F. and S. L. Bullock (2016). "Augmenting CRISPR applications in Drosophila with tRNA-flanked sgRNAs." Nat Methods **13**(10): 852-854.

Prazak, L., M. Fujioka and J. P. Gergen (2010). "Non-additive interactions involving two distinct elements mediate sloppy-paired regulation by pair-rule transcription factors." Dev Biol **344**(2): 1048-1059.

Quiring, R., Walldorf, U., Kloter, U., and Gehring, W. J. (1994). "Homology of the *eyeless* gene of Drosophila to the *Small eye* gene in mice and *Aniridia* in humans " Science **265**(5 August 1994): 785-789.

Rebay, I., Fleming, R., Fehon, R.G., Cherbas, L., Cherbas, P., and Artavanis-Tsakonas, S. (1991). "Specific EGF repeats of Notch mediate interactions with Delta and Serrate: Implicationsfor Notch as a multifunctional receptor." Cell **67**: 687-699.

Reddy, B. V., C. Rauskolb and K. D. Irvine (2010). "Influence of fat-hippo and notch signaling on the proliferation and differentiation of Drosophila optic neuroepithelia." Development **137**(14): 2397-2408.

Reichardt, I. and J. A. Knoblich (2013). "Cell biology: Notch recycling is numbed." Curr Biol **23**(7): R270-272.

Ren, Q., C. P. Yang, Z. Liu, K. Sugino, K. Mok, Y. He, M. Ito, A. Nern, H. Otsuna and T. Lee (2017). "Stem Cell-Intrinsic, Seven-up-Triggered Temporal Factor Gradients Diversify Intermediate Neural Progenitors." Curr Biol **27**(9): 1303-1313.

Rhyu, M., S. , Jan, Lily, Y., and Jan Yuh Nung (1994). "Asymmetric segregation of Numb protein during division of the sensory organ precursor cell confers distinct fates to daughter cells." Cell **76**: 477-491.

Rister, J., Razzaq, A., Boodram, P.,Desai, N., Tsanis, C., Chen, H., Jukam, D., and Desplan, C. (2015). "Single-base pair differences in a shared mtif determine differential Rhodopsin expression." Science **350**(6265): 1258-1261.

Robinson, J. T., H. Thorvaldsdottir, W. Winckler, M. Guttman, E. S. Lander, G. Getz and J. P. Mesirov (2011). "Integrative genomics viewer." Nat Biotechnol **29**(1): 24-26.

Roegiers, F. and Y. N. Jan (2004). "Asymmetric cell division." Curr Opin Cell Biol **16**(2): 195-205.

San Juan, B. P., I. Andrade-Zapata and A. Baonza (2012). "The bHLH factors Dpn and members of the E(spl) complex mediate the function of Notch signalling regulating cell proliferation during wing disc development." Biol Open **1**(7): 667-676.

Sandelin, A., W. Alkema, P. Engstrom, W. W. Wasserman and B. Lenhard (2004). "JASPAR: an open-access database for eukaryotic transcription factor binding profiles." Nucleic Acids Res **32**(Database issue): D91-94.

Schindelin, J., I. Arganda-Carreras, E. Frise, V. Kaynig, M. Longair, T. Pietzsch, S. Preibisch, C. Rueden, S. Saalfeld, B. Schmid, J. Y. Tinevez, D. J. White, V. Hartenstein, K. Eliceiri, P. Tomancak and A. Cardona (2012). "Fiji: an open-source platform for biological-image analysis." Nat Methods **9**(7): 676-682.

Schmid, A., Chiba, A. and Doe, C.Q. (1999). "Clonal analysis of Drosophila embryonic neuroblasts: neural cell types, axon projections and muscle targets " Development **126**: 4653-4689.

Schmidt, H., Rickert, C., Bossing, T., Vef, O., Urban, J. and Technau, G.M. (1997). "The embryonic CNS lineages of Drosophila melanogaster II. Neuroblast lineages derived from the dorsal part of the neurectoderm " Developmental Biology **189**: 186-204.

Selleck, S. B. a. S. H. (1991). "The influence of retinal innervation on neurogenesis in the first optic ganglion of Drosophila " Neuron **6**: 83-99.

Shlyueva, D., G. Stampfel and A. Stark (2014). "Transcriptional enhancers: from properties to genome-wide predictions." Nat Rev Genet **15**(4): 272-286.

Sladitschek, H. L., U. M. Fiuza, D. Pavlinic, V. Benes, L. Hufnagel and P. A. Neveu (2020). "MorphoSeq: Full Single-Cell Transcriptome Dynamics Up to Gastrulation in a Chordate." Cell **181**(4): 922-935 e921.

Small, S. and D. N. Arnosti (2020). "Transcriptional Enhancers in Drosophila." Genetics **216**(1): 1-26.

Southall, T. D., K. S. Gold, B. Egger, C. M. Davidson, E. E. Caygill, O. J. Marshall and A. H. Brand (2013). "Cell-type-specific profiling of gene expression and chromatin binding without cell isolation: assaying RNA Pol II occupancy in neural stem cells." Dev Cell **26**(1): 101-112.

Spitz, F. and E. E. Furlong (2012). "Transcription factors: from enhancer binding to developmental control." Nat Rev Genet **13**(9): 613-626.

Stothard, P. (2000). "The Sequence Manipulation Suite: Javascript programs for analyzing and formatting protein and DNA sequences " BioTechniques **28**(6): 1102-1104.

Stoykova, A., Fritsch, R., Walther, C., and Gruss, P. (1996). "Forebrain patterning defects in *Small eye* mutant mice " Development **122**: 3453-3465.

Stratmann, J., H. Gabilondo, J. Benito-Sipos and S. Thor (2016). "Neuronal cell fate diversification controlled by sub-temporal action of Kruppel." Elife **5**.

Suzuki, T., M. Kaido, R. Takayama and M. Sato (2013). "A temporal mechanism that produces neuronal diversity in the Drosophila visual center." Dev Biol **380**(1): 12-24.

Syed, M. H., B. Mark and C. Q. Doe (2017). "Steroid hormone induction of temporal gene expression in Drosophila brain neuroblasts generates neuronal and glial diversity." Elife **6**.

Takemura, S. Y., Z. Lu and I. A. Meinertzhagen (2008). "Synaptic circuits of the Drosophila optic lobe: the input terminals to the medulla." J Comp Neurol **509**(5): 493-513.

Tanaka-Matakatsu, M., J. Miller and W. Du (2015). "The homeodomain of Eyeless regulates cell growth and antagonizes the paired domain-dependent retinal differentiation function." Protein Cell **6**(1): 68-78.

Tomarev, S. I., Callaerts, P., Kos, L., Zinovieva,R., Halder, G., Gehring, W.J., and, Piatigorsky,J. (1997). "Squid Pax-6 and eye development." PNAS **94**: 2421-2426.

Tran, K. D. and C. Q. Doe (2008). "Pdm and Castor close successive temporal identity windows in the NB3-1 lineage." Development **135**(21): 3491-3499.

Trimarchi, J. M., M. B. Stadler and C. L. Cepko (2008). "Individual retinal progenitor cells display extensive heterogeneity of gene expression." PLoS One **3**(2): e1588.

Ulvklo, C., R. MacDonald, C. Bivik, M. Baumgardt, D. Karlsson and S. Thor (2012). "Control of neuronal cell fate and number by integration of distinct daughter cell proliferation modes with temporal progression." Development **139**(4): 678-689.

Urbach, R. and G. M. Technau (2003). "Molecular markers for identified neuroblasts in the developing brain of Drosophila." Development **130**(16): 3621-3637.

van den Ameele, J. and A. H. Brand (2019). "Neural stem cell temporal patterning and brain tumour growth rely on oxidative phosphorylation." Elife **8**.

van Steensel, B., and Henikoff, S. (2000). "Identification of in vivo DNA targets of chromatin proteins using tethered Dam methyltransferase." Nature Biotechnology **18**: 424-428.

van Steensel, B. and J. Dekker (2010). "Genomics tools for unraveling chromosome architecture." Nat Biotechnol **28**(10): 1089-1095.

Venken, K. J., J. W. Carlson, K. L. Schulze, H. Pan, Y. He, R. Spokony, K. H. Wan, M. Koriabine, P. J. de Jong, K. P. White, H. J. Bellen and R. A. Hoskins (2009). "Versatile

P[acman] BAC libraries for transgenesis studies in Drosophila melanogaster." Nat Methods **6**(6): 431-434.

Walsh, K. T. and C. Q. Doe (2017). "Drosophila embryonic type II neuroblasts: origin, temporal patterning, and contribution to the adult central complex." Development **144**(24): 4552-4562

Wang, H., G. W. Somers, A. Bashirullah, U. Heberlein, F. Yu and W. Chia (2006). "Aurora-A acts as a tumor suppressor and regulates self-renewal of Drosophila neuroblasts." Genes Dev **20**(24): 3453-3463.

Weng, M., K. L. Golden and C. Y. Lee (2010). "dFezf/Earmuff maintains the restricted developmental potential of intermediate neural progenitors in Drosophila." Dev Cell **18**(1): 126-135.

White, K. and Kankel, D. (1978). "Patterns of cell division and cell movement in the formation of the imaginal nervous system in Drosophila melanogaster" Developmental Biology **65**: 296-321.

Wray, G. A., M. W. Hahn, E. Abouheif, J. P. Balhoff, M. Pizer, M. V. Rockman and L. A. Romano (2003). "The evolution of transcriptional regulation in eukaryotes." Mol Biol Evol **20**(9): 1377-1419.

Yasugi, T., A. Sugie, D. Umetsu and T. Tabata (2010). "Coordinated sequential action of EGFR and Notch signaling pathways regulates proneural wave progression in the Drosophila optic lobe." Development **137**(19): 3193-3203.

Yasugi, T., D. Umetsu, S. Murakami, M. Sato and T. Tabata (2008). "Drosophila optic lobe neuroblasts triggered by a wave of proneural gene expression that is negatively regulated by JAK/STAT." Development **135**(8): 1471-1480.

Yoon, K. J., F. R. Ringeling, C. Vissers, F. Jacob, M. Pokrass, D. Jimenez-Cyrus, Y. Su, N. S. Kim, Y. Zhu, L. Zheng, S. Kim, X. Wang, L. C. Dore, P. Jin, S. Regot, X. Zhuang, S. Canzar, C. He, G. L. Ming and H. Song (2017). "Temporal Control of Mammalian Cortical Neurogenesis by m(6)A Methylation." Cell **171**(4): 877-889 e817.

Yu, H. H., T. Awasaki, M. D. Schroeder, F. Long, J. S. Yang, Y. He, P. Ding, J. C. Kao, G. Y. Wu, H. Peng, G. Myers and T. Lee (2013). "Clonal development and organization of the adult Drosophila central brain." Curr Biol **23**(8): 633-643.

Zacharioudaki, E., S. S. Magadi and C. Delidakis (2012). "bHLH-O proteins are crucial for Drosophila neuroblast self-renewal and mediate Notch-induced overproliferation." Development **139**(7): 1258-1269.

Zaffran, S., Das, G., and Frasch, M. (2000). "The NK-2 homeobox gene scarecrow (scro) is expressed in pharynx, ventral nerve cord and brain of Drosophila embryos." Mechanisms of Development **94**(1-2): 237-241.

Zhu, H., S. D. Zhao, A. Ray, Y. Zhang and X. Li (2022). "A comprehensive temporal patterning gene network in Drosophila medulla neuroblasts revealed by single-cell RNA sequencing." Nat Commun **13**(1): 1247.

Zhu, L. J., R. G. Christensen, M. Kazemian, C. J. Hull, M. S. Enuameh, M. D. Basciotta, J. A. Brasefield, C. Zhu, Y. Asriyan, D. S. Lapointe, S. Sinha, S. A. Wolfe and M. H. Brodsky (2011). "FlyFactorSurvey: a database of Drosophila transcription factor binding specificities determined using the bacterial one-hybrid system." Nucleic Acids Res **39**(Database issue): D111-117.

Zhu, S., S. Lin, C. F. Kao, T. Awasaki, A. S. Chiang and T. Lee (2006). "Gradients of the Drosophila Chinmo BTB-zinc finger protein govern neuronal temporal identity." Cell **127**(2): 409-422.

Zimmer, C., M. C. Tiveron, R. Bodmer and H. Cremer (2004). "Dynamics of Cux2 expression suggests that an early pool of SVZ precursors is fated to become upper cortical layer neurons." Cereb Cortex **14**(12): 1408-1420.